2022

Reproductive Resilience of Aedes Aegypti Mosquitoes

Krithika Venkataraman

Reproductive resilience of *Aedes aegypti* mosquitoes

A Thesis Presented to the Faculty of
The Rockefeller University
in Partial Fulfillment of the Requirements for
the degree of Doctor of Philosophy

by
Krithika Venkataraman
June 2022

Reproductive resilience of *Aedes aegypti* mosquitoes

Krithika Venkataraman, Ph.D.

The Rockefeller University 2022

Female *Aedes aegypti* mosquitoes impose a severe global public health burden as vectors of viruses that cause dengue, chikungunya, yellow fever, and Zika, and parasites that cause lymphatic filariasis. Under optimal environmental conditions, *Aedes aegypti* females have access to human hosts that provide blood proteins required for egg development, conspecific males that provide sperm required for fertilization, and freshwater in natural or manmade containers that serves as an egg-laying substrate suitable for offspring survival during larval and pupal stages. As global temperatures rise, *Aedes aegypti* females are faced with climate challenges like intense droughts and intermittent bouts of precipitation, which create unpredictable, suboptimal conditions for egg-laying. Yet, this species is highly invasive, adeptly domesticated, and continues to expand its stronghold across most continents. How do female *Aedes aegypti* mosquitoes successfully reproduce when freshwater availability is unpredictable? What behavioral and molecular adaptations have evolved to ensure the reproductive flexibility and resilience of this species when they are faced with intense droughts and changing climates?

Here we show that the reproductive behaviors of adult *Aedes aegypti* females are tightly interconnected and centered on precise spatiotemporal control of egg-laying in a manner that balances intrinsic physiological needs with extrinsic environmental

constraints to ensure maximal fitness. Specifically, in drought-like conditions simulated in the laboratory, females that have mated and blood fed will retain mature eggs in their ovaries for extended periods, while maintaining the viability of these eggs until they can be laid in freshwater. Using transcriptomic and proteomic profiling of *Aedes aegypti* ovaries, we identify two previously uncharacterized genes that we name *tweedledee* and *tweedledum,* each encoding a small, secreted protein that both show ovary-enriched, temporally-restricted expression during egg retention. These genes are mosquito-specific, linked within a syntenic locus, and rapidly evolving under positive selection, raising the possibility that they serve an adaptive function. A CRISPR-Cas9-mediated mutation that disrupts both *tweedledee* and *tweedledum* together demonstrates that they are specifically required for extended retention of viable eggs. These results highlight an elegant example of taxon-restricted genes at the heart of an important adaptation that equips *Aedes aegypti* females with “insurance” to flexibly extend their reproductive schedule without losing reproductive capacity, thus allowing this species to exploit unpredictable habitats in a changing world.

For Amma and Appa, foremost – my parents, my first teachers, and my best friends – whose love, faith, championship, and unconditional support keeps me grounded.

For my siblings – my babies and my sweetest cheerleaders – who breathe life and purpose into me daily. You two are my light and love.

For my grandparents – on whose shoulders the rest of us stand.

ACKNOWLEDGMENTS

I am deeply thankful to my family, friends, and mentors who have personally and professionally supported me over the past 7 years. This milestone is collectively ours.

A huge thank you to Leslie Vosshall, first and foremost – a fantastic PhD advisor, formidable leader, tireless ally, and an excellent role model. She has not only taught me to critically evaluate scientific data but has also shown me how to consider the practicality of doing top-notch science while leading a happy team fueled by camaraderie. Leslie has never failed to provide me with the cheerleading I needed on tough days or shied away from difficult conversations when a project proved to no longer yield fruit. From Leslie I have learned how to ask for and receive feedback, how to be constructive and efficient in my planning, and how to strategically address the elephant in the room as a step towards solving problems, no matter the context. I am also especially grateful for the freedom I have had to explore my curiosities, take risks, and hone my scientific intuition as a PhD student, and for the space, time, and support Leslie provided for me to be human.

Thank you to my thesis committee, Daniel Kronauer and Shai Shaham, for your time, your enthusiasm, and your ideas from molecular biology to evolution. Conversations with you both have brought so much energy to my scientific journey and have shown me how to weigh the risks and rewards of different ideas. I am a better scientist for all the rigor you have emphasized in our meetings. Thank you also to Li Zhao, with whom I've had many exciting discussions about our curious findings, and who has provided

insight with unwavering passion throughout our collaboration. I am so delighted to have Hopi Hoekstra as my external examiner – your work has been such an inspiration, and I have loved following your approach to studying naturalistic behaviors. Thank you for your time and interest in our work, and for all your insightful questions!

I am indebted to the Vosshall Lab staff, past and present, who have been an integral part of the lab's fabric. Barbara Ghelardi, your efficiency is a force to be reckoned with, and I appreciate how you look out for each of us, making sure we are well-stocked! Libby Mejia and Gloria Gordon – your warmth, your care, and your check-ins – both as individuals and as a unit – have been what made coming to lab every day feel like coming home to family. Our lab managers, Isabel Gutierrez and Emely Zeledon have shown me how to keep a team motivated and cohesive, and I'm grateful to have been supported by them. I have been fortunate to overlap with several wonderful Research Assistants in the Vosshall Lab – Ali Ehrlich, Zhongyan Gong, Anjali Pandey, Kyrollos Barsoum, Zach Gilbert, Laura Dedmon, Nia Lyn, M Dougherty, and Mona Liu. You have all made my experience truly vibrant with your conversations and ideas.

To the postdocs in the lab with whom I have discussed countless ideas, shared my delight in new results, and troubleshooted experiments on the daily – thank you for your mentorship and friendship. Takeshi Morita (whose expansive knowledge I have learned much from, and whose quiet, consistent kindness is unparalleled), Ellen De Obaldia (i.e., the best bay mate and a big part of my support system), Trevor Sorrells (with whom I have loved sharing music, art, theater and good food as much as exciting

science ideas), Andreas Keller (whom it has been a joy to know and learn from recently through his olfactory art journey!), and Meg Younger (whom I can count on for great pep talks and timely perspective). A special shoutout to Ben Matthews, Laura Duvall, Nadav Shai and Leah Houri-Zeevi, all of whom I have closely worked with. Ben, where do I even begin? My first mentor in the Vosshall lab, who got me excited about mosquito behavior and who has been an inspiration for so much of my thesis work. You are a model for how to be a kind, collaborative scientist. Laura – it has been such a joy chatting with you about everything from wild glitter mosquito ideas to drag shows, and I'm especially grateful for the opportunity to have worked with you on our fluorescent mosquito methods papers over the dreary pandemic, and to have shared glamorous evenings of conversation. Nadav – having you across from me in lab and your regular check-ins have brought me comfort and calm in a much-needed way and has made me feel at home in science and in lab. Our time collaborating has given me so much to look forward to during otherwise tough times. Leah – thank you for sharing your energy and excitement with me, and for being patiently, unwaveringly around. I think so fondly of the times that we have spent together (with your lovely, welcoming family!), be it baking cookies, being drenched at cancelled concerts, zoo-hopping, or sharing weekly Matto breakfast at the park!

Being a graduate student in the Vosshall lab has been a special experience, thanks to the friends I have found in my fellow graduate students. My day ones: Nipun Basrur – our adventures in the city, on Broadway, on hikes, and trying recipes from home regularly have given me lots to look forward to; Margo Herre – I have learned so much

from watching you do science and have admired your grace and generosity during our collaboration, which was foundational for my thesis. I'm so thankful for our friendship, walks and chats! Veronica Jové – thank you for being such a thoughtful colleague and great friend, and for always going out of your way to show up and help me think through the good or the bad. Our Vanguard adventure with Libby will always be one of my favorite Rockefeller memories! Thank you to Moli Liu, Josh Zeng, Emily Dennis, and Román Corfas, the senior graduate students who led the way and gave me sage, timely advice. To the newer graduate students in the lab: Adriana Rosas – your friendship and kindness has been an integral part of my support system these past 2 years, and I can't wait for more jazz/snow adventures; Yael Tsitohay – I'm thrilled to have a Smithie in lab, and I feel so at home talking to you about family, life, and science (in French or English!); Lola Neal – what a joy it has been to work with you and to welcome you to Rockefeller and the lab, and thank you for being an amazing neighbor; Priyanka Lakhiani – I am so grateful for your generosity in teaching me new skills, being patient and flexible, and for our soul-soothing yoga classes together; and Olivia Goldman – I admire your fearlessness, your allyship, your incredible multitasking skills, and the important work you put in to make academic science inclusive.

A big thank you to the Dean's Office – Sid Strickland, Emily Harms, Andrea Morris, Cris Rosario, Stephanie Fernandez, Kristen Cullen, and Marta Delgado. We are so fortunate to benefit from your compassion, efficiency, and tireless efforts to remove all red tape so that we can do unhindered science. I am also grateful to the countless staff (security, catering/food services, janitorial), administrators, and facilitators who have kept the

Rockefeller campus and the Vosshall Lab well-oiled, safe, and a joyous place to do science. I have worked with multiple resource centers at Rockefeller who have provided invaluable support. A special thank you to those who have collaborated and taught me so much – Henrik Molina and Justine Fidelin at the Proteomics Core; Jim Petrillo and Dan Gross at the PIT; Christina Pyrgaki, Kate Cialowicz, Carlos Rico, Tao Tong, and Alison North at the BIRC; Tom Carroll and Doug Barrows at the BRC; Connie Zhao at the Genomics Core; and Caroline Jiang from the biostatistics team. A big thank you to Jeanne Garbarino and the RockEDU team for your mentorship lessons – your work is phenomenal and participating in it has deeply enriched my time at Rockefeller. I have also been incredibly lucky to be on the Insight Lecture committee for several years. This has fueled my ideas and grown my inspiration over the years, and I'm grateful to Jesse Ausubel for the opportunity.

I have been fortunate to have mentored several extremely talented scientists during my time here – Jieqing Zhao, Osasere Imade, Sarah Zylka, and Lola Neal. It has been most rewarding working with and collaborating with all of you, and it gives me immense pleasure watching your journeys unfold. The future of science and the world is bright.

To my friends outside of lab at Rockefeller – Stephanie Marcus, Fanny Matheis, and Sarah Baker – sharing adventures with you (and with your families) in New York and beyond has made graduate school such a special experience, and I'm forever grateful for our time spent together. Thank you for being my core crew. Thank you also to my friends, Cheng Lyu, Christina Wang, Ariën Schiepers, and Astrid Hoffius – I cherish all

the great memories! To my friends from Smith – Jamie Samdahl and Metasebia Aberra, who have been my support system despite the miles between us and have made the past 10+ years in the US so memorable, thank you for your cheerleading and cold-calling. Stanzin Dawa – who has been my family, and who has literally looked after me during the worst and best times and has been around for absolutely everything in my life since 2011. Here's to many more memories, Aunty – love you. Gemma Regan-Mochrie – there is no version of graduate school or London and New York that I could imagine without you, and there's no better person to have been in such synchrony with through these years. David Fesser, you have been the best travel buddy, and I cannot wait to explore more of the world with you post-pandemic! My Bengaluru friends, Neeraja Ramakrishnan, Arun Radhakrishnan, Ajay Ravindran – thank you for living through the cringeworthy but irreplaceable memories with me, and for being up for adventure always. Ritika Chandy – you are the best, and I'm beyond lucky to have you as my friend and sister until the end of time.

Everything I have been able to do, see, learn and experience has been thanks to my fantastic family, who are my #1 support system. I am grateful to all my cousins, aunts, and uncles spread across the world who remind me who I am and who never give up on me, wherever I may end up on my adventure. I have been fortunate to have had my maternal grandmother, Chichu, visit me first at Smith and then at Rockefeller, and share in my excitement over the years. Early in my time at Rockefeller, while mid-experiment, I received news of my maternal grandfather, Ammalam's, passing. While at Smith, I lost my paternal grandmother, Paati, and before that, my paternal grandfather, Thatha. I

wish you three were still here today to see me reach this PhD milestone – a first within our close family. We all stand on your shoulders.

To my baby brother, Krishna, who insists he's not a baby – I am so proud of the person you are growing to be, the important friend you have become, and your unmatched sense of empathy sets an example for me daily. I am thrilled to see your curiosity develop and I admire the calm with which you handle life. Bubs, you are wise beyond your years, and I will always adore you most embarrassingly. To my baby sister Keerthana, my sunshine, my most relentless cheerleader, my sweetest best friend, and the other half of my heart – you are everything I could wish for and more in a sister and friend. I have loved sharing books and science with you, as much as our duplicate papa hugs and adventures. Your strength and resilience are unmatched, and I cannot wait for the next phase of our journey together, exploring the world and living our bucket lists with peace and ease. I am so proud of you today and always. Finally, to my parents – Amma and Appa. This is for you. Watching you both has taught me how to be kind, curious, and persevering, as well as how to discern when to be trusting, forgiving, and brave. From you both, I have learned generosity and the power of unwavering support and companionship, as well as how to stay true to my core values. Thanking my lucky stars every day – I love you.

TABLE OF CONTENTS

LIST OF FIGURES

LIST OF TABLES

CHAPTER 1. Innovations for survival and reproduction in dynamic ecosystems

1.1 Adaptations enable survival and reproduction in changing habitats

Extraordinary adaptations are ubiquitous across the animal kingdom within every habitat. Adaptations can be behavioral, physiological, or structural, and are evolutionarily selected to enable members of a species to persist by providing survival value. Ecosystems within which animals exist are in constant flux. When faced with changing habitats, animals must act flexibly and appropriately to survive and reproduce. For example, when a river-dwelling African lungfish (*Protopterus annectens*) experiences food and water scarcity during drought, it burrows into the dried riverbed, forming a cocoon with secreted mucus. There, it can survive for years while remaining metabolically dormant but within a week of rainfall, it reawakens and resumes normal metabolism (Chng et al., 2017; Heimroth et al., 2018). Among birds, species like the Eurasian blackcap (*Sylvia atricapilla*) exhibit genetically-encoded seasonal migratory behaviors that rapidly evolve in the face of changing resource availability, resulting in new migratory routes and destinations (Berthold et al., 1992; Berthold and Querner, 1981; Delmore et al., 2020). Land mammals such as marsupials alter the timing of their reproductive cycle in response to offspring-derived cues (Renfree, 1979). Tammar wallaby (*Macropus eugenii)* mothers can newly conceive while carrying previously birthed offspring in their pouches, but they developmentally arrest conceived embryos at the 100-cell stage, only resuming embryonic development after the pouch offspring has finished suckling and left to live independently (Renfree, 1979; Tyndale-Biscoe et al., 1974). Such adaptations enable animals to flexibly allocate both the extrinsic and

intrinsic resources required for reproduction and survival as appropriate to their availability and their utility.

1.2 Taxon-restricted genes underlie tailored adaptations in a diverse world

How are novel adaptations encoded by the genome of a species? Historically, studies have focused on genes that are conserved across clades and that comprise a large proportion of all genomes, reflecting the depth of shared ancestry between species. As gene conservation is often accompanied by functional conservation, the study of conserved genes has highlighted many of the genetic components that are essential for organismal function across Metazoa (Johnson, 2018). Standalone, an understanding of conserved genes is insufficient for explaining the range of striking differences in traits observed from bees to blue whales. How then do we understand the exquisite biodiversity of the natural world? How do novel traits arise? Two alternate mechanisms exist. First, old genes are integrated into new gene networks, or co-opted to encode novel phenotypes (Khalturin et al., 2009). Second, novel protein-coding genes newly arise, such as from genome rearrangements (Stewart and Rogers, 2019), from alternate reading frames of old genes (Guan et al., 2018), or from previously non-coding sequences (Zhao et al., 2014). These young genes, comprising 10-20% of genomes, are taxonomically restricted to a specific clade (Johnson, 2018; Khalturin et al., 2009), and may encode proteins with new domains, structures, and functions (Bungard et al., 2017).

Adaptations, especially those relevant to reproduction or expansion into new ecological niches, have been shown in recent studies across diverse species to arise from taxon-restricted, rapidly evolving genes with tissue-restricted and/or sexually dimorphic expression (Guillén et al., 2014; Schmidt et al., 2013; Witt et al., 2021). For example, a mouse *de novo* gene, *Gm13030,* with female-biased, oviduct-specific expression shows strong estrous cycle-dependent control (Xie et al., 2019). In homozygous *Gm13030* mutant females, three *Dcpp* genes known to promote embryo implantation are upregulated. Mutant females progress normally through their first estrous cycle but undergo premature implantation in their second estrous cycle, resulting in inappropriately early second litters and higher infanticide rates – both likely maladaptive phenotypes (Xie et al., 2019). In *Rhagovelia antilleana* water strider insects, a pair of taxon-restricted genes (*gsha* and *mogsha*) are required for the development of a midleg fan structure specific to this genus (Santos et al., 2017). The fan endows *Rhagovelia* with the biomechanical capabilities needed to perform a rowing behavior on the surface of rapidly moving streams where they are typically found (Santos et al., 2017). Other non-*Rhagovelia* species occupying the same streams rarely perform these rowing behaviors and instead occupy static surfaces on leaves, suggesting the fan is central to *Rhagovelia's* ability to walk on water (Santos et al., 2017). *Hormaphis cornu* aphids secrete salivary gland-enriched BICYCLE proteins, which come from a large family of rapidly evolving secreted molecules. The aphids pierce their stylet into mesophyll cells of the *Hamamelis virginiana* witch hazel leaf, where they deposit BICYCLE proteins. This triggers the formation of galls on the witch hazel leaf, which provides the aphid with the shelter and nutrition required for subsequent development (Korgaonkar et al., 2021).

Such phenotypic novelties may therefore endow species across the tree of life with the ability to expand into new ecological niches, perform new behaviors, and provide an overall survival advantage.

1.3 Mosquito species exploit a remarkable range of habitats worldwide

Especially as pertaining to reproduction, mosquitoes have evolved some of the most effective adaptations. They are Dipterans – two-winged flies – that belong to the monophyletic family, Culicidae (Harbach, 2013). Approximately 3,500 named species of mosquito exist, of which only a small proportion spread diseases of major global public health importance (Harbach, 2013). Mosquito species span an impressive range of habitats across continents, ranging from the savannas and grasslands in Africa; the rainforests across Asia or South America; ponds in the Arctic, and manmade construction sites or containers abundant in cities from North America to Europe to Australia (Cornel et al., 2018; DeSiervo et al., 2020; Liang et al., 2018; Powell et al., 2018; Spielman and D'Antonio, 2001). Species differ in their blood-feeding capacity; their preference for blood meal hosts and egg-laying sites; the optimal conditions required for larval and pupal survival; and the ability of eggs laid to remain in a state of developmental arrest known as diapause for prolonged periods (Day, 2016). These differences in adaptations reflect the range of ecologies within which mosquito species exist, each with distinct combinations of selective pressures that shape the reproductive characteristic of the species.

1.4 Reproductive modes in blood-feeding vs. non-blood-feeding mosquitoes

Most mosquito species do not require a blood meal for developing eggs and lack the capacity for blood-feeding (Basrur et al., 2020; McBride et al., 2014). One of the largest mosquitoes, *Toxorhynchites speciosus* (elephant mosquito), and one of the smallest, *Wyeomiia smithii* (pitcher plant mosquito) rely on larval nutrition to develop eggs (Armbruster et al., 1997; Armbruster et al., 2001; Steffan, 1980). *Toxorhynchites speciosus* are predatory in the larval stage; for nutrition, they cannibalize larvae of competing mosquito species, and even conspecifics (Steffan, 1980). *Wyeomia smithii* mosquitoes exclusively live inside the pitcher plant and for most populations, the host prey capture environment provides the resources required for nutrition and reproduction, although a few populations in distinct geographic locations do blood feed to reproduce (Armbruster et al., 1997; Armbruster et al., 2001; Bradshaw et al., 2018). Blood-feeding vector species notorious for transmitting deadly infections belong predominantly to three genera: *Anopheles, Culex,* and *Aedes,* and these require a vertebrate blood meal to develop eggs (Spielman and D'Antonio, 2001). Blood-feeding is a sexually dimorphic trait in these disease vector species, with only females bearing the capacity to engorge on and digest blood (Basrur et al., 2020; Lehane, 2005).

1.5 Egg-laying strategies of blood-feeding mosquitoes

Following differences in how nutrients required for egg development are obtained, female mosquitoes that are ready to deposit eggs display a wide range of egg-laying behaviors. This includes variations in the size of individual eggs, the size of the egg clutch, preference for specific egg-laying substrates, and the degree of flexibility in the

timing of an egg-laying event (Afify and Galizia, 2015; Bentley and Day, 1989; Day, 2016; Matthews et al., 2019; Wallis, 1954). Before a female makes an egg-laying decision, she must integrate information regarding her internal physiology (e.g., nutritional and mating status) as well as her external environment (e.g., relative humidity, temperature, pH, salinity, presence of predators vs. competitors). The integrated information must encompass both spatial and temporal considerations. Are her eggs mature and ready to be laid? If so, is the located egg-laying substrate suitable for offspring survival? If environmental conditions are unfavorable, are the eggs laid able to remain viable but in diapause until conditions become optimal for hatching? Should the female distribute her eggs across multiple egg-laying substrates – a phenomenon known as skip oviposition – which allows the mother to hedge her bets (Colton et al., 2003)? These decision points are linked, and each species employs a strategy that is appropriate to its ecological niche (Wallis, 1954).

Some species like *Aedes triseriatus,* the Eastern tree hole mosquito, are oviposition specialists – they select egg-laying substrates from a relatively narrow range of options and so are often constrained in the ecological niches they may inhabit. Other species like *Culex nigripalpus,* the Florida SLE mosquito, are generalists, laying eggs in an opportunistic fashion across more diverse egg-laying substrates, which allows them flexibility to move between a broader range of habitats (Day, 2016).

The egg-laying site selection strategy of a species depends on the type of eggs they lay. Eggs may be laid singly, or carefully stacked into rafts or clusters (Figure 1.1).

Species can be permanent water mosquitoes, which lay eggs directly on the surface of water bodies that remain stably available, or they can be floodwater mosquitoes, which lay eggs on moisture adjacent to temporary water bodies that dry out and become re-flooded depending on weather patterns (Clements, 2000). Typically, eggs laid on water by permanent water mosquito species hatch rapidly following embryonic development. Eggs laid adjacent to water on moisture in unpredictable climates by floodwater mosquitoes can developmentally arrest to remain viable in diapause for several months before hatching when water becomes available again (Bentley and Day, 1989; Curtin and Jones, 1961; Day, 2016; Du and Millar, 1999; Wallis, 1954). Across Culicidae, eggs that are desiccation resistant are laid by species belonging to only a few genera: *Aedes, Ochlerotatus, Psorophora, Haemagogus,* and *Opifex* (Clements, 2000). Among prominent disease vector mosquitoes, *Culex* species lay several hundred eggs typically in the form of rafts which float atop water and are oriented such that larvae can directly swim into the water upon hatching (Figure 1.1). Most *Anopheles* species lay eggs singly on the surface of water (Figure 1.1), and these eggs hatch rapidly within days of being deposited once embryos have developed. Many *Aedes* species also lay eggs singly. These eggs that are laid at the water's edge are desiccation-resistant and enter a diapause state until hatching conditions are suitable (Figure 1.1). Such strategies and characteristics exist on a continuum in many species or populations, with flexibility to switch between them as the environment demands (Day, 2016; Wallis, 1954).

Figure 1.1 Eggs laid by disease vector mosquitoes
Eggs laid by mosquitoes from the three primary disease vector genera: *Anopheles* (left), *Aedes* (center), and *Culex* (right).
Photograph credits: *Aedes*, adapted from (Isoe et al., 2019); *Culex, Anopheles,* from Centers for Disease Control/CDC.

1.6 *Aedes aegypti* mosquitoes are invasive despite dependence on freshwater – a fluctuating resource

Domesticated *Aedes aegypti* mosquitoes that lay eggs at the edge of freshwater and go through an aquatic life cycle as larvae and pupae are very susceptible to fluctuating precipitation patterns and climate change-driven catastrophes like drought (Caldwell et al., 2021; Cook et al., 2020; Gu et al., 2020; Hopp and Foley, 2003). Despite climate variations, *Aedes aegypti* mosquitoes are highly invasive on almost every continent (Figure 1.2) and pose a serious, immediate, and growing threat to global public health (Brown et al., 2014; Kraemer et al., 2015a; Kraemer et al., 2019; Lounibos and Kramer, 2016). In biting multiple humans across their cycles of reproduction, female *Aedes aegypti* mosquitoes transmit viral infections such as yellow fever, Zika, dengue, and chikungunya, and parasitic infections such as lymphatic filariasis (WHO, 2017).

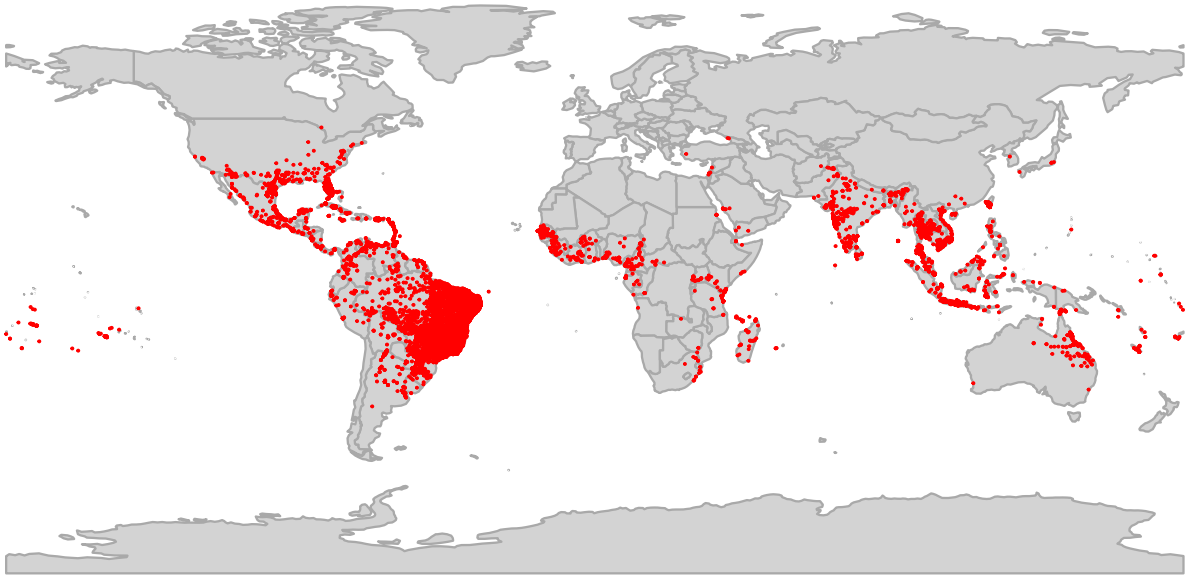

Figure 1.2 Occurrences of *Aedes aegypti* mosquitoes globally from 1960-2013
Red points indicate occurrences of *Aedes aegypti* from 1960-2013. Global geographical distribution re-plotted using occurrence data from (Kraemer et al., 2015a), which provides further information on what constitutes an occurrence.

Where did *Aedes aegypti* originate? How did it come to invade much of the planet? The ancestral form of *Aedes aegypti* originated in sub-Saharan Africa, where it was found in forests. This ancestral population still exists as the forest form (*Aedes aegypti formosus*), feeds on blood from a variety of mammals to develop eggs, which are laid in tree holes or pools of organic matter-filled water (Gloria-Soria et al., 2016; McBride, 2016; McBride et al., 2014; Powell et al., 2018; Powell and Tabachnick, 2013). The form of *Aedes aegypti* (*Aedes aegypti aegypti*) found across much of the world today is highly domesticated and its establishment is directly connected to a dark, shameful, and unforgivable part of human history: the slave trade. Thought to have initially been spread in part by eggs attached to human containers during the transportation of African people as slaves to the Americas, the invasion of this species has been further enabled by urbanization and the lack of screening for invasive species during continued global

trade (Gloria-Soria et al., 2016; McBride, 2016; McBride et al., 2014; Powell et al., 2018; Powell and Tabachnick, 2013).

Human activities have also influenced *Aedes aegypti*'s invasiveness indirectly, through the acceleration of climate change (WHO, 2017). Over the past century, global temperatures have steadily increased (Figure 1.3A), and along with it the proportion of the planet that can support *Aedes aegypti*'s survival has also expanded (Figure 1.3B) (Caldwell et al., 2021; Kraemer et al., 2019; Ryan et al., 2019). Current projections for global temperatures over the next century are dire. Without significant mitigation of greenhouse gas emissions from human activities, global warming is strongly predicted to continue posing a problem for the health of the planet (IPCC, 2021). Notably, a major consequence of this is the likely increase in the number of regions globally where *Aedes aegypti*-borne disease transmission can occur due to their increased temperature suitability for the *Aedes aegypti* life cycle (Ryan et al., 2019).

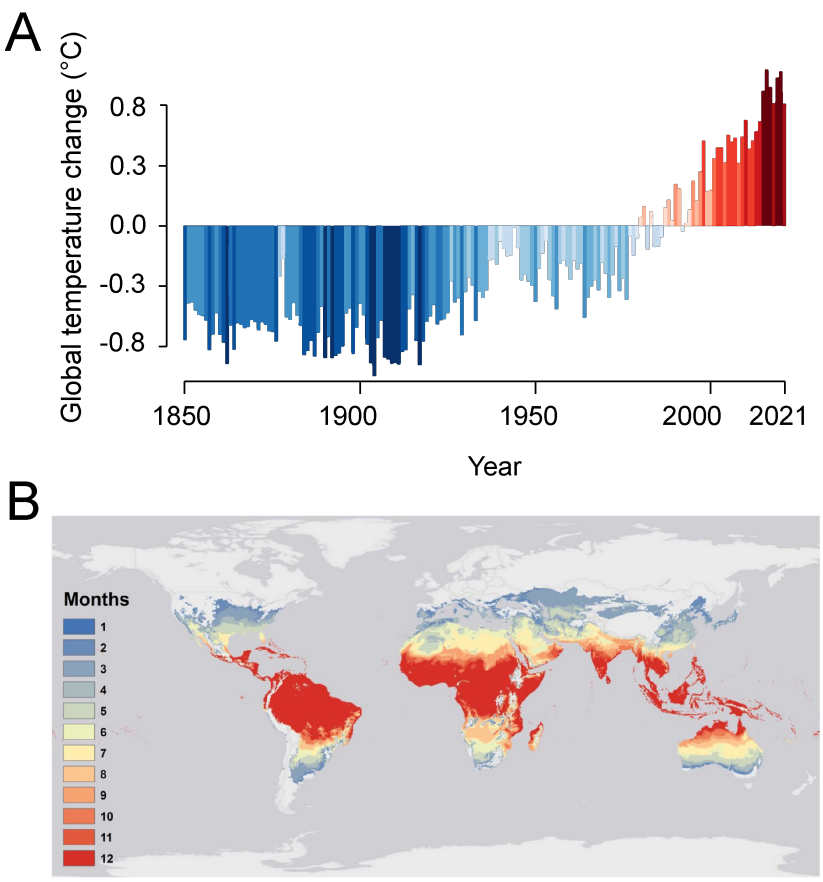

Figure 1.3 Global temperature increases expand the regions suitable for *Aedes aegypti* mosquitoes
(**A**) Changes in global temperature from 1850-2021. Adapted from Ed Hawkins, University of Reading (https://showyourstripes.info/c).
(**B**) World map showing the current suitability of locations for *Aedes aegypti*-borne disease transmission based on mean temperatures. Adapted from (Ryan et al., 2019).

What reproductive strategies have domesticated *Aedes aegypti* evolved that allow them to exploit and thrive in human settlements? Domestic strains of *Aedes aegypti* prefer hunting and biting humans over other vertebrate hosts (Harrington et al., 2001; Harrington et al., 2014; McBride et al., 2014; Rose et al., 2020) and prefer laying eggs on moist surfaces proximal to freshwater in natural and manmade containers found around human settlements (Bentley and Day, 1989; Matthews et al., 2019). Female *Aedes aegypti* typically mate once in their lifetime (Gwadz and Craig Jr., 1968), storing

sperm in specialized organs called spermathecae from which sperm are released to fertilize eggs post-ovulation, as eggs are in transit through the reproductive tract *en route* to being laid (Degner and Harrington, 2016; Jones and Wheeler, 1965). Once laid at the edge of freshwater, eggs darken and harden, and embryogenesis occurs within the eggshell (Li, 1994). After this, if conditions are suboptimal for hatching (Rezende et al., 2008), a developmental arrest state called diapause is triggered to prevent embryo desiccation for up to 3-6 months. Embryos then hatch when pools of freshwater become available again, and when aquatic larval and pupal development can be completed before eclosion to the terrestrial adult stage (Clements, 1963a).

The steps in the reproductive sequence of an adult *Aedes aegypti* female are precisely orchestrated. While mating and host-seeking can occur in any order as the availability of conspecific males and human hosts, respectively, allows, both these behaviors must precede egg-laying, the final step in the reproductive sequence of the female before she parts with her offspring. Appropriate selection of an egg-laying substrate, and precise timing of the egg-laying event are therefore crucial decision points that determine fitness outcomes, and that must accordingly balance internal physiological needs with constraints posed by the external environment.

1.7 Summary of key contributions from this study

The increase in global temperatures thus far recorded and currently projected for the coming century suggest changes to other climate variables, such as precipitation seasonality. Notably, greater intensity and frequency of climate catastrophes like floods and droughts are expected (IPCC, 2021). These precipitation-related facets of climate

change will have serious ramifications for *Aedes aegypti* mosquitoes that lead a freshwater-centric lifestyle, and for the spread of the diseases that they transmit. Despite its importance, the basis of the reproductive resilience of *Aedes aegypti* in the face of unpredictable climates is not well understood. Our study focuses on how females time their egg-laying event based on freshwater availability – a crucial final step in each reproductive cycle of an adult female *Aedes aegypti* mosquito. We explore the behavioral and molecular mechanisms that underpin the reproductive success of this species in unpredictable environments. Here we show that under drought-like conditions simulated in the laboratory, *Aedes aegypti* females will robustly retain eggs in their ovaries until freshwater is located. Under normal conditions when freshwater is plentiful, females will lay eggs 3-4 days after a blood meal. We restricted access to freshwater for 4-12 days post-blood meal. A considerable proportion of eggs laid after extended retention to at least 12 days post-blood-meal were viable, hatching at high rates. We identified two previously uncharacterized, tightly linked genes – here named *tweedledee* and *tweedledum* for the curious pair of characters in Lewis Carroll's 1871 book, “Through the Looking-Glass and What Alice Found There” – that are adult female-specific and ovary-enriched in their expression. The expression of these genes is dramatically upregulated in the ovaries only during the period in which females retain eggs, and the genes are spatially limited to cells that encapsulate mature eggs. Both genes are taxon-restricted, with no detectable orthology except in *Aedes albopictus,* a similarly invasive disease vector mosquito species that is ~70 million years diverged from *Aedes aegypti* (Chen et al., 2015). In *Culex quinquefasciatus* and several *Anopheles* mosquito species, we identify “*conceptualogs*,” which we define as genes

with no sequence homology to *tweedledee* or *tweedledum*, but which bear other featural similarities with them, such as synteny, gene structure, gene size, and the presence of signal peptides in the predicted proteins. *Aedes aegypti tweedledee* and *tweedledum,* as well as the *Anopheles gambiae conceptualog*, are rapidly evolving genes within their respective species, and show strong signatures of positive selection. Using loss-of-function mutagenesis to make a mutation that disrupts both genes simultaneously, we show that *Aedes aegypti tweedledee* and *tweedledum* are specifically required for extended retention of viable eggs under suboptimal drought conditions. Without *tweedledee* or *tweedledum* as in the double mutants*,* mated, blood-fed *Aedes aegypti* females lose their reproductive “insurance.” As a result, when egg retention is triggered by restricted freshwater access due to drought-like conditions, most of the eggs they have matured no longer generate viable offspring if laid. Our results suggest that the taxon-restricted genes, *tweedledee* and *tweedledum,* play a crucial role in maintaining the reproductive resilience of female *Aedes aegypti* mosquitoes faced with fluctuating precipitation cycles and unpredictable drought-like conditions. The ecological flexibility of *Aedes aegypti* mosquitoes makes it likely that they will expand into new parts of the globe where they were previously absent (Caldwell et al., 2021; Ryan et al., 2019). We propose that these genes, which allow *Aedes aegypti* females to maintain reproductive capacity, constitute an integral part of the mechanisms allowing the ecological flexibility of this species. The following chapters are based on the content of a bioRxiv pre-print posted on March 2, 2022 (Venkataraman et al. DOI: 10.1101/2022.03.01.482582).

CHAPTER 2. Mosquito reproduction is coordinated, flexible, and resilient

2.1 Innate reproductive behaviors are tightly linked in *Aedes aegypti* mosquitoes

The innate behaviors of an adult female *Aedes aegypti* mosquito are centered on the appropriate selection of a reproductive strategy that balances tradeoffs between internal energetic resources and external environmental conditions. To ensure that the timing and sequence of steps in the reproductive cycle of a female *Aedes aegypti* mosquito are appropriate for maximal reproductive output, the innate behaviors enabling access to blood meal sources, male sperm, and freshwater egg-laying substrates are interconnected (Figure 2.1). Each behavior proceeds only when the necessary "checkpoints" have been cleared (Clements, 1963b). For example, females will not lay most, if any, of their eggs before they have mated (Villarreal et al., 2018). Females will suppress their attraction to hosts while eggs are developing and only restore attraction once eggs are laid (Duvall et al., 2019; Klowden, 1994; Klowden and Lea, 1978, 1979a, b; Liesch et al., 2013). Females will not lay eggs both until and unless they locate freshwater, retaining them in their ovaries as needed (Day, 2016; Judson, 1968; Matthews et al., 2019). This interconnectedness of innate behaviors ensures that reproductive steps proceed in the order required for offspring survival.

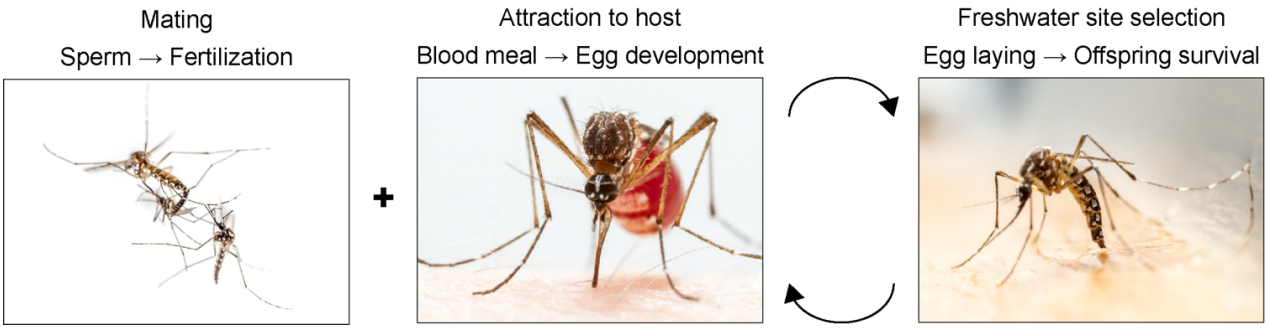

Figure 2.1 Innate reproductive behaviors of *Aedes aegypti* females
Left: *Aedes aegypti* male and female mating.
Center: Female blood feeding from a human host.
Right: Female laying eggs in water.
Photographs: Alex Wild.

2.2 Host-seeking is strongly correlated with ovary state

Aedes aegypti females require protein from a vertebrate blood meal to mature each clutch of eggs, typically over 3-4 days (Klowden, 1994). Once mature, if freshwater was unavailable, we found that mated females retained eggs in their ovaries. When tested using a live human stimulus olfactometer (Basrur et al., 2020), we found that females retaining eggs continued to suppress their host-seeking drive for both moderate (6 days post-blood-meal, Figure 2.2A) or extended (12 days post-blood-meal, Figure 2.2B) periods of time after blood-feeding. Females fully restored attraction to human hosts only after finding freshwater and laying eggs, irrespective of when after egg retention they laid eggs (Figure 2.2). At this point, females were ready to initiate a second cycle of reproduction. The dynamics of mosquito attraction to humans was similar across multiple cycles of reproduction (Figure 2.2C), which suggests that attraction to humans – a *de facto* protein-feeding drive – is strongly dependent on reproductive physiology.

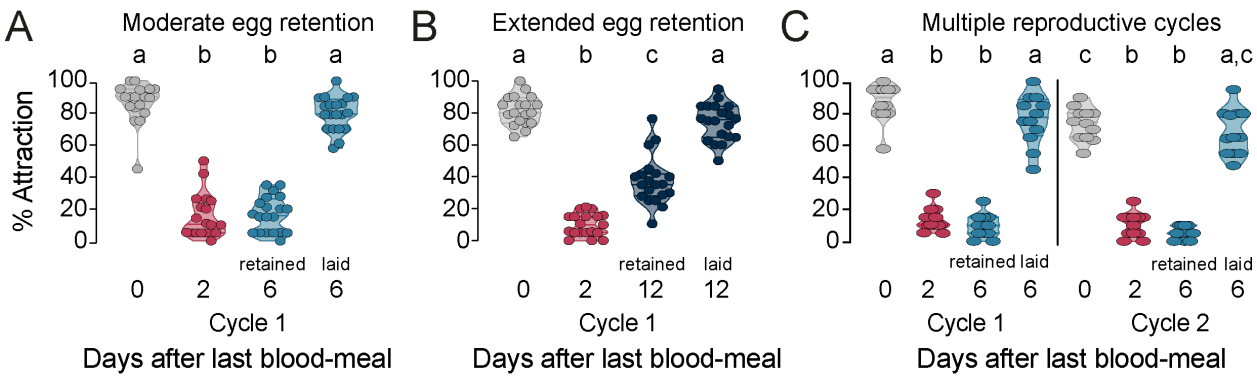

Figure 2.2 Blood-feeding suppresses attraction until eggs are laid
(**A-C**) Attraction of wild type females to a human forearm at the indicated reproductive state and cycle. Females are mated for all host-seeking experiments. Each point represents a single trial with ~20 females, n=12-20 trials/group. Data are plotted as violin plots with median and 1st/3rd quartiles and showing all data points. Data labeled with different letters are significantly different: (**A**) Kruskal-Wallis, Dunn's multiple comparisons test, $p<0.05$. (**B, C**) one-way ANOVA, Tukey's multiple comparisons test, $p<0.05$.

How soon after laying eggs do females restore attraction to hosts? When *Aedes aegypti* females locate a potential egg-laying substrate, they contact it with their legs, proboscis, and ovipositor to evaluate its suitability for egg-laying before depositing eggs individually (Matthews et al., 2019). Using separate egg-laying vials for each female (Figure 2.3A), we found that ~80% of mated females 6 days post-blood-meal completed egg-laying within 3 hours of gaining access to freshwater (Figure 2.3B). When collected after the 3-hour period allotted for egg-laying and assayed in the olfactometer with a live human stimulus, females showed restored attraction to humans within 2 hours of completing egg-laying (Figure 2.3C-D). Due to technical limitations of our egg-laying and host-seeking assays, we cannot conclude whether egg-laying triggers restored attraction on shorter timescales, but future manipulations that force rapid egg-laying may be useful for determining the timing of restored attraction with greater resolution.

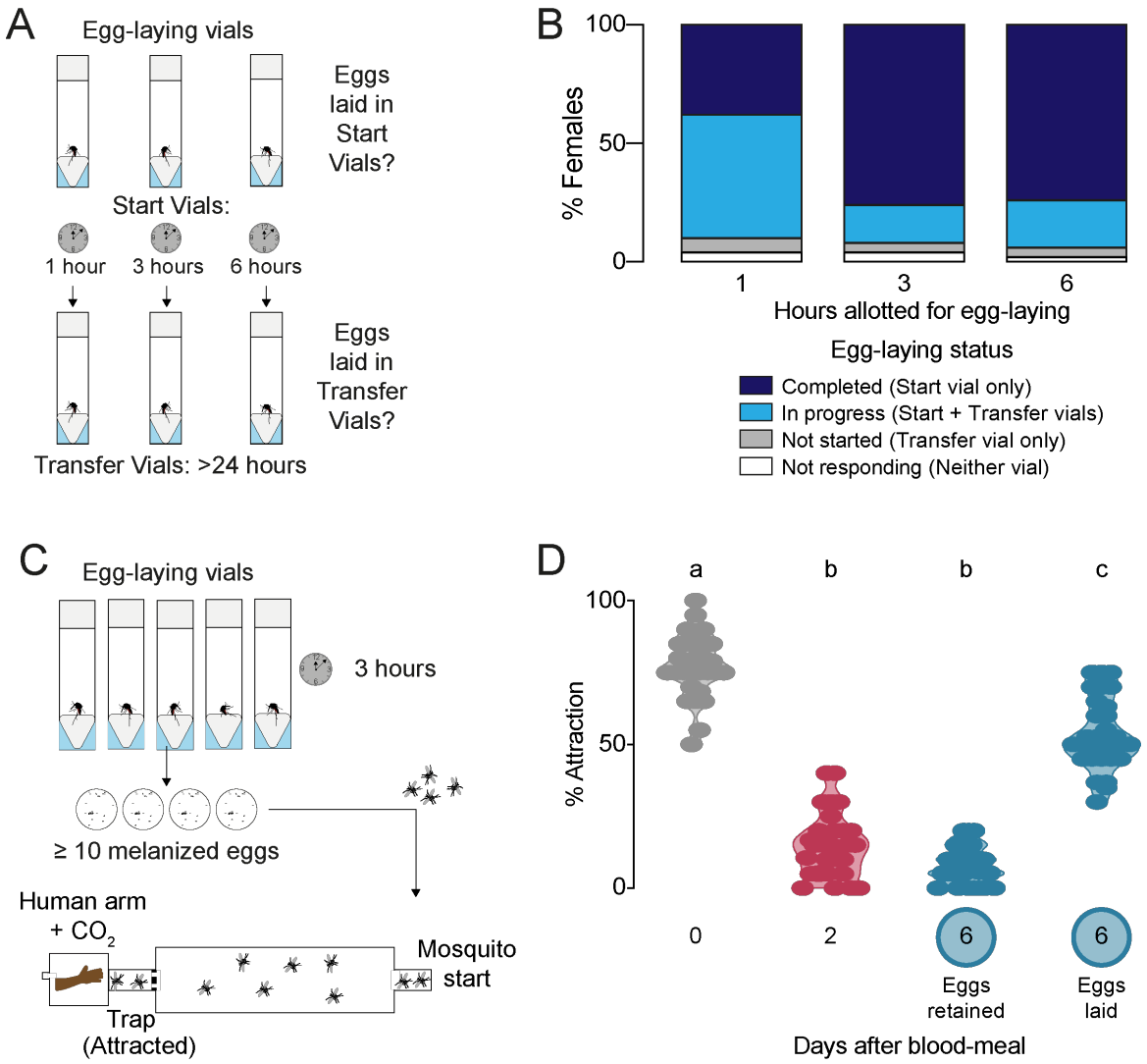

Figure 2.3 Timing of egg-laying and return to human host-seeking
(**A**) Assay schematic to determine the length of time taken for individual wild type females to complete egg-laying.
(**B**) Temporal dynamics of egg-laying (n=50 females/time-point) according to criteria indicated in legend at right.
(**C**) Cartoon of independent assay to verify and collect females that have restored attraction to humans as soon after egg-laying as possible. Females were given 3 hours for egg-laying based on results in (B) and only females that had laid at least 10 melanized eggs – those presumed to have completed egg-laying – were chosen for subsequent testing of attraction to humans within an additional 2 hours using a long-range, live human stimulus olfactometer.
(**D**) Attraction of wild type females to a human forearm at indicated reproductive state. Violin plot with median and 1st/3rd quartiles and showing all data points. Each point represents a single trial with a group of ~20 female mosquitoes with n=30-31 replicates/group. Data labeled with different letters are significantly different (one-way ANOVA, Tukey's multiple comparisons test, $p<0.0001$).

2.3 Host-seeking and mating are decoupled, but both are coupled to egg-laying

Mating to obtain sperm, as well as host-seeking to engorge on a blood meal are both required for a female to successfully reproduce. Under controlled laboratory conditions, we found that virgin and mated females were both attracted to human hosts prior to blood-feeding, and mated females showed significantly stronger levels of attraction (Figure 2.4). After blood-feeding, irrespective of their mating status, females suppressed their attraction to human hosts while developing eggs (Figure 2.4). These data suggest that mating and host-seeking/blood-feeding behaviors are decoupled in *Aedes aegypti*, allowing the females flexibility to mate and blood-feed in any order according to the availability of males and blood meal hosts, respectively (Figure 2.4).

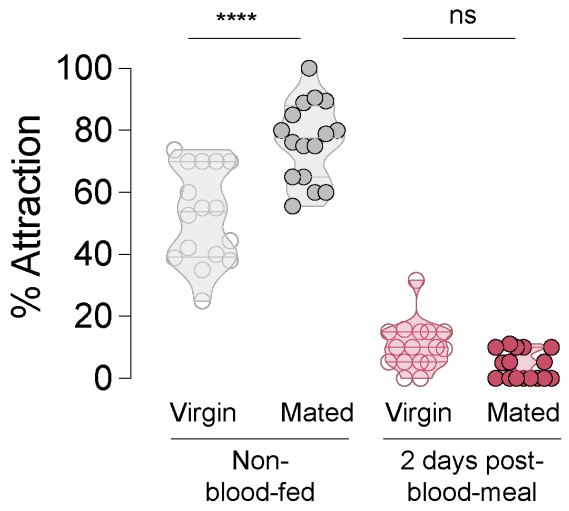

Figure 2.4 Mating enhances attraction, while blood-feeding suppresses attraction
Attraction of wild type females to a human forearm at the indicated reproductive state. Each point represents a single trial with ~20 females, n=16/group. Data are plotted as violin plots with median and 1st/3rd quartiles and showing all data points. One-way ANOVA, Holm-Šídák's test comparing virgin and mated groups within each time-point; n.s.: not significant, ****p<0.0001.

Our data (Figure 2.2) support previous findings that mated females without access to freshwater egg-laying substrates robustly retain the eggs in their ovaries (Day, 2016;

Matthews et al., 2019). When provided access to freshwater 6 days post-blood-meal (Figure 2.5), virgin females, in contrast to mated females, laid few eggs, if any. This ensures that eggs that are unfertilized and that are therefore inviable are not wasted.

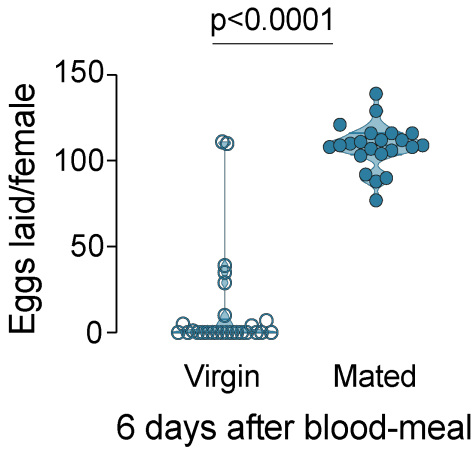

Figure 2.5 Virgin females lay few eggs compared to mated females
Number of eggs laid by mated or virgin females. Data represent eggs laid by a single female, n=22-26 females/group, shown as a violin plot with median and 1st/3rd quartiles with all data points. Mann-Whitney test, p<0.0001.

Together, these data demonstrate that egg-laying, the ultimate step in the reproductive sequence of a female, is tightly coupled to both mating and blood feeding and requires both to occur. Our results in this chapter are largely consistent with decades of laboratory and field observations (Afify and Galizia, 2015; Bentley and Day, 1989; Brown et al., 1994; Day, 2016; Duvall et al., 2019; Hudson, 1956; Judson, 1968; Klowden, 1994; Klowden, 1995; Klowden, 1996, 1999a, b; Klowden and Lea, 1978, 1979b; Liesch et al., 2013; Matthews et al., 2019) and demonstrate a strong basis for conducting further studies to understand the basis of egg-laying behavior using the Liverpool laboratory strain of *Aedes aegypti,* which is described as the wild type in all experiments described.

2.4 Egg-laying decisions are timed based on context

When a mated female mosquito has converted blood meal nutrients into mature eggs over 3-4 days, she must integrate internal information about her mating and egg development status with externally-derived chemosensory cues from potential egg-laying substrates to make subsequent, contextually appropriate egg-laying decisions (Afify and Galizia, 2015; Bentley and Day, 1989; Matthews et al., 2019). Under optimal environmental conditions of abundant freshwater, a female readily lays her eggs at the edge of freshwater 3-4 days after the blood meal, but under drought-like conditions, females robustly retain eggs within their ovaries (Figure 2.6).

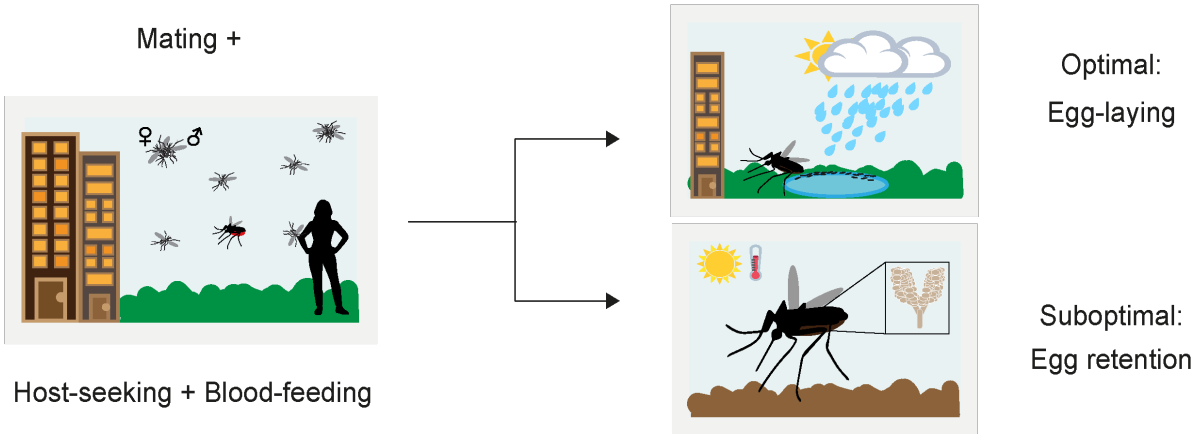

Figure 2.6 Context considerations for egg-laying decisions
Schematic of the reproductive decision point of a female mosquito after egg maturation under optimal and suboptimal egg-laying conditions of freshwater abundance and scarcity, respectively.

How does egg retention during drought affect subsequent egg-laying and egg viability? We measured egg retention in the laboratory by simulating drought-like conditions of varying durations (Figure 2.7A). Females that engorged on a full blood meal laid ~100-110 eggs at the edge of freshwater 4 days after a blood meal, of which ~70% hatched (Figure 2.7B-D). Even though the number of eggs laid decreased with increasing length

of egg retention, the proportion of viable eggs remained consistently high even after extended egg retention to at least 12 days post-blood-meal (Figure 2.7B-D). These results show that wild type *Aedes aegypti* mosquitoes demonstrate reproductive resilience during drought by retaining viable eggs until freshwater becomes available.

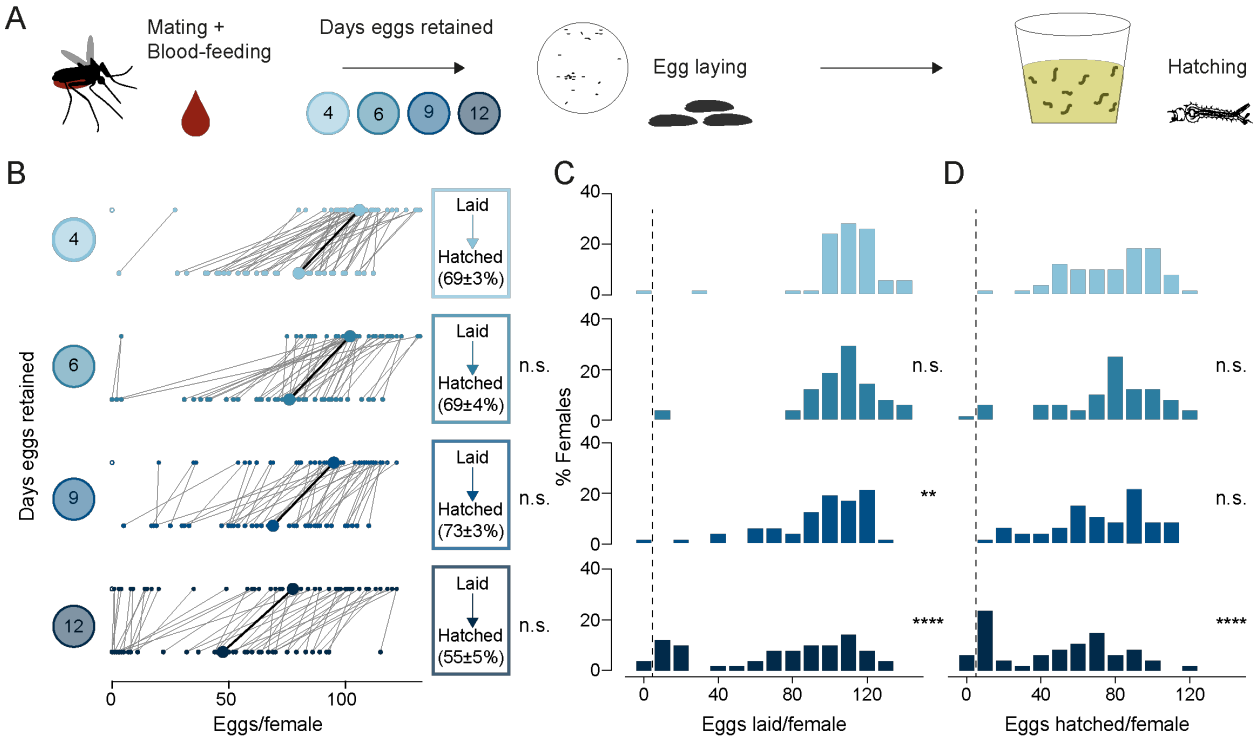

Figure 2.7 *Aedes aegypti* female reproduction is drought-resilient
(**A**) Schematic of experiment to test effect of egg retention on egg-laying and hatching. (**B**) Number of eggs laid by (top) and hatched from (bottom) single females that experienced the indicated egg retention periods. Females laying no eggs are depicted by open circles. Lines connect eggs laid by and hatched from the same individual. Larger circles and bold lines represent medians. Boxes show hatching rate (mean±S.E.M) from each egg retention group. n=46-50 females/group.
(**C, D**) Distribution of eggs laid (C) and eggs hatched (D) after the indicated length of egg retention, analyzed from data in (B). Zero values are binned separately for each group. All other bins are groups of 10 starting with [1-10] and with closed/inclusive intervals. The groups for number of eggs laid (C), number of eggs hatched (D), and % hatched (B, boxes), respectively, at 6-, 9-, and 12-days post-blood-meal are compared to 4 days post-blood-meal to determine significant difference (Kruskal-Wallis, Dunn's multiple comparison test; n.s.: not significant, $p>0.05$; **$p<0.01$; ****$p<0.0001$).

Because precise temporal control of egg-laying without loss of viability is an adaptation that maximizes the reproductive resilience and the fitness of *Aedes aegypti* females, understanding its basis will illustrate how this species is able to invade otherwise inhospitable ecological niches. Despite the importance of this question, little is known about how females retain viable eggs in their ovaries during periods of prolonged drought.

CHAPTER 3. *tweedledee* and *tweedledum* expression is ovary enriched and temporally regulated by egg retention

3.1 *tweedledee* and *tweedledum* are massively upregulated in ovaries with mature eggs

How female *Aedes aegypti* mosquitoes carrying mature eggs in their ovaries maintain the potential for subsequent fertilization, laying, and hatching of their eggs after different lengths of retention remains unexplored. To identify candidate genes regulating the retention of viable eggs in *Aedes aegypti* ovaries post-maturation, we used bulk RNA-sequencing (RNA-seq) to profile ovaries across 11 different time-points in their first cycle of reproduction (Figure 3.1A). Principal component analysis (PCA) of the ovary RNA-seq dataset shows that replicates within each reproductive stage cluster together, and that principal components 1 and 2 (PC1 and PC2) separate the reproductive stages from each other (Figure 3.1B). These data reflect the major transcriptional changes in the ovary across the reproductive cycle and highlight that each stage is distinctly and tightly regulated.

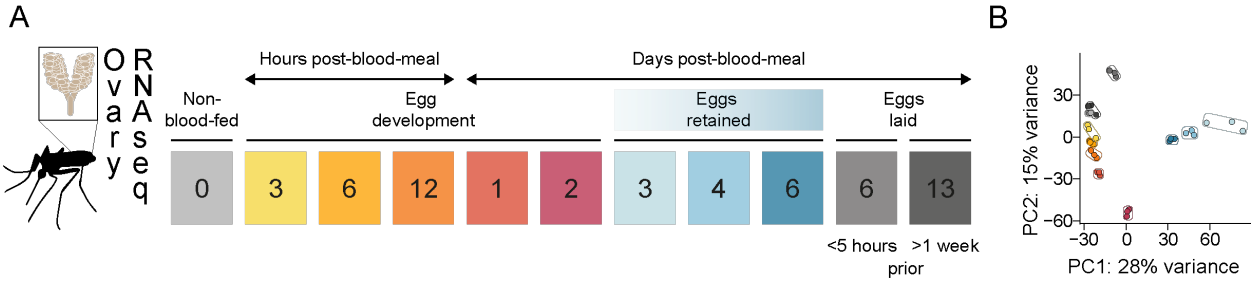

Figure 3.1 Bulk RNA-seq of *Aedes aegypti* ovaries across reproduction
(**A**) Reproductive time-points sampled for bulk ovary RNA-seq, n=3 replicates/group, 11 groups.
(**B**) Principal component analysis (PCA) of DESeq2-normalized, transformed counts from ovary RNA-seq.

Ovaries carrying mature eggs occupy much of the female mosquito's abdomen, requiring redirection of her energy resources towards maintaining her eggs. Therefore, we hypothesized that candidate regulators of viable egg retention would be abundantly expressed across egg retention time-points (Figure 3.2A), with specific upregulation at time-points when eggs are retained compared to pre-blood meal or during egg development (Figure 3.2B). We expected that post-egg-laying, the expression of these genes would eventually decline as the female transitions out of her reproductive state (Figure 3.2B). We also speculated that, given the distinct natural histories and diverse egg-laying strategies across insects (Bentley and Day, 1989; Day, 2016; Wallis, 1954), genes regulating viable egg retention in *Aedes aegypti* may be taxon-restricted within mosquitoes (Figure 3.2C). Filtering based on these steps, and by confirming the presence of candidates in an ovary proteome dataset that we generated (see Figure 3.3C), we identified two genes that satisfy our criteria as candidate regulators of viable egg retention (Figure 3.2D). These previously uncharacterized genes, *LOC5563800* and *LOC5566109*, which we named *tweedledee* and *tweedledum* respectively, show similar and striking patterns of regulation in our transcriptomic dataset (Figure 3.2D). *tweedledee* is expressed in females before a blood meal and during egg development, but its expression increases 3 orders of magnitude during periods of egg retention. The regulation of *tweedledum* is even more remarkable. It is present at less than 1 transcript per million (TPM) at non-blood-fed and egg production stages but rises to 10,000 TPM during egg retention.

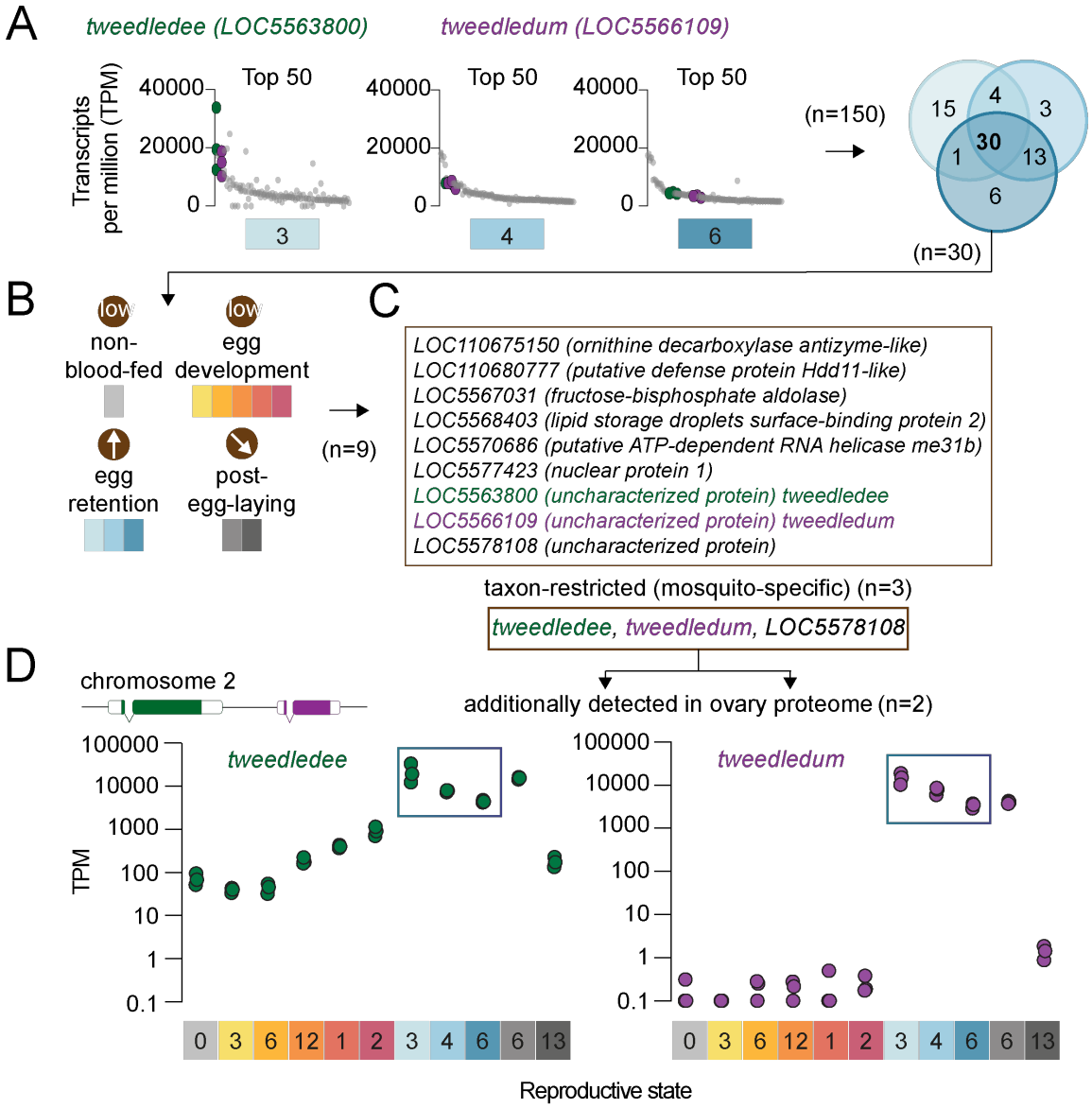

Figure 3.2 Logic to filter candidate regulators of viable egg retention from ovary RNA-seq

(A) Top 50 most abundant transcripts ranked by median transcripts per million (TPM) for egg retention groups, 3-, 4-, and 6-days post-blood-meal (total=150 transcripts). Gray dots represent replicates for each transcript in the top 50, green dots indicate *tweedledee,* and purple dots represent *tweedledum.* Venn diagram of the number of overlapping transcripts between the top 50 genes across egg retention groups, with 30 transcripts shared between all three groups.

(**B**) Logic of expression pattern for selecting candidate genes expected to underlie robust retention of viable eggs.

(**C**) Genes with expression dynamics that follow filtering criteria in B.

(**D**) Transcript expression pattern in the ovaries of *tweedledee* (top) and *tweedledum* (bottom) which were filtered as candidates for further validation. The blue rectangle indicates the period of egg retention.

3.2 *tweedledee* and *tweedledum* expression is adult specific and tissue restricted

Using published transcriptomes of developmental stages (Akbari et al., 2013; Matthews et al., 2018) and multiple adult tissues (Akbari et al., 2013; Matthews et al., 2016) from *Aedes aegypti* mosquitoes, we confirmed that *tweedledee* and *tweedledum* are adult specific (Figure 3.3A, 3.4) and female enriched (Figure 3.3B). They both show ovary-enriched expression with strong upregulation post-egg maturation in the females (Figure 3.3B), with some expression in male reproductive tissues (Figure 3.3A). In addition to specific upregulation during egg retention, *tweedledee* shows basal, constitutive expression across several conditions and tissues, whereas the spatiotemporal expression of *tweedledum* is more tightly restricted (Figures 3.2D, 3.3).

Gene expression in the ovary is uniquely poised to impact gene expression in the embryo; the maternal germline expresses several genes, the products of which are transferred into the oocyte while in the ovary, and still persistent in the earliest stages of embryonic development post-fertilization, during the maternal-zygotic transition (Akbari et al., 2013). Expression of *tweedledee* and *tweedledum* is negligible at 0-1 TPM in embryos, while in ovaries collected in the same experiment at 72 hours post-blood-meal with mature eggs, expression of *tweedledee* and *tweedledum* is ~10,000 TPM (Figure 3.4). We suggest that this expression pattern is most consistent with *tweedledee* and *tweedledum* being ovary somatic tissue-specific genes, many of which are well established as critical components providing the oocyte protection within the ovary (Figure 3.4). Our results in Chapters 3.3 and Chapter 4 further support this hypothesis.

Overall, these data show the exquisite specificity of *tweedledee* and *tweedledum* expression in ovaries bearing mature eggs, strengthening the possibility that the genes are candidate regulators of viable egg retention.

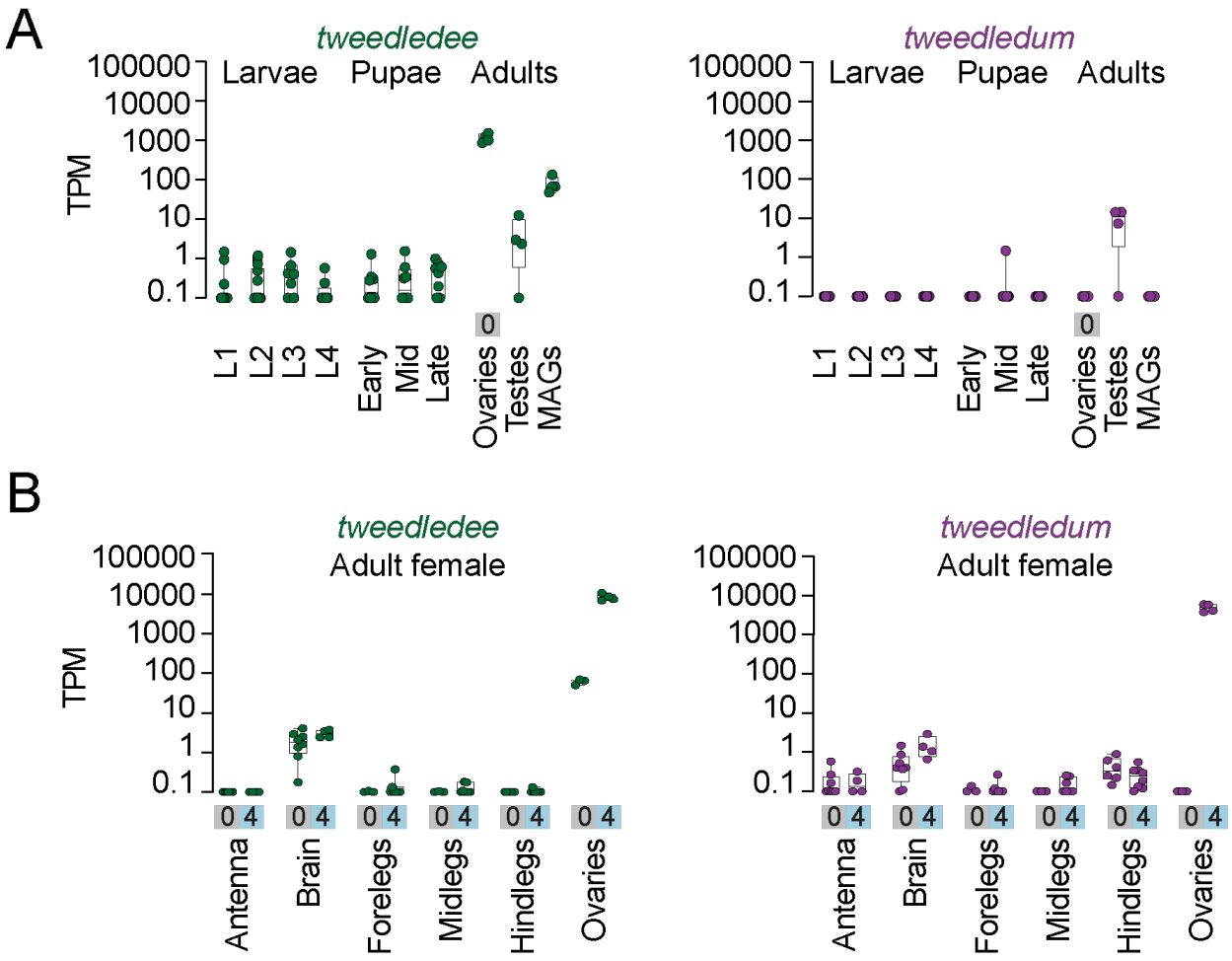

Figure 3.3 Candidate regulators of viable egg retention are adult specific and ovary enriched
(**A**) TPM values for *tweedledee* (left) and *tweedledum* (right) during larval, pupal, and adult stages of development [data from (Matthews et al., 2018)], MAGs = male accessory glands, n=4-13 replicates/group.
(**B**) TPM values for *tweedledee* (left) and *tweedledum* (right) in adult female tissues (data originally from (Matthews et al., 2016), reanalyzed in (Matthews et al., 2018), n=3-8 replicates/group.
Box plots: median, 1st/3rd quartile, minimum to maximum whiskers.

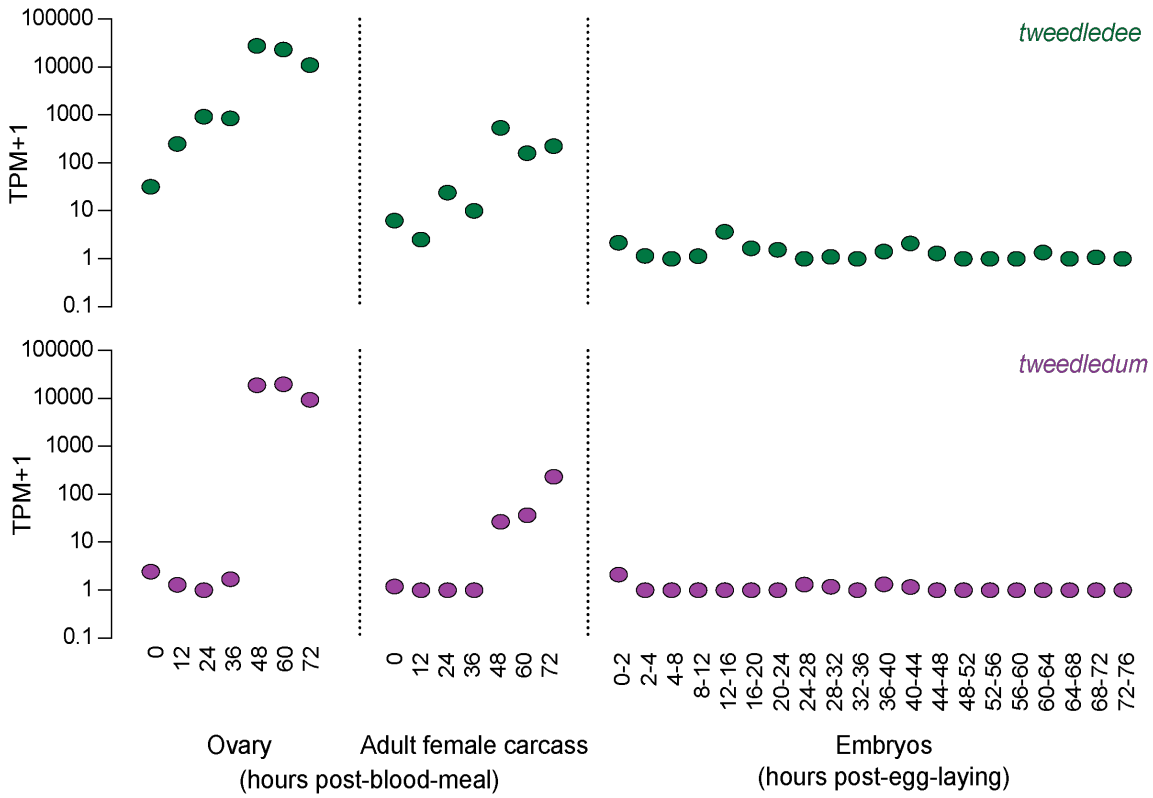

Figure 3.4 Candidate regulators of viable egg retention are expressed at negligible levels in embryos
TPM+1 values for *tweedledee* (top) and *tweedledum* (bottom) in adult female ovaries and adult female carcasses with ovaries removed at time-points post-blood-meal, and in embryos at time-points post-egg-laying. Data originally from(Akbari et al., 2013), reanalyzed in (Matthews et al., 2018).

3.3 tweedledee and tweedledum proteins are upregulated in ovaries with mature eggs

We next performed quantitative proteomics profiling of the female ovaries across a subset of reproductive time points corresponding to non-blood-fed, egg development, egg retention, and post-egg-laying states (Figure 3.5A). PCA shows that replicates within each stage again clustered together as in the RNA-seq dataset, and all reproductive states formed distinct clusters in PC1 and PC2, reflective of the ovaries being tightly and distinctly controlled across these different reproductive states (Figure 3.5B). Both tweedledee and tweedledum protein were notably upregulated at the egg retention phase of the reproductive cycle (Figure 3.5C). Because tweedledee and tweedledum expression levels remain high in the ovaries when sampled <5 hours post-egg-laying when all mature eggs have been laid, we speculate that these genes are expressed in somatic tissues in the ovary (Figure 3.5C).

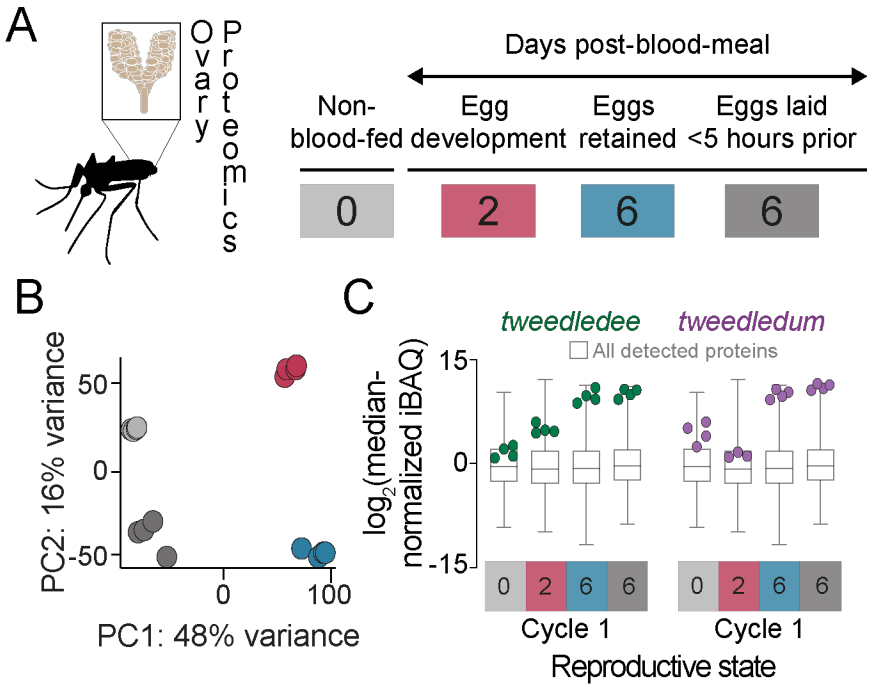

Figure 3.5 tweedledee and tweedledum proteins are upregulated in ovaries with mature eggs
(**A**) Reproductive time-points sampled for ovary proteomics, n=4 replicates/group, 4 groups.
(**B**) PCA of iBAQ values from ovary proteomics.
(**C**) Distribution of iBAQ values as a metric of abundance for all proteins detected per group in ovary proteomics. Overlaid green dots represent individual replicate values for tweedledee and purple dots represent replicates for tweedledum. All values are pre-imputation and represent log_2-transformed median iBAQ signals normalized by subtracting the median iBAQ signal for the group.
Box plots: median, 1st/3rd quartile, minimum to maximum whiskers.

3.4 tweedledee and tweedledum proteins circulate in the hemolymph of females carrying mature eggs

tweedledee and *tweedledum* are predicted to encode proteins with N-terminal signal peptides. To test if they are secreted, we profiled the proteome of the circulating hemolymph, the insect equivalent of blood. We collected hemolymph samples across non-blood-fed, egg development, egg retention, and post-egg-laying states in the first and second cycles of reproduction (Figure 3.6A). The hemolymph is in close apposition to the ovaries, and its contents during distinct reproductive time-points reflect interorgan communication (Anderson and Spielman, 1971; Hansen et al., 2014; Sun et al., 2000). PCA of the hemolymph proteome showed that at 2 days post-blood-meal, the composition of the circulating fluid is most distinct (separated by PC1) from other profiled time-points (Figure 3.6B). These findings are consistent with our expectations, as this is the only time-point profiled during which eggs are likely to still be maturing and during which the hemolymph is therefore transporting components for egg maturation (Hagedorn, 1974; Hagedorn and Fallon, 1973). Notable examples of hemolymph-transported proteins include the vitellogenins (yolk protein precursors), which we detect in our dataset (https://doi.org/10.5281/zenodo.5945525). These proteins are synthesized in the fat body, an analog of the vertebrate liver, and transported via the hemolymph to the ovaries where they are packaged into maturing eggs (Fallon et al., 1974; Hagedorn, 1974). We detected tweedledee and tweedledum proteins in the hemolymph and found that they were both strongly upregulated in each of the reproductive cycles during egg retention and within 5 hours of egg-laying compared to pre-blood-meal, during egg development, or >1-week post-egg-laying (Figure 3.6C).

These data together suggest that somatic ovary cells secrete tweedledee and tweedledum, and that their expression in the ovary and secretion into the circulating hemolymph are both tightly regulated by egg retention state.

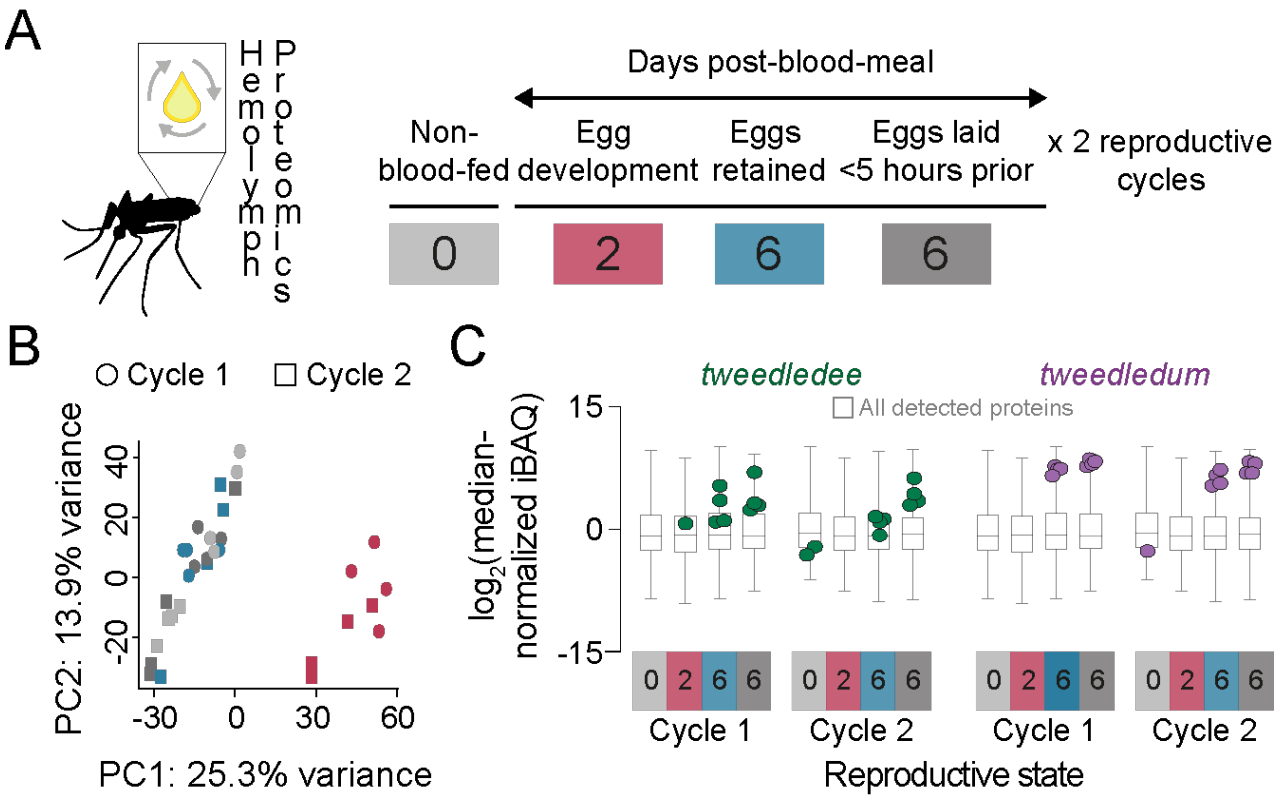

Figure 3.6 tweedledee and tweedledum circulate in the hemolymph during egg retention
(**A**) Reproductive time-points sampled for hemolymph proteomics, n=4 replicates/group, 8 groups.
(**B**) PCA of iBAQ values from hemolymph proteomics.
(**C**) Distribution of iBAQ values as a metric of abundance for all proteins detected per group in hemolymph proteomics. Overlaid green dots represent individual replicate values for tweedledee and purple dots represent replicates for tweedledum. All values are pre-imputation and represent log_2-transformed median iBAQ signals normalized by subtracting the median iBAQ signal for the group.
Box plots: median, 1st/3rd quartile, minimum to maximum whiskers.

CHAPTER 4. *tweedledee* and *tweedledum* are expressed in cells encapsulating mature eggs

Within the ovaries, the development of mature eggs is housed in individual chambers/follicles, encapsulated within a membrane of follicular epithelial cells (Bertram, 1959; Parks and Larsen, 1965) (Figure 4.1A). The follicles undergo massive changes post-blood-meal (Figure 4.1B) and post-egg-laying (Figure 4.1C). Changes occur in both the composition of cell types as well as their spatial distribution within the follicle. At the point of egg-laying, mature eggs transit out of their individual chambers and enter the calyx, a continuous tube through the center of the ovary connected to the oviducts (Bertram, 1959; Curtin and Jones, 1961) . Eggs transit into the oviducts and are fertilized in the reproductive tract by sperm released from sperm storage organs, the spermathecae, before being ejected through the ovipositor (Bertram, 1959; Curtin and Jones, 1961; Degner and Harrington, 2016).

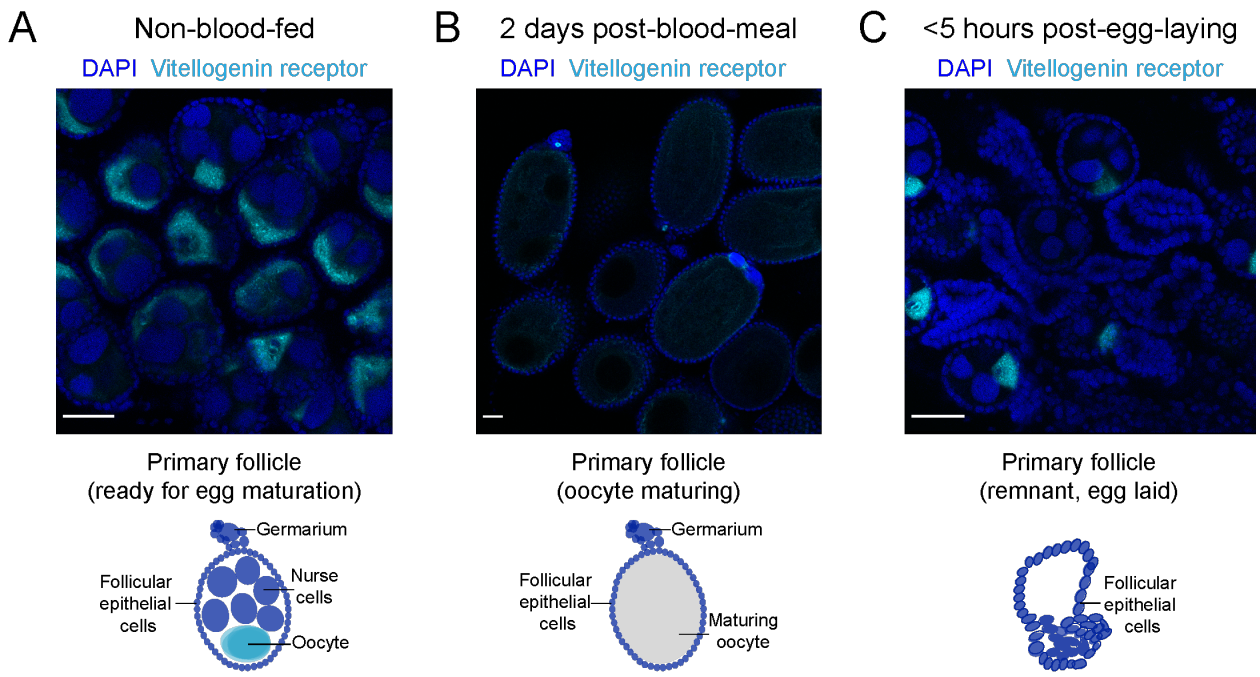

Figure 4.1 Follicles undergo massive changes after blood-feeding and egg-laying
(**A**) Top: Single confocal section of whole-mount fluorescence RNA *in situ* hybridization of a non-blood-fed ovary with the vitellogenin receptor probe in teal and DAPI staining in blue. Bottom: Cartoon cross-section of one primary follicle while in the non-blood-fed state. Secondary follicle not shown.
(**B**) Top: Single confocal section of whole-mount fluorescence RNA *in situ* hybridization of an ovary 2 days post-blood-meal during egg development with the vitellogenin receptor probe in teal and DAPI staining in blue. Bottom: Cartoon cross-section of one primary follicle while egg maturation is in progress. Secondary follicle not shown.
(C) Top: Single confocal section of whole-mount fluorescence RNA in situ hybridization of an ovary 6 days post-blood-meal within 5 hours of egg-laying, with the vitellogenin receptor probe in teal and DAPI staining in blue. Note: both primary follicle remnants and secondary follicles are visible at this time-point, and cartoon only depicts the primary follicle remnant. Bottom: Cartoon cross-section of one primary follicle remnant when eggs have been laid <5 hours prior.
Scale bars: 50 μm.

4.1 *tweedledee,* but not *tweedledum* is expressed in the ovary's calyx cells

Using whole-mount ovary fluorescence RNA *in situ* hybridization we show that *tweedledee,* but not *tweedledum* transcripts are detectable in non-blood-fed ovaries (Figure 4.2). *tweedledee* expression in non-blood-fed ovaries is restricted to calyx cells, and it is markedly absent in the primary follicles (Figure 4.2). The primary follicles are

comprised of seven nurse cells and an oocyte surrounded by somatic follicular epithelial cells (Valzania et al., 2019). Once the female consumes a blood meal, the primary follicle develops into an egg, with the surrounding follicular epithelial cells secreting eggshell proteins and other components onto it (Isoe et al., 2019; Valzania et al., 2019). The oocyte is characteristically marked by *vitellogenin receptor* (*LOC5569465*) expression (Figure 4.1-4.2). The *vitellogenin receptor* gene enables receptor-mediated endocytosis of yolk precursor proteins into the egg after a blood meal (Sappington et al., 1996).

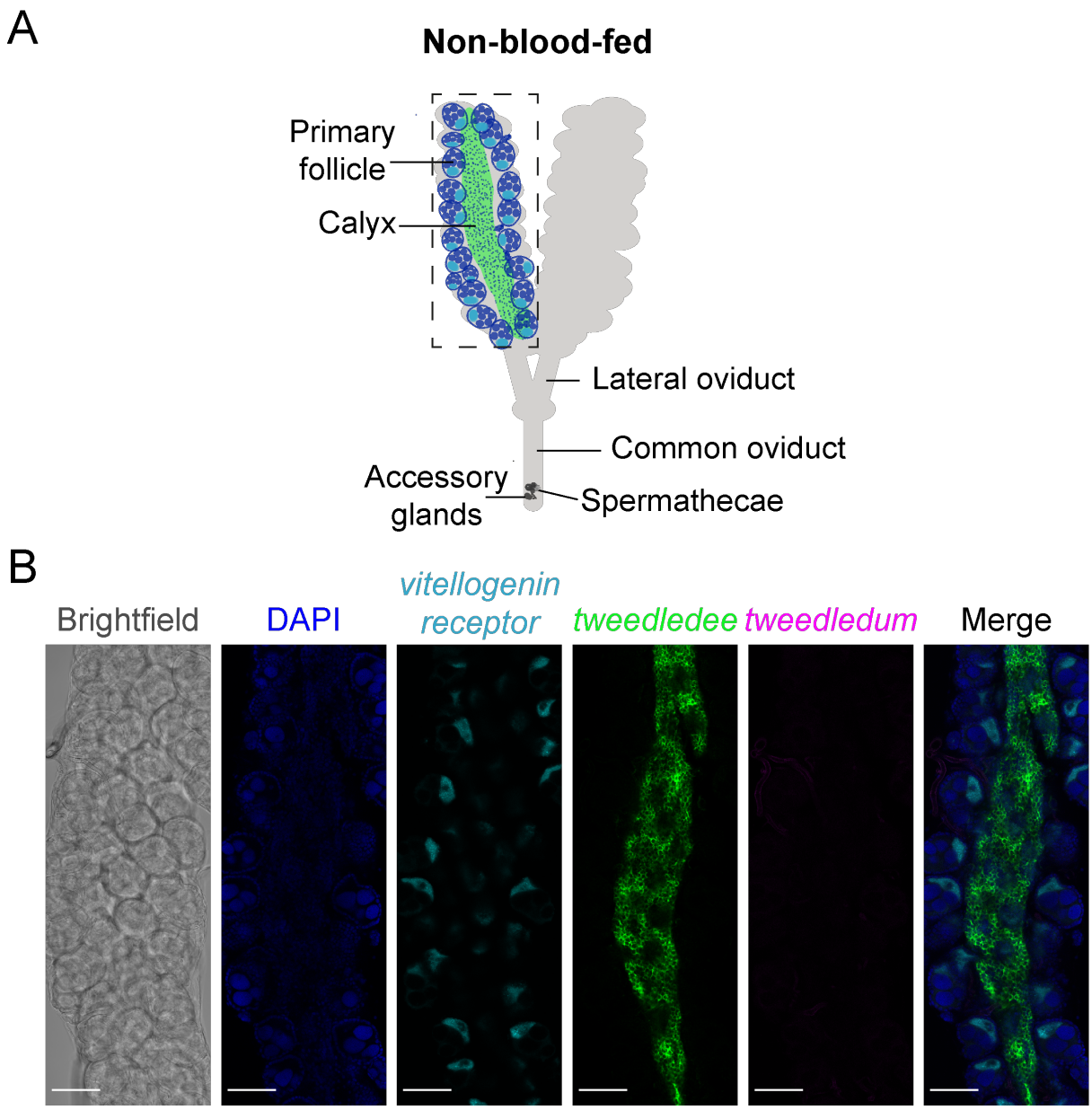

Figure 4.2 *tweedledee* but not *tweedledum* is expressed in the calyx of non-blood-fed ovaries
(**A**) Cartoon of a pair of ovaries and the female reproductive system, with left ovary representing a cross-section of one ovary while in the non-blood-fed state.
(**B**) Single confocal section of whole-mount fluorescence RNA *in situ* hybridization of a non-blood-fed ovary with the indicated probes. Scale bars: 100 μm.

4.2 *tweedledee* and *tweedledum* are expressed in somatic cells that contact eggs

Because of technical limitations of performing RNA *in situ* hybridization on intact ovaries both during egg development and during retention of fully mature eggs due to optical opacity of the ovary and difficulties with probe penetration, we utilized ovaries 6 days post-blood-meal within 5 hours of egg-laying to identify the cells expressing *tweedledee* and *tweedledum* (Figure 4.3). Since ovary RNA-seq data suggest both transcripts are abundantly expressed <5 hours post-egg-laying (Figure 3.2D), we postulated that this time-point would allow us to identify which cells express *tweedledee* and *tweedledum*. Ovaries collected within 5 hours of egg-laying have two different types of egg follicles (Figure 4.3): the remnants of primary follicles which held mature eggs prior to laying and a secondary follicle that was previously attached to the primary follicle, and that is ready to develop into a new egg upon consumption of a second blood meal (Bertram, 1959; Riehle and Brown, 2002; Valzania et al., 2019). *tweedledee* was detected in the calyx through which eggs transit (Figure 4.3B) as well as in the follicular epithelial cells of the primary follicle remnants (Figure 4.3A-D). *tweedledum* was also expressed in the follicular epithelial cells of primary follicle remnants, and solely in these cells together with *tweedledee* (Figure 4.3). Notably, neither of the transcripts were expressed in secondary follicles (Figure 4.3).

Figure 4.3 *tweedledee* and *tweedledum* are expressed in cells encapsulating mature eggs

(**A, B**) Left: Single confocal section of whole-mount fluorescence RNA *in situ* hybridization of an ovary <5 hours post-egg-laying with all eggs laid (A) or with two eggs in transit indicated by white arrows (B) with the indicated probes. Right: cartoons representing cross-section through a post-egg-laying ovary with probe expression patterns depicted in different ovary structures.

(**C, D**) Left: Single confocal section of whole-mount fluorescence RNA *in situ* hybridization of an ovary <5 hours post-egg-laying with the indicated probes showing a secondary follicle ready to develop into an egg upon consumption of a second blood meal (C) and a post-egg-laying follicle that is the remnant of a primary follicle which previously contained an egg (D). Right: cartoons depicting *tweedledee* and *tweedledum* expression pattern uniquely in the primary follicle remnant (D), but not in the secondary follicle expressing vitellogenin receptor (C).

Scale bars: 100 μm in A-B, and 10 μm in C-D.

A Post-egg-laying (<5 hours): all eggs laid

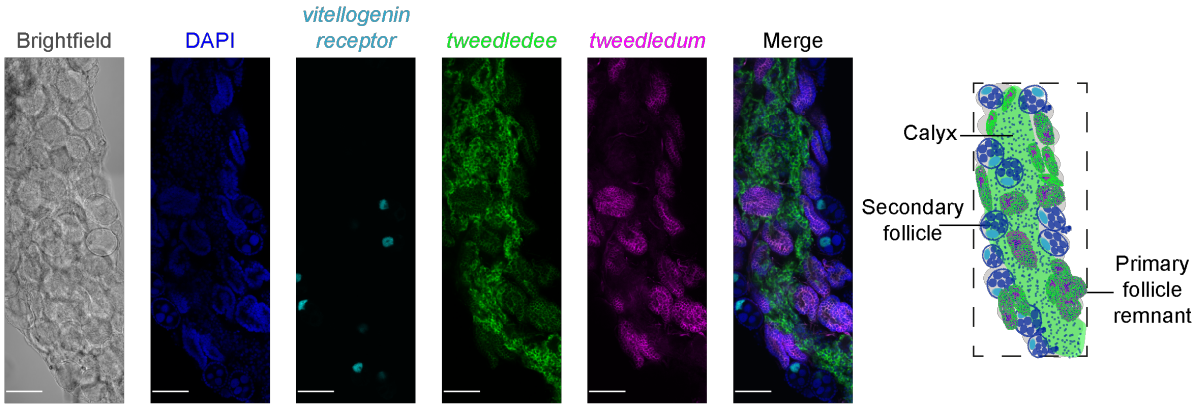

B Post-egg-laying (<5 hours): eggs in transit

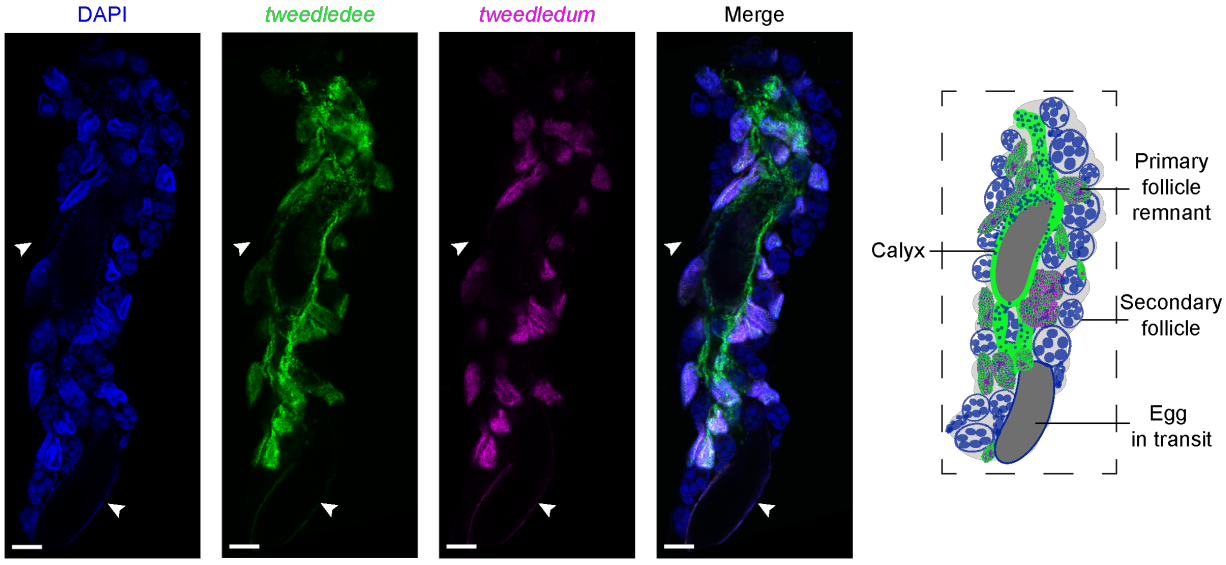

C Post-egg-laying (<5 hours): secondary follicle

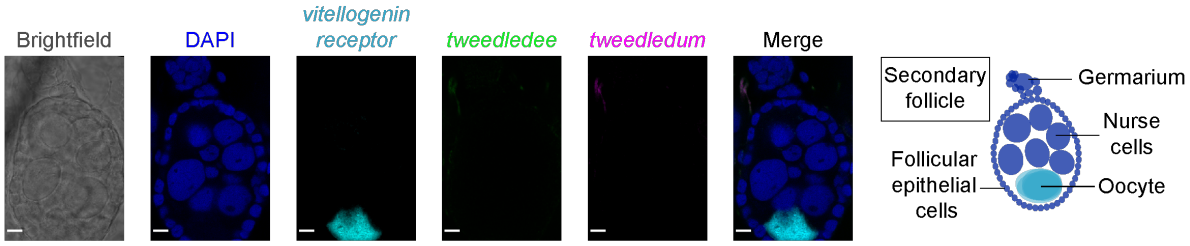

D Post-egg-laying (<5 hours): primary follicle remnant

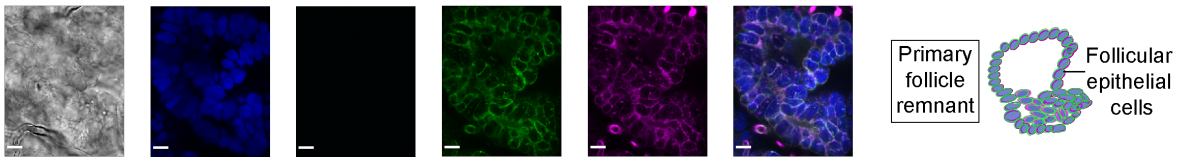

We additionally examined *tweedledee* and *tweedledum* expression >1-week post-egg-laying when the gross morphology of the ovary resets, bearing closer resemblance overall to non-blood-fed ovaries. At this time-point, *tweedledum* expression was again undetectable, and *tweedledee* was exclusively expressed in the calyx (Figure 4.4).

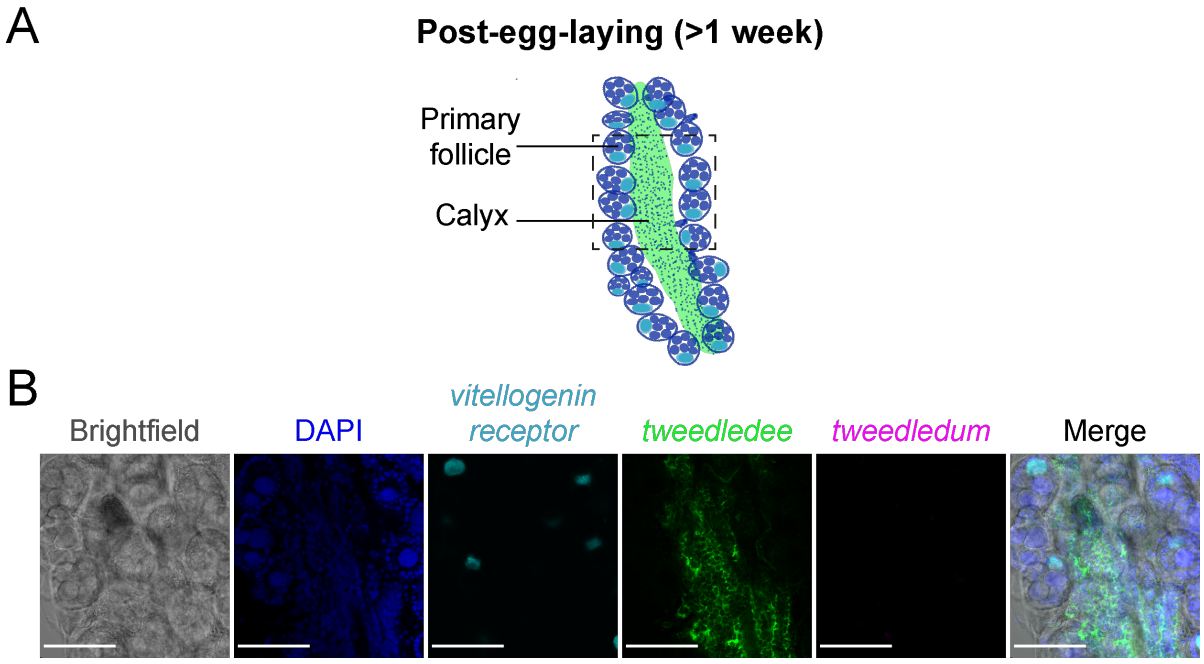

Figure 4.4 Gross ovary morphology and *tweedledee* and *tweedledum* expression reset by a week post-egg-laying
(**A**) Cartoon of a single ovary cross-section post-egg-laying.
(**B**) Single confocal section of whole-mount fluorescence RNA *in situ* hybridization of an ovary >1-week post-egg-laying with the indicated probes. Scale bars: 100 μm.

The patterns of *tweedledee* and *tweedledum* expression detected using RNA *in situ* hybridization in non-blood-fed ovaries (Figure 4.2) and in ovaries <5 hours (Figure 4.3) or >1-week post-egg-laying (Figure 4.4) validate the expression patterns from the respective time-points in the ovary RNA-seq data (Figure 3.2D).

Overall, the robust expression of *tweedledee* and *tweedledum* in the follicular epithelial cells of primary follicle remnants and the added expression of *tweedledee* in the calyx suggests that these genes, either independently or together, are poised to play a role in protecting eggs specifically during egg retention and while they are being laid.

CHAPTER 5. *tweedledee* and *tweedledum* are linked, mosquito-specific, and rapidly evolving

We examined the *Aedes aegypti* genome for clues on the function and evolutionary origin of *tweedledee* and *tweedledum*. The genes are located next to each other on chromosome 2, and both have a short first exon and a longer second exon (Figure 5.1A). These genes are predicted to encode small proteins (tweedledee: 216 amino acids; tweedledum: 116 amino acids), both with N-terminal signal peptides but no other known domains (Figure 5.1B). Although similar in many respects, the two genes and their encoded proteins bear no meaningful sequence similarity to each other; any conserved residues are dispersed across the proteins, leaving open the question of whether tweedledum resulted from a partial duplication of tweedledee (Figure 5.1C).

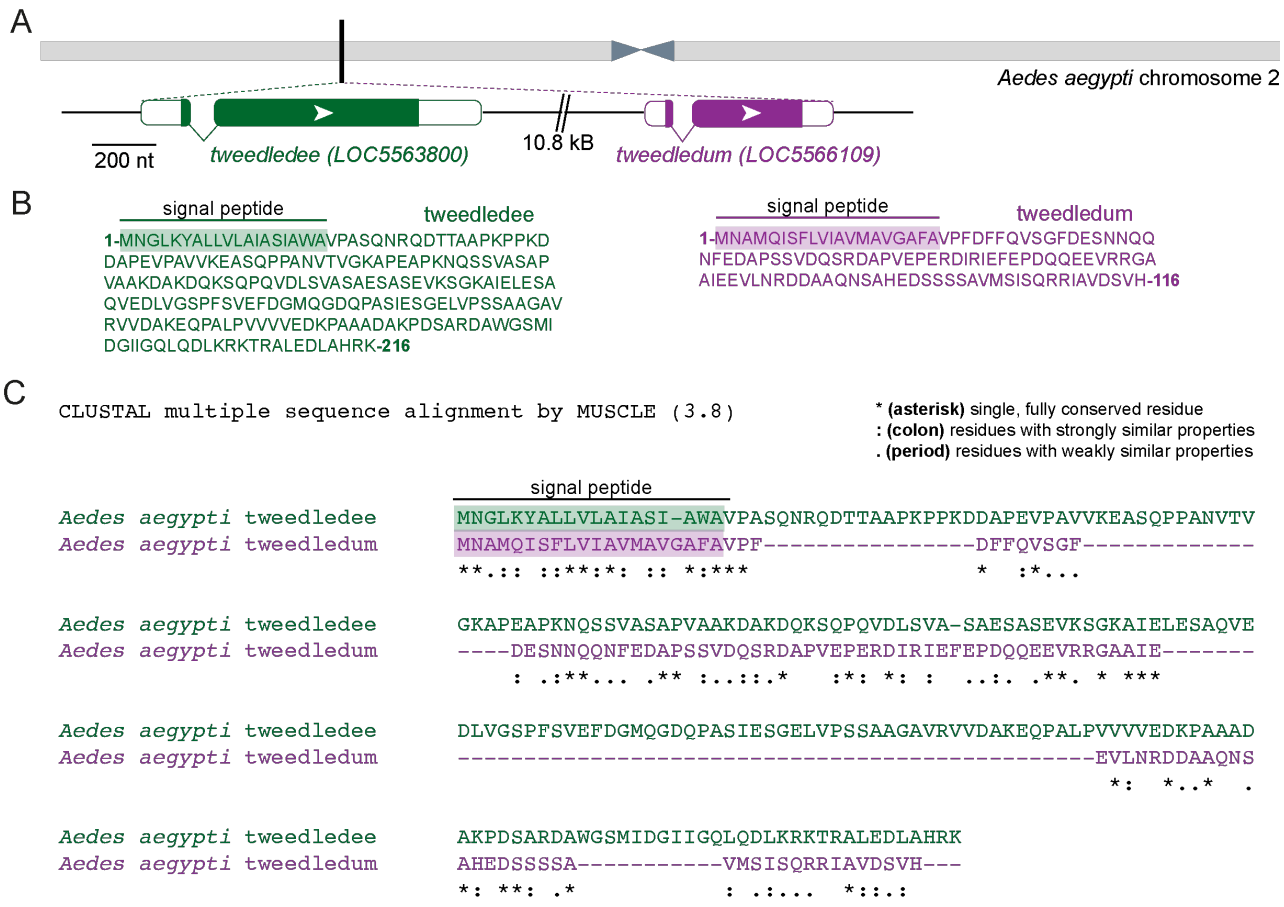

Figure 5.1 *tweedledee* and *tweedledum* are linked, and encode signal peptides
(**A**) Chromosomal location and gene structure of *tweedledee* and *tweedledum*.
(**B**) Amino acid sequences of tweedledee (left) and tweedledum (right) with predicted N-terminal signal peptides indicated.
(**C**) Protein sequence alignment by MUSCLE 3.8 (Madeira et al., 2019) of tweedledee and tweedledum.

5.1 Properties of *tweedledee* and *tweedledum:* GC and amino acid content

We calculated the guanine+cytosine (GC) content for all protein-coding genes in the *Aedes aegypti* genome. This metric is indicative of gene and transcript thermal stability, and thus also an important determinant shaping interactions between a species and its environment (Šmarda et al., 2014). Compared to all protein-coding genes, *tweedledee* (50% GC) and *tweedledum* (48% GC) fall in the 94th and 89th percentile, respectively (Figure 5.2A). Within the distribution of protein-coding genes containing a predicted

signal peptide, the percentiles for *tweedledee* and *tweedledum* remain similar at 95th and 88th, respectively (Figure 5.2A).

We then calculated the proportion of each amino acid residue in tweedledee and tweedledum and compared it to the average proportion of each amino acid residue across all proteins in the *Aedes aegypti* genome that contain a predicted signal peptide (Figure 5.2B). In all cases, we performed comparisons on proteins in their functional secreted form, with signal peptides cleaved *in silico*. Both tweedledee and tweedledum share compositional biases with each other relative to other secreted proteins encoded by the *Aedes aegypti* genome. They both show an underrepresentation of leucine, threonine, and glycine, an overrepresentation of aspartate, glutamate, alanine, valine, and serine, and entirely lack cysteine, tyrosine, and tryptophan (Figure 5.2B).

Notably, compared to the average proportion across all proteins predicted to encode signal peptides in the *Aedes aegypti* genome, tweedledee has an above-average proportion of prolines, while the proline content of tweedledum is average. This is consistent with our observation that tweedledee and tweedledum are on the high 'tail' of the GC-content distribution in the *Aedes aegypti* genome, as proline residues are encoded by nucleotide sequences that are GC-rich (CCT, CCC, CCA, CCG). What consequences might high GC and proline content have for the protein? High GC-content promotes intrinsic protein disorder, as GC-rich codons encode disordered amino acids like proline (Heames et al., 2020). Young and *de novo* genes in several species including *Drosophila melanogaster* are also more likely to encode proteins with

elevated disorder compared to conserved proteins (Heames et al., 2020). Taken together, these observations suggest that tweedledee and tweedledum proteins may have a high degree of intrinsic disorder.

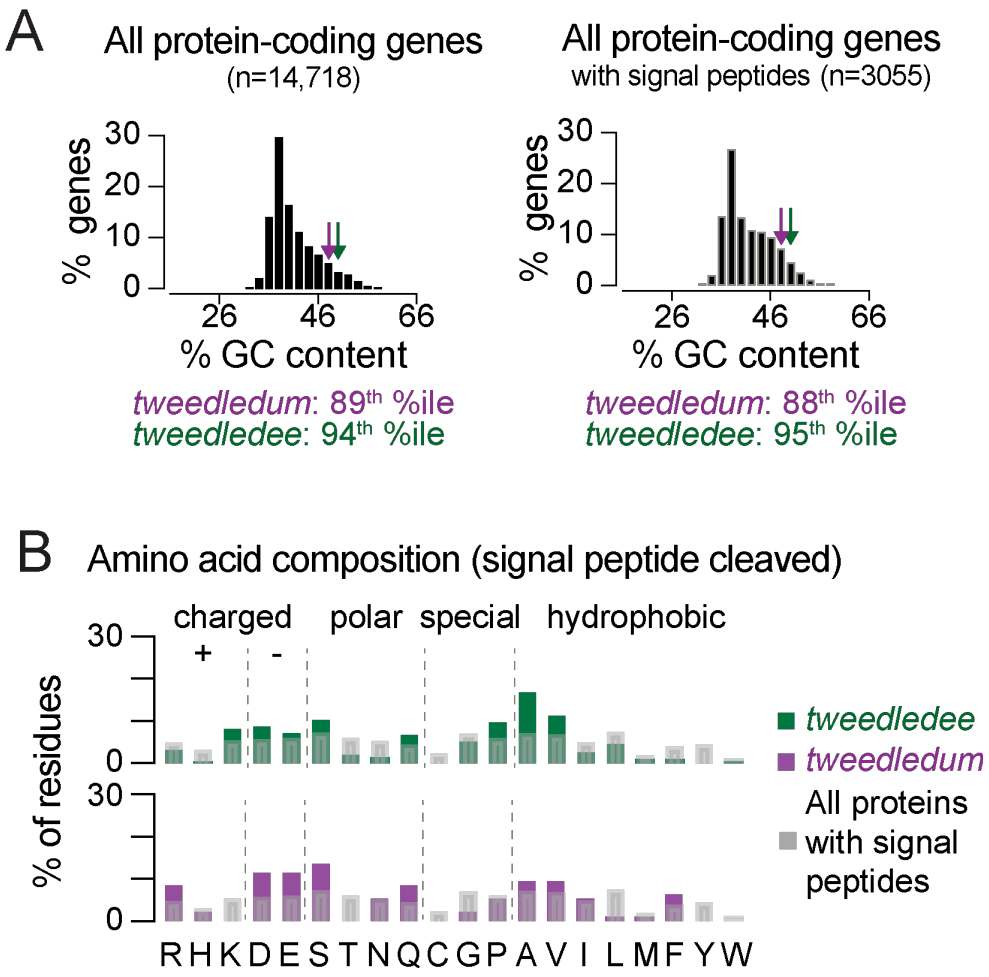

Figure 5.2 *tweedledee* and *tweedledum* share similar properties
(**A**) GC content of all protein-coding genes in the *Aedes aegypti* (AaegL5) genome (left) and of all protein-coding genes with predicted signal peptides (right), with *tweedledee* and *tweedledum* indicated by arrows.
(**B**) Amino acid composition of *Aedes aegypti* tweedledee and tweedledum, as compared to mean percent residue for all proteins with predicted signal peptides in the *Aedes aegypti* genome (AaegL5), calculated after signal peptide cleavage.

5.2 Evolutionary origins of *tweedledee* and *tweedledum*

To explore the evolutionary history and origin of these genes, we searched for putative homologs. Using BLASTp, the only orthologs identifiable in Genbank for both tweedledee and tweedledum with E-values < 0.05 are in *Aedes albopictus,* another invasive mosquito vector ~70 million years diverged from *Aedes aegypti* (Chen et al., 2015). In both *Aedes aegypti* and *Aedes albopictus, tweedledee* and *tweedledum* or their respective orthologs are flanked by two conserved genes, *peritrophin-like* and *scratch* (annotated as *escargot* in *Aedes aegypti,* see Methods) (Figure 5.3A). Using *peritrophin-like* and *scratch* as "anchor" genes, we searched for other syntenic loci potentially containing *tweedledee* or *tweedledum* homologs in other mosquito species (Figure 5.3A). We found syntenic loci in several other mosquitoes, but not in any non-mosquito species, including *Drosophila melanogaster* flies. The *Drosophila melanogaster scratch* gene is located on chromosome 3L and is not near any *peritrophin-like* genes. There are several genes adjacent to *Drosophila melanogaster scratch*, but none have the gene or protein structure of *tweedledee* and *tweedledum*. In *Culex quinquefasciatus, Anopheles gambiae,* and several other *Anopheles* mosquito species both within and outside of the *Anopheles gambiae* complex, there are syntenic loci with conserved *peritrophin-like* and *scratch* genes (Figure 5.3A). In these *Culex* and *Anopheles* cases, the conserved genes flank a single uncharacterized gene (Figure 5.3A). We termed these single uncharacterized genes in non-*Aedes* mosquitoes "*conceptualogs*," since they bear no sequence homology to *tweedledee* or *tweedledum* in *Aedes,* but they are like *tweedledee* and *tweedledum* in many other aspects. First, they are all two exons long, with a short first exon and a longer second exon (Figure

5.3C). Second, they are predicted to encode proteins of similar length ranging between 190 and 269 amino acids (Figure 5.3A-B), and third, they are predicted to contain N-terminal signal peptides (Figure 5.3C). Ordered by the topology of the mosquito phylogenetic tree, the protein sequences of tweedledee and tweedledum in *Aedes* or of the conceptualogs in *Anopheles* diverge more rapidly than the protein sequences of their flanking anchor genes within their respective genera (Figure 5.3A). In comparing the amino acid content of all conceptualogs (with signal peptides cleaved) to each other and to the *Aedes* tweedledee and tweedledum, we observed several similarities despite the rapid protein sequence divergence: all genes have no or very few cysteine or tryptophan residues, and an overrepresentation of glutamate and alanine (Figure 5.3B). Exonic sequences of *tweedledee*, *tweedledum*, and the *conceptualogs* in *Culex* and *Anopheles* also show strong similarities in the relative locations of their signal peptides and disordered domains as predicted by SignalP and IUPred2A, respectively (Figure 5.3C). All genes in the *tweedleedee/tweedledum* or *conceptualog* locus referenced here are listed in Table 1.

To assess whether the molecular evolution of *Aedes aegypti tweedledee* and *tweedledum* relative to the outgroup, *Aedes albopictus*, and of the *Anopheles gambiae conceptualog* relative to the outgroup, *Anopheles stephensi*, is adaptive, we computed the ratio of non-synonymous (dN, amino acid-altering) to synonymous (dS, silent) mutations at each site (Yang and Bielawski, 2000). By calculating the distribution of dN/dS values for all protein-coding genes with unique outgroup orthologs in the *Aedes aegypti* and *Anopheles gambiae* genomes, we found that *tweedledee*, *tweedledum*, and the *conceptualog* are in the 98^{th,} 92nd, and 99th percentile, respectively (Figure 5.3D).

This suggests that compared to most protein-coding genes in mosquitoes, amino acid-altering mutations are more likely to reach fixation for *tweedledee*, *tweedledum*, and the *Anopheles conceptualog*. A sliding-window analysis of dN/dS values across the coding sequences of *Aedes aegypti tweedledee* and *tweedledum* revealed that these high gene-wide dN/dS values are likely driven by rapid sequence divergence in specific regions around the middle of the gene (Figure 5.3E). These analyses together suggest that *tweedledee, tweedledum*, and the *conceptualogs* likely shared a common ancestor, and that the genes are evolving rapidly under strong selective pressure across the mosquito phylogeny.

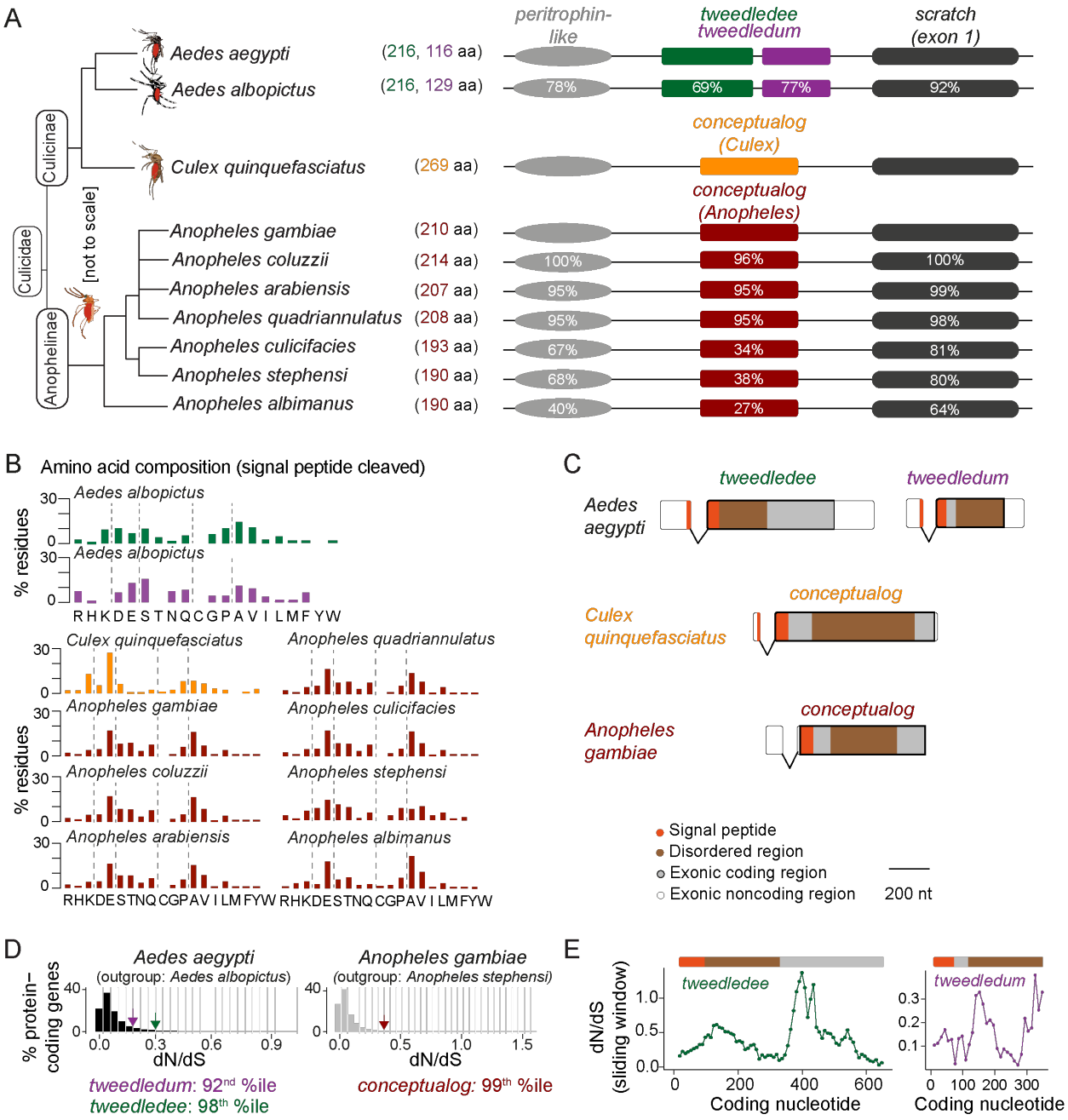

Figure 5.3 *tweedledee*, *tweedledum*, and *conceptualogs* are rapidly evolving under positive selection across the mosquito phylogeny

(**A**) Syntenic loci in *Aedes*, *Culex*, and *Anopheles* mosquito species are shown (not to scale), ordered by the topology of the mosquito phylogenetic tree. The protein length of tweedledee, tweedledum, or the conceptualog is shown in parentheses next to the species name. Protein sequence identity is shown for each gene as calculated using a reference species for each genus, either *Aedes aegypti* or *Anopheles gambiae*. For *scratch,* protein sequence identity was calculated by aligning exon 1 of each species due to a fragmented annotation in multiple reference genomes (see Methods). Accession numbers for all genes are at https://doi.org/10.5281/zenodo.5945525.

(**B**) Amino acid composition of tweedledee and tweedledum in *Aedes albopictus* and of the conceptualogs in *Culex* and *Anopheles* species.
(**C**) Gene structures of *Aedes aegypti tweedledee* and *tweedledum* and the *conceptualog* in *Culex quinquefasciatus* and *Anopheles gambiae* are shown to scale with signal peptide and disordered domains annotated. The 3'UTR of *Anopheles gambiae conceptualog* is lacking in the current genome annotation.
(**D**) The distribution of dN/dS values for 8,030 protein-coding genes in *Aedes aegypti* and 9,958 protein-coding genes in *Anopheles gambiae*. *tweedledee*, *tweedledum* and the *conceptualog* are shown with arrows.
(**E**) dN/dS values were calculated for a 102-nucleotide sliding window size of 34 nucleotides each with a 3 amino acid overlap across the coding sequence of *Aedes aegypti tweedledee* and *tweedledum*. Coding sequences were aligned to orthologs in *Aedes albopictus*.

Table 1. List of genes in the syntenic *tweedledee, tweedledum* locus across mosquito species

	Species	Assembly Version	RefSeq Gene ID	GenBank Gene ID	Gene Name	Additional Notes
tweedledee, tweedledum, conceptualogs	*Aedes aegypti*	GCF_002204515.2	5563800	AAEL005212	*tweedledee*	Gene name newly assigned; previously known as uncharacterized protein LOC5563800
	Aedes aegypti	GCF_002204515.2	5566109	AAEL005192	*tweedledum*	Gene name newly assigned; previously known as uncharacterized protein LOC5566109
	Aedes albopictus	GCF_006496715.1	109405118 109408065 115270160	-		ortholog to *tweedledee* Note: three putative orthologs exist in the genome
	Aedes albopictus	GCF_006496715.1	109408096 115269714 115269715	-		ortholog to *tweedledum* Note: three putative orthologs exist in the genome
	Culex quinquefasciatus	GCF_015732765.1	119770141	-		conceptualog
	Anopheles gambiae	GCF_000005575.2	1270273	AGAP006792		conceptualog
	Anopheles coluzzii	GCF_016920705.1	120949978	-		conceptualog
	Anopheles arabiensis	GCF_016920715.1	120893416	-		conceptualog
	Anopheles quadriannulatus	GCA_000349065.1	-	AQUA017315		conceptualog
	Anopheles culicifacies	GCA_000473375.1	-	ACUA016129		conceptualog
	Anopheles stephensi	GCF_013141755.1	118509842	-		conceptualog
	Anopheles albimanus	GCF_013758885.1		118465173		conceptualog
scratch	*Aedes aegypti*	GCF_002204515.2	Exon 1: 110675127	-	*scratch*	Exons are annotated as multiple genes. Exon 1 was used for multiple sequence alignment

	Species	Assembly Version	RefSeq Gene ID	GenBank Gene ID	Gene Name	Additional Notes
			Exon 2: 5566146			
	Aedes albopictus	GCF_006496715.1	109405162 109408066	-	*scratch*	Note: two putative orthologs exist in the genome; 109405162 was used for analyses
	Culex quinquefasciatus	GCF_015732765.1	6051351	-	*scratch*	
	Anopheles gambiae	GCF_000005575.2	1270274	AGAP006791	*scratch*	
	Anopheles coluzzii	GCF_016920705.1	120949053	-	*scratch*	
	Anopheles arabiensis	GCF_016920715.1	-	Exon 1: AARA009125 Exon 2: AARA009124	*scratch*	Exons are annotated as multiple genes. Exon 1 was used for multiple sequence alignment
	Anopheles quadriannulatus	GCA_000349065.1	-	Exon 1: AQUA003880 Exon 2: AQUA003879	*scratch*	Exons are annotated as multiple genes. Exon 1 was used for multiple sequence alignment
	Anopheles culicifacies	GCA_000473375.1	-	Exon 1: ACUA001197 Exon 2: ACUA022497	*scratch*	Exons are annotated as multiple genes. Exon 1 was used for multiple sequence alignment
	Anopheles stephensi	GCF_013141755.1	118510563	-	*scratch*	
	Anopheles albimanus	GCF_013758885.1	118462524	-	*scratch*	
peritrophin-like	*Aedes aegypti*	GCF_002204515.2	110675944	-	*peritrophin-like*	

	Species	Assembly Version	RefSeq Gene ID	GenBank Gene ID	Gene Name	Additional Notes
	Aedes albopictus	GCF_006496715.1	109408095 115269716	-	*peritrophin-like*	Note: two putative orthologs exist in the genome; 109408095 was used for analyses
	Culex quinquefasciatus	GCF_015732765.1	119770697	-	*peritrophin-like*	
	Anopheles gambiae	GCF_000005575.2	1270272	AGAP006793	*peritrophin-like*	
	Anopheles coluzzii	GCF_016920705.1	120949175	-	*peritrophin-like*	
	Anopheles arabiensis	GCF_016920715.1	-	AARA009126	*peritrophin-like*	
	Anopheles quadriannulatus	GCA_000349065.1	-	AQUA003881	*peritrophin-like*	
	Anopheles culicifacies	GCA_000473375.1	-	ACUA015145	*peritrophin-like*	
	Anopheles stephensi	GCF_013141755.1	118509254	-	*peritrophin-like*	
	Anopheles albimanus	GCF_013758885.1	118465172	-	*peritrophin-like*	

5.3 *In silico* predictions of three-dimensional structure are low confidence for tweedledee, tweedledum, and conceptualogs

The respective tweedledee proteins in *Aedes aegypti* and *Aedes albopictus* are orthologous, as are the respective tweedledum proteins in these *Aedes* species. However, neither of the *Aedes aegypti* proteins bear meaningful sequence homology with the *Culex quinquefasciatus* or *Anopheles gambiae* conceptualogs (Figure 5.4). For further insight into function of these proteins, we turned to *in silico* structure prediction using AlphaFold2 in collaboration with Dr. Junhui Peng in Dr. Li Zhao's laboratory at The Rockefeller University (Figure 5.5). AlphaFold2 yielded low-confidence predictions for tweedledee, tweedledum, their orthologs in *Aedes albopictus,* and their conceptualogs in *Culex quinquefasciatus* and *Anopheles gambiae* (Figure 5.5A). The predicted structures for the respective proteins between the *Aedes* species all had some commonalities: they each had flexible helices, with disordered regions (Figure 5.5A). The conceptualogs in *Culex quinquefasciatus* and *Anopheles gambiae* also contained flexible helices with disordered regions (Figure 5.5A). However, when comparing *Aedes* tweedledee with the conceptualogs of *Culex quinquefasciatus* and *Anopheles gambiae,* we found that the location of the helices varies across genera, and do not share meaningful sequence similarity (Figure 5.5B). These results are not surprising, given that AlphaFold2 performs best with larger proteins and the availability of homologs in other species that can be used to generate multiple sequence alignments (Jumper et al., 2021; Tunyasuvunakool et al., 2021).

Figure 5.4 Multiple sequence alignment of tweedledee, tweedledum, and conceptualogs across mosquito phylogeny

Protein sequence alignment by MUSCLE 3.8 (Madeira et al., 2019) of tweedledee, tweedledum, and the conceptualogs in *Aedes, Culex, and Anopheles* species.

A

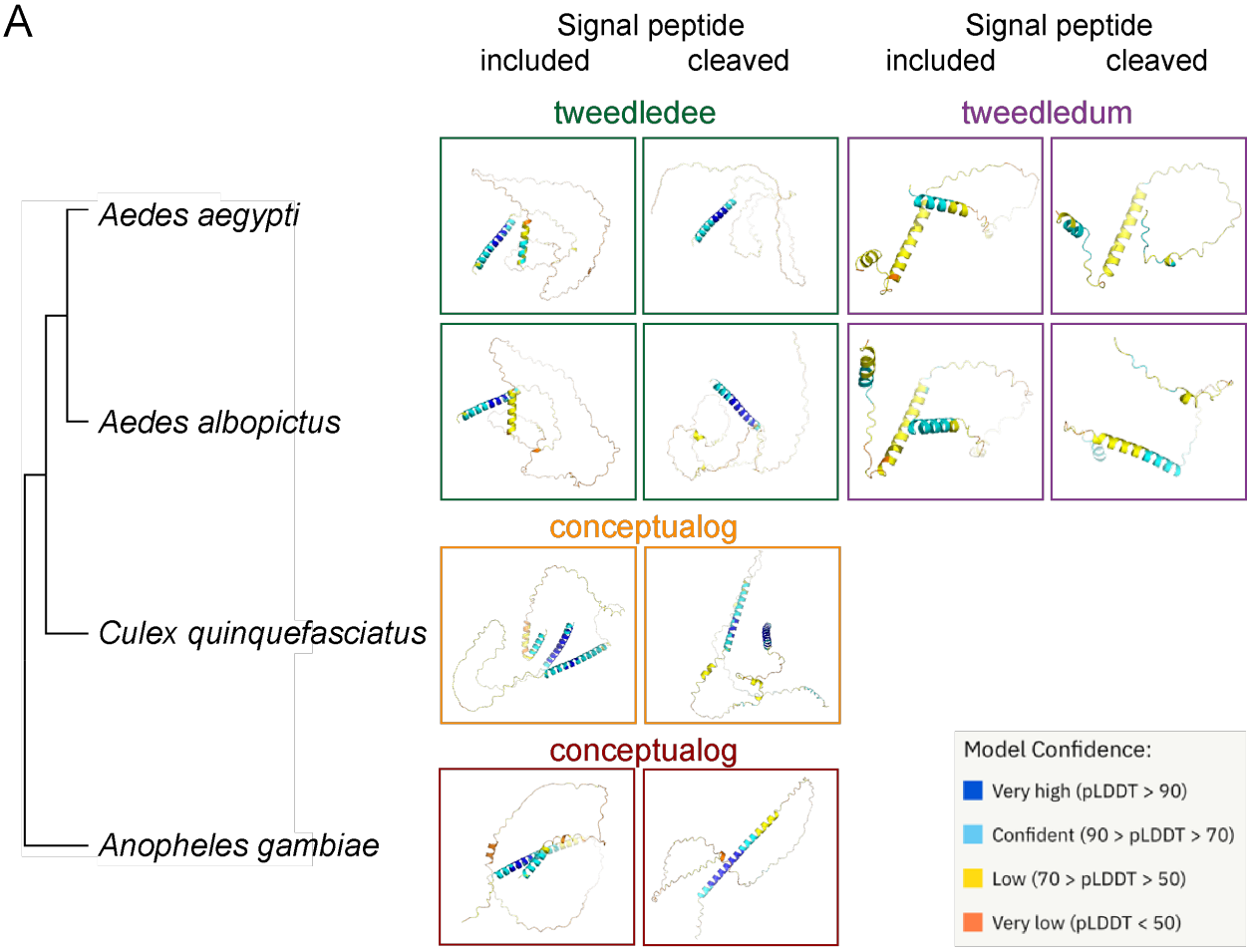

B

```
CLUSTAL multiple sequence alignment by MUSCLE (3.8)
Alpha helix

Anopheles gambiae (conceptualog)      EDAQSYATPAETVQETQHPETDHMEKKNESVSESQLNDEQNAESFLNLLSG
Culex quinquefasciatus (conceptualog) --GKAEQVPKAAPAPKPACGNDKELRQRV-------------EAIIAEL--
Aedes aegypti (tweedledee)            -----PALPVVVVEDKPAAADAKPDSARDAW-----------GSMID----
Aedes albopictus (tweedledee)         -------LPVVVVDDKQASSGAKADSGRDAW-----------GSLIDGIIG
                                             *  .   .      :    .               :::
```

*** (asterisk)** single, fully conserved residue
: (colon) residues with strongly similar properties
. (period) residues with weakly similar properties

Figure 5.5 AlphaFold2 predictions for tweedledee, tweedledum, and conceptualogs

(**A**) Protein structure predictions by AlphaFold2 (Jumper et al., 2021) of tweedledee and tweedledum in *Aedes aegypti* and *Aedes albopictus,* and of the conceptualogs in *Culex quinquefasciatus* and *Anopheles gambiae.*

(**B**) Protein sequence alignment by MUSCLE 3.8 (Madeira et al., 2019) of the respective flexible helices predicted by AlphaFold2 in *Aedes aegypti* tweedledee, *Aedes albopictus* tweedledee, and *Culex quinquefasciatus* and *Anopheles* gambiae conceptualogs.

Our evolutionary and *in silico* structural analyses of *tweedledee* and *tweedledum* make them curiouser and curiouser. As small genes that are rapidly evolving under positive selection only within *Aedes* mosquitoes, could they be playing a functional role that is specific to *Aedes aegypti*? Are the *conceptualogs* in other mosquito species functionally similar to *Aedes tweedledee* and *tweedledum*? Our analyses suggest this possibility, while also highlighting that rapid evolution of *tweedledee, tweedledum, and the conceptualogs* across divergent mosquito species likely reflects distinct selective pressures present in the variety of ecological niches occupied by *Aedes, Culex,* and *Anopheles* mosquitoes.

CHAPTER 6. *tweedledee* and *tweedledum* are required for viable egg retention

6.1 CRISPR-Cas9 mutagenesis to generate *tweedledee* and *tweedledum* double mutants

Under fluctuating climate conditions of intermittent precipitation, retaining viable eggs for extended durations is likely to be an adaptive reproductive strategy for *Aedes aegypti* females. To test whether *tweedledee* and *tweedledum* are required under drought-like conditions for females to retain viable eggs for extended periods after blood feeding, we used CRISPR-Cas9 to generate a large deletion at the *tweedledee* and *tweedledum* locus, here referred to as *Δdeedum* double mutants (Figure 6.1). The 11.7 kb deletion starts within *tweedledee* exon 2 and ends in exon 2 of *tweedledum* (Figure 6.1A). The gene fusion resulting from the large deletion and several additional indels is predicted, *in silico,* to encode a protein with amino acids 1-53 of tweedledee conserved before the breakpoint junction, following which a frameshift is introduced that leads to fusion with 68 missense amino acids before a stop codon (Figure 6.1A). This deletion event in *Δdeedum* is predicted to produce null mutations in both *tweedledee* and *tweedledum*.

To unambiguously identify and routinely genotype the mutants, we developed a strategy using polymerase chain reaction (PCR) with three pairs of primers. This strategy, using primer combinations flanking each of the genes individually, as well as the entire *tweedledee* and *tweedledum* locus, allowed us to distinguish between wild type, +/*Δdeedum,* and *Δdeedum/Δdeedum* animals (Figure 6.1B). Primer and sgRNA sequences used are available at https://doi.org/10.5281/zenodo.5945525.

A

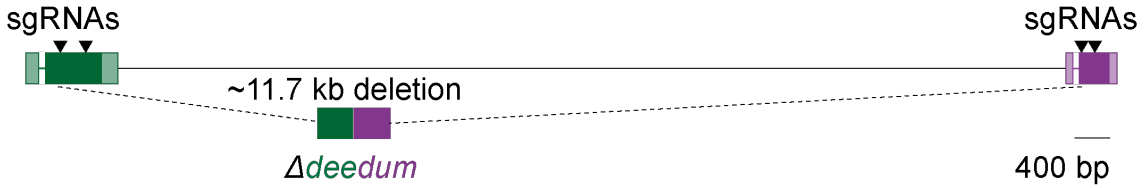

B

PCR primer combinations		PCR product size with indicated DNA template genotype		
		+/+	+/*deedum*	*deedum*/*deedum*
tweedledee-F	*tweedledee-R*	1143 bp	1143 bp	No product
tweedledum-F	*tweedledum-R*	751 bp	751 bp	No product
tweedledee-F	*tweedledum-R*	Too large to amplify	867 bp	867 bp

Figure 6.1 CRISPR-Cas9 mutagenesis/genotyping strategy for *Δdeedum* mutants
(**A**) Schematic of *Δdeedum* mutant that deletes both *tweedledee* and *tweedledum*.
(**B**) Genotyping strategy for *Δdeedum* double mutants.
sgRNA and primer sequences are at https://doi.org/10.5281/zenodo.5945525.

6.2 *Δdeedum* mutants host-seek and blood-feed at comparable rates to wild type

To characterize the reproductive behaviors of *Δdeedum* double mutant females compared to wild type females, we mated them to sibling males of their respective genotypes. To assess the general health of females, we tested their level of attraction to human hosts (Figure 6.2A) and their blood meal consumption (Figure 6.2B). Like wild type females, *Δdeedum* double mutant females were strongly attracted to a live human arm in a single stimulus olfactometer assay (Figure 6.2A). They approximately doubled their body weight from engorging on a blood meal (Figure 6.2B), and when presented with the same live arm stimulus 6 days following the blood meal while retaining eggs, they showed a suppressed host-seeking drive like wild type females (Figure 6.2A). Both wild type and *Δdeedum* females restored attraction to human hosts by 6 days after the blood meal if they had been provided freshwater to lay eggs 3-5 days after the blood meal (Figure 6.2A). Together, these host-seeking and blood-feeding results suggest that *Δdeedum* mutants are healthy, and that loss of *tweedledee* and *tweedledum* together does not affect attraction to human hosts, modulation of attraction following a blood meal and following egg-laying, or the ability to engorge on a full blood meal – all crucial behavioral checkpoints for reproductive success.

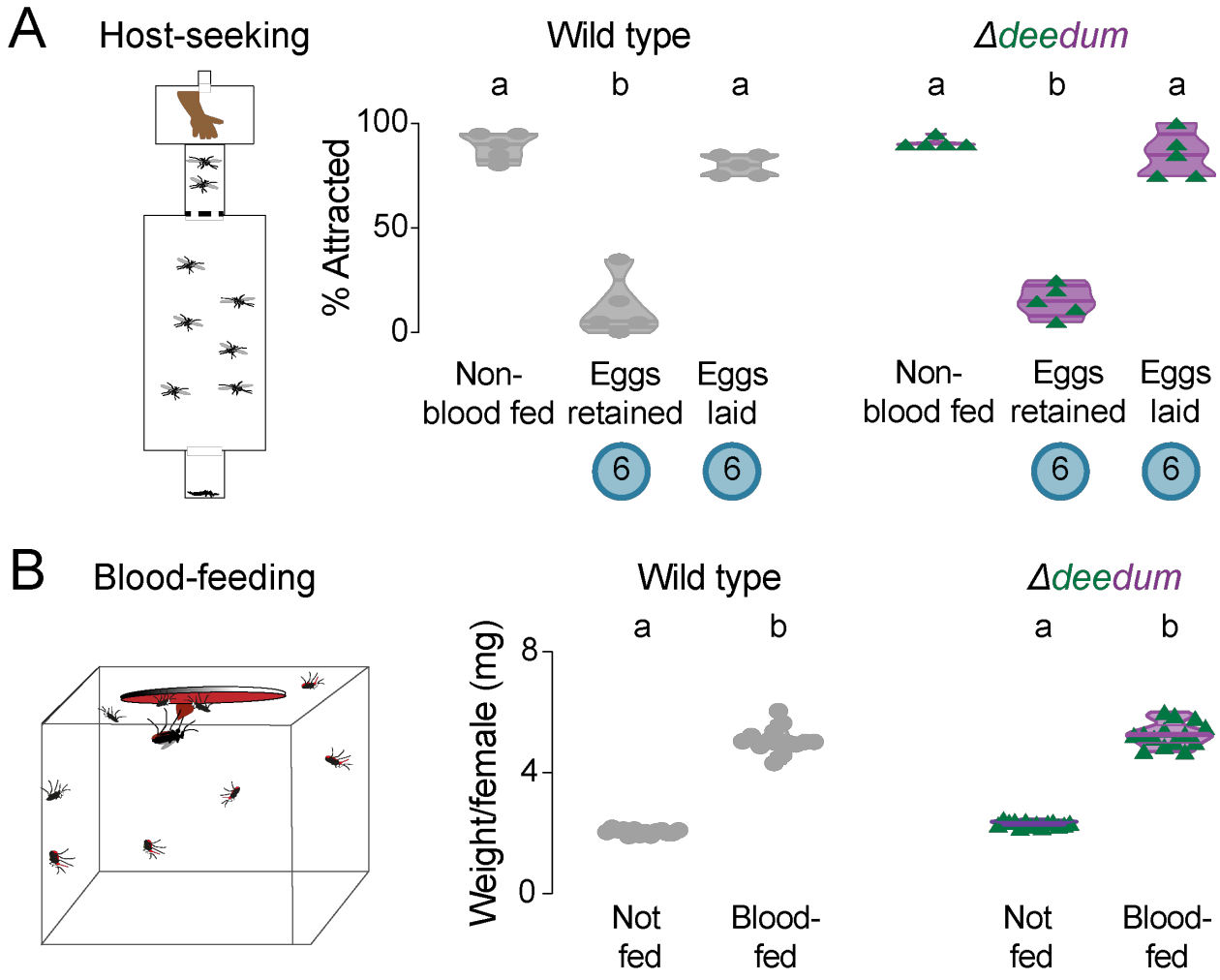

Figure 6.2 *Δdeedum* females host-seek and blood-feed at similar rates to wild type
(**A**) Attraction of wild type and *Δdeedum* mutant females to a human forearm. Data are plotted as violin plots with median and 1st/3rd quartiles and showing all data points. Each point represents a single trial with ~20 females, n=5 trials/group. Significantly different groups are indicated by different letters (one-way ANOVA, Holm-Šídák's multiple comparisons test, $p<0.0001$).
(**B**) Averaged weights of 5 females of the indicated genotype not fed or blood fed, n=14 groups of 5 females per group. Data are plotted as violin plots with median and 1st/3rd quartiles and showing all data points. Significantly different groups are indicated by different letters (one-way ANOVA, Tukey's multiple comparisons test, $p<0.0001$).

6.3 *Δdeedum* ovaries and spermathecae visually appear grossly normal following egg retention

We next asked whether *Δdeedum* double mutant females have morphologically healthy ovaries and spermathecae with visually normal eggs and sperm, respectively. *Δdeedum* females that consumed a full blood meal developed mature eggs and retained them for at least 12 days after the blood meal in their ovaries. There were no grossly observable morphological defects in *Δdeedum* eggs or ovaries compared to wild type when ovaries were dissected and photographed 6 days (Figure 6.3A) or 12 days (Figure 6.3B) after the blood meal. Spermathecae, the organs specialized for sperm storage following a single mating event contained sperm that appeared motile in both wild type and *Δdeedum* mutants at both time-points (Figure 6.3).

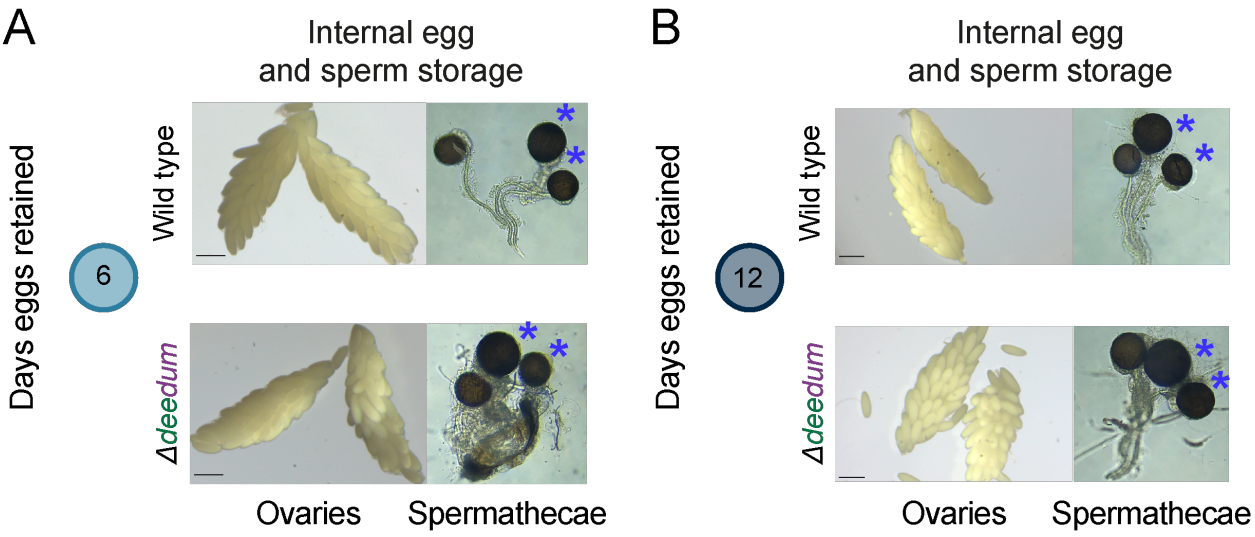

Figure 6.3 *Δdeedum* ovaries and spermathecae visually appear grossly normal after moderate or extended egg retention
(**A, B**) Wild type (top) and *Δdeedum* (bottom) ovaries and spermathecae after 6 days post-blood-meal, reflecting moderate egg retention (A) and 12 days post-blood-meal, reflecting extended egg retention (B).
Blue asterisks (*) indicate spermathecae filled with motile sperm.

6.4 *Δdeedum* mutants lose reproductive resilience with increasing egg retention

Our findings in Chapter 6.1-6.3 show that the reproductive organs of *Δdeedum* mutant females visually appear grossly normal and that their attraction to human hosts, modulation of attraction after a blood meal, and blood meal sizes are comparable to wild type. We next tested the egg retention and egg-laying behaviors of *Δdeedum* females compared to wild type to assess how the mutants compare in their reproductive resilience during droughts of different durations (Figure 6.4A). We blood fed wild type and *Δdeedum* mutant females, and withheld access to a freshwater substrate for either 6 days (Figure 6.4B-D) or 12 days (Figure 6.4E-G), corresponding to moderate or extended drought-like conditions (Figure 6.4A). When we provided freshwater 6 days after the blood meal, 98% of wild type females compared to 90% of *Δdeedum* females laid at least one egg (Figure 6.4B-D). While wild type females laid a median of 109 eggs, *Δdeedum* mutant females laid a median of 85 eggs. Of the females that laid any eggs, 98% of the wild type females compared to 82% of *Δdeedum* females produced at least one viable offspring (Figure 6.4B-D). Of the eggs laid by the respective genotypes, 73% of wild type eggs hatched, while only 36% of *Δdeedum* eggs hatched (Figure 6.4B-D). Deleting *tweedledee* and *tweedledum* therefore had a considerable effect on egg viability during moderate egg retention.

If instead we withheld freshwater for 12 days after the blood meal before providing it to females, 98% of wild type females still laid at least one egg compared to 82% of *Δdeedum* females (Figure 6.4E-G). Of the females that laid eggs, 100% of the wild type females still produced at least one viable offspring compared to only 56% of *Δdeedum*

females (Figure 6.4E-G). Wild type animals laid a median of 98 eggs of which 58% hatched (Figure 6.4E-G). *Δdeedum* females laid a median of 43 eggs after this extended retention, but in stark contrast to wild type, only 15% of the eggs laid hatched (Figure 6.4E-G). Therefore, as the duration of drought increased, females lacking *tweedledee* and *tweedledum* lost their ability to remain reproductively resilient.

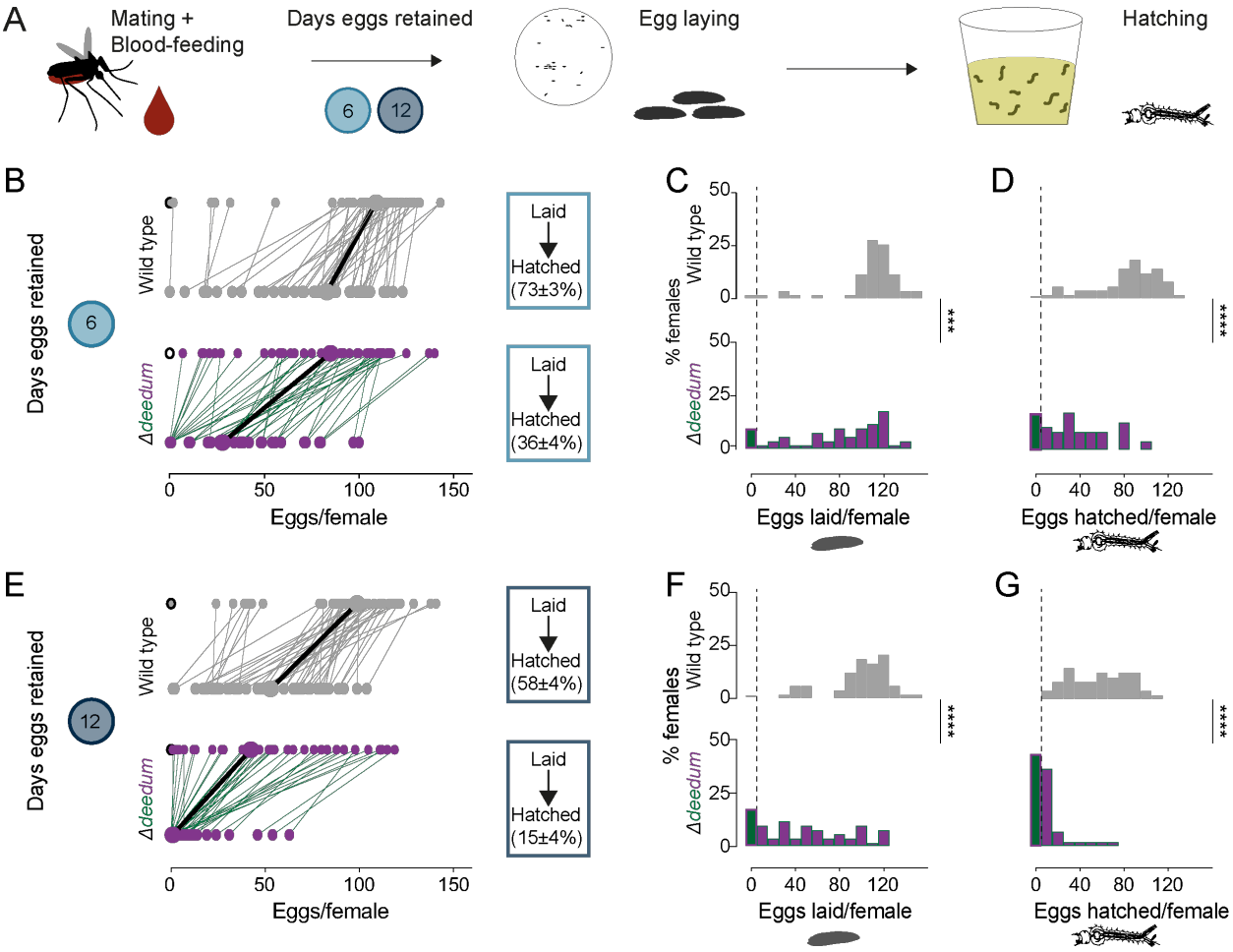

Figure 6.4 *Δdeedum* mutants increasingly lose the ability to maintain egg viability with increased egg retention time
(**A**) Schematic of experiment to test effect of moderate (6 days) and extended (12 days) egg retention on egg-laying and hatching.
(**B, E**) Number of eggs laid by (top) and hatched from (bottom) single wild type and *Δdeedum* mutant females 6 days (B) and 12 days (E) post blood-meal, depicting moderate and extended egg retention, respectively. Females laying no eggs are depicted by open circles. Lines connect eggs laid by and hatched from the same

individual. Larger circles and bold lines represent medians. Boxes show (mean ± S.E.M) of % eggs hatched from each egg retention group, n = 48-50 females/ group.
(**C, F**) Distribution of eggs laid after egg retention in wild type and *⊿deedum* mutant females 6 days (C) or 12 days (F) post-blood-meal. Zero values are binned separately for each group. All other bins are groups of 10 starting with [1-10] and with closed/inclusive intervals. (C, F) The groups between each genotype for eggs laid were compared at each of the time points to determine significant difference (Mann-Whitney tests, *** $p<0.001$; **** $p<0.0001$).
(**D, G**) Distribution of eggs hatched after egg retention in wild type and *⊿deedum* mutant females 6 days (D) or 12 days (G) post-blood-meal. Zero values are binned separately for each group. All other bins are groups of 10 starting with [1-10] and with closed/inclusive intervals. (D, G) The groups between each genotype for eggs hatched were compared at each of the time points to determine significant difference (Mann-Whitney tests, *** $p<0.001$; **** $p<0.0001$).
Distributions in (C, D) are analyzed from data in (B) and distributions in (F, G) are analyzed from data in (E).

6.5 The*Δdeedum* mutant phenotype is recessive

At both 6 days (Figure 6.5A) and 12 days (Figure 6.5B) post-blood-meal, heterozygous females laid a similar number of eggs to wild type females, indicating that the *Δdeedum* phenotype is largely recessive.

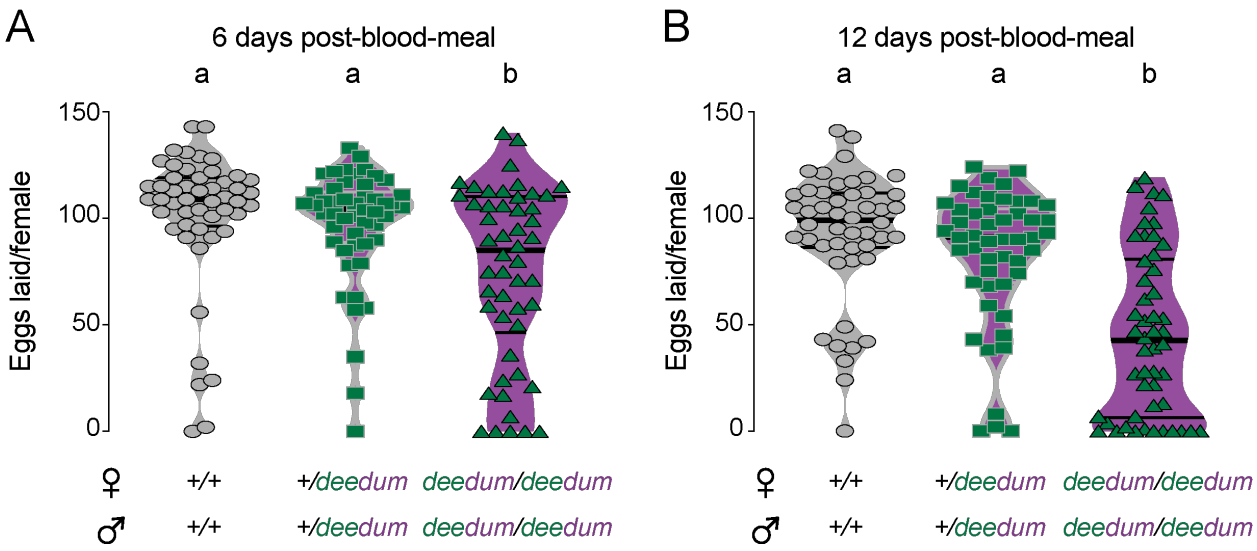

Figure 6.5 The reproductive resilience phenotype of *Δdeedum* is recessive
(**A-B**) Eggs laid by females of the indicated genotype 6 (A), or 12 (B) days post-blood-meal. The genotype of the males to which they were mated is indicated below the female genotypes. Data are plotted as violin plots with median and 1st/3rd quartiles and showing all data points. Each point represents the eggs laid by a single female (A: n=50/genotype; B: n=48-50/genotype). Data labeled with different letters are significantly different (Kruskal-Wallis, Dunn's multiple comparisons test, $p<0.05$). Egg-laying data for wild type and *Δdeedum* groups are re-plotted from Figure 6.4, and heterozygote groups were age-matched and tested together with the wild type and *Δdeedum* groups.

6.6 The *Δdeedum* mutant phenotype is maternally-derived

Aedes aegypti females undergo profound changes in physiology and behavior upon mating (Alfonso-Parra et al., 2016; Duvall et al., 2017; League et al., 2021; Villarreal et al., 2018). To ask if the genotype of the male with which the female had mated had an influence on these female reproductive resilience phenotypes, we mated both wild type and *Δdeedum* females to wild type males instead of sibling males of their respective genotypes. We tested the number of eggs laid by females after extended retention and found that *Δdeedum* females laid significantly fewer eggs compared to wild type females (Figure 6.6). These data suggest that the decreased fitness after egg retention seen in *Δdeedum* females is largely a maternally-derived phenotype.

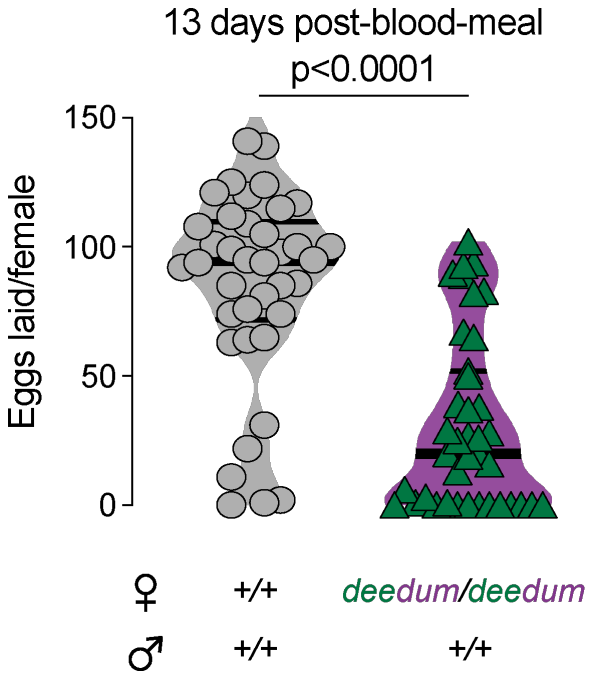

Figure 6.6 Loss of fitness after egg retention in *Δdeedum* females is a maternally-derived phenotype
Eggs laid by females of the indicated genotype after extended retention (13 days post-blood-meal). The genotype of the males to which they were mated is indicated below the female genotypes. Data are plotted as violin plots with median and 1st/3rd quartiles and showing all data points. Each point represents the eggs laid by a single female, n=38-39/genotype. Significance is established by Mann-Whitney test, p<0.0001.

Together, these data illustrate that *tweedledee* and *tweedledum* are required in the female for maintaining egg viability specifically when she retains eggs in her ovary for moderate or extended periods post-blood-meal, such as during suboptimal egg-laying conditions like drought. The loss of resilience observed in *Δdeedum* is a time-restricted phenotype – resilience of the mutants worsens considerably compared to wild type as egg retention time increases. We speculate that *tweedledee* and *tweedledum* may therefore be an "insurance" mechanism to protect eggs prior to egg-laying in case environmental conditions are suboptimal for egg-laying – the final step in an adult female's reproductive sequence (Figure 6.7). We also note that the loss of reproductive resilience in *Δdeedum* mutants compared to wild type is observed across different egg-laying assay configurations, suggesting that the phenotype is a biological phenomenon independent of the specific egg-laying chamber configuration provided.

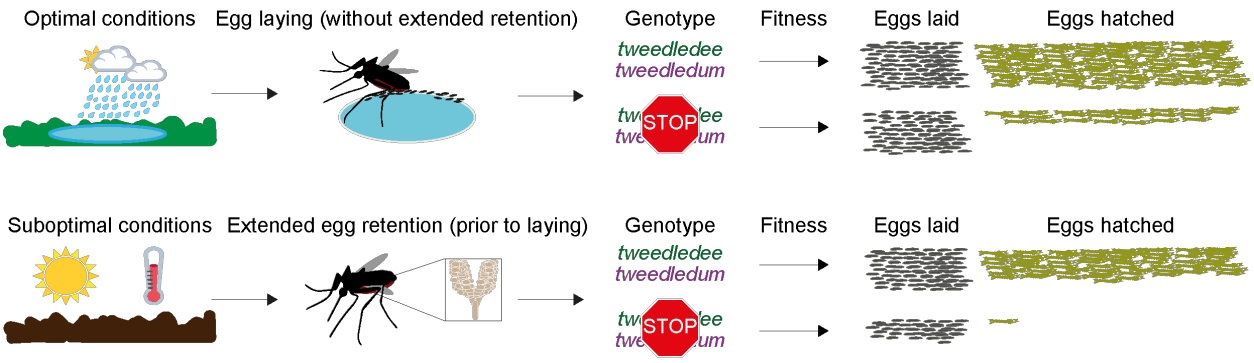

Figure 6.7 Summary of *tweedledee* and *tweedledum* function in drought resilience of female *Aedes aegypti* mosquitoes

6.7 Can *tweedledee* or *tweedledum* alone confer reproductive resilience?

In this study we generated a deletion that disrupted both *tweedledee* and *tweedledum*. This left open the question of whether both genes contribute to reproductive resilience during drought, or whether loss of either of the genes alone would lead to loss of egg viability following retention. Since our CRISPR-Cas9 strategy for generating the *Δdeedum* double mutant involved injecting embryos with a mixture of guides targeting both *tweedledee* and *tweedledum*, we also isolated a mutant with a deletion in *tweedledee* alone (*Δdee* single mutant) and an independent mutant with a deletion in *tweedledum* alone (*Δdum* single mutant). To date, owing to practical and technical challenges, we have been unable to establish a homozygous *Δdee* single mutant strain, leaving open the question of whether *tweedledee* alone could confer reproductive resilience.

6.8 Generation and phenotyping of *Δdum* single mutant

We recovered and successfully established a *Δdum* single mutant (Figure 6.8) and observed that it had a phenotype largely overlapping with that of *Δdeedum* (Figures 6.9-6.11). The *Δdum* mutant has a deletion of 175 bp within the second exon of *tweedledum*, and the resulting gene fusion is predicted, *in silico,* to encode a protein with the first 17 amino acids of tweedledum conserved before the breakpoint junction, after which a frameshift adds 7 missense amino acids followed by a stop codon (Figure 6.8A-B).

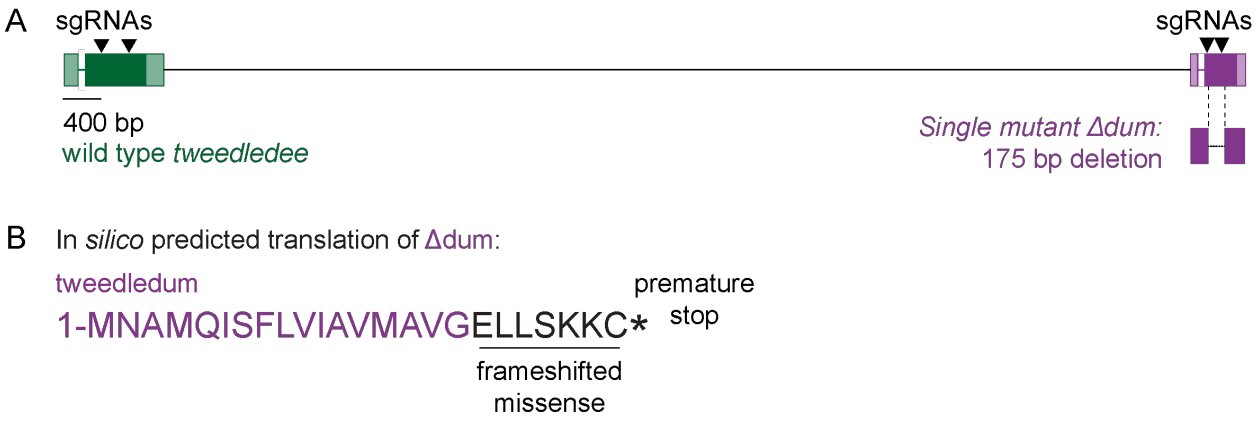

Figure 6.8 Generation of *tweedledum* single mutant (*Δdum*)
(**A**) Schematic of *Δdum* mutant that deletes *tweedledum,* but not *tweedledee*.
(**B**) *In silico* predicted translation of Δdum.

Δdum mutants engorged on blood meals to approximately double their body weight (Figure 6.9). They retained eggs and motile sperm in their visually healthy ovaries and spermathecae, respectively, for moderate (6 days post-blood-meal, Figure 6.10A) or extended (Figure 6.10B) durations post-blood-meal, suggesting good overall health.

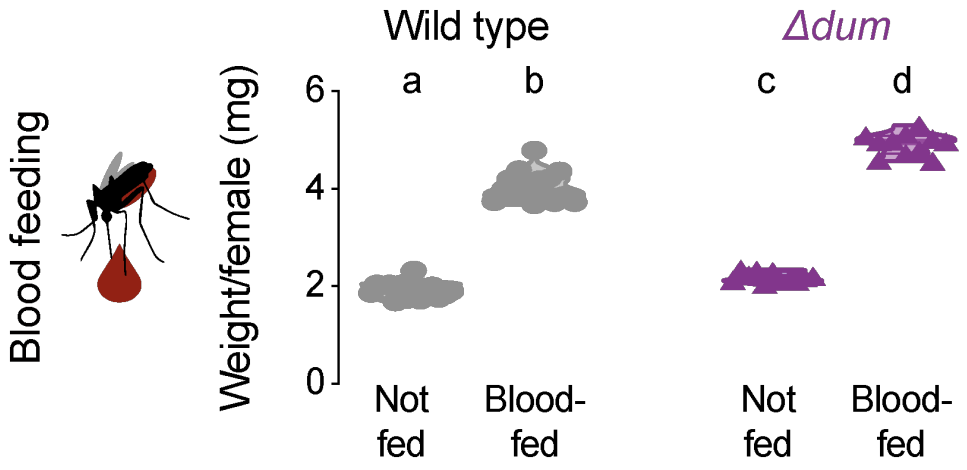

Figure 6.9 *Δdum* mutant engorge on blood to double their body weight
Averaged weights of 5 females of the indicated genotype not fed or blood fed, n=11-16 groups of 5 females per group. Data are plotted as violin plots with median and 1st/3rd quartiles and showing all data points. Significantly different groups are indicated by different letters (one-way ANOVA, Tukey's multiple comparisons test, $p<0.05$).

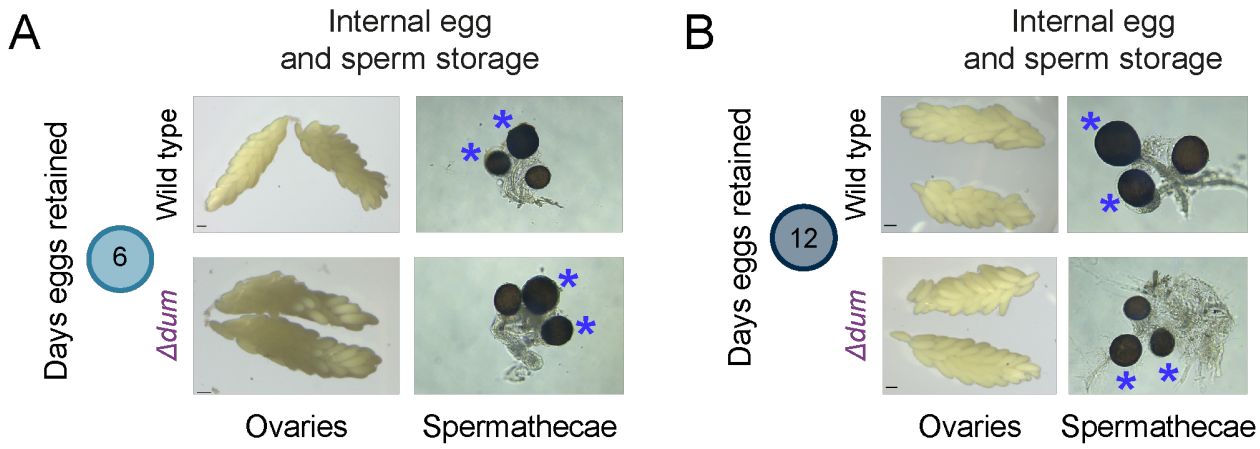

Figure 6.10 *Δdum* ovaries and spermathecae visually appear grossly normal after moderate or extended egg retention
(**A, B**) Wild type (top) and *Δdum* (bottom) ovaries and spermathecae 6 days post-blood-meal, reflecting moderate egg retention (A) and 12 days post-blood-meal, reflecting extended egg retention.
Blue asterisks (*) indicate spermathecae filled with motile sperm.

How reproductively resilient are females lacking functional tweedledum protein during drought conditions? *Δdum* mutants laid a similar number of eggs compared to wild type after moderate retention (Figure 6.11A-B) but laid significantly fewer eggs after extended retention (Figure 6.11C-D). Of the eggs laid after extended retention, a starkly smaller proportion from *Δdum* mutants compared to wild type generated viable offspring (Figure 6.11C,E).

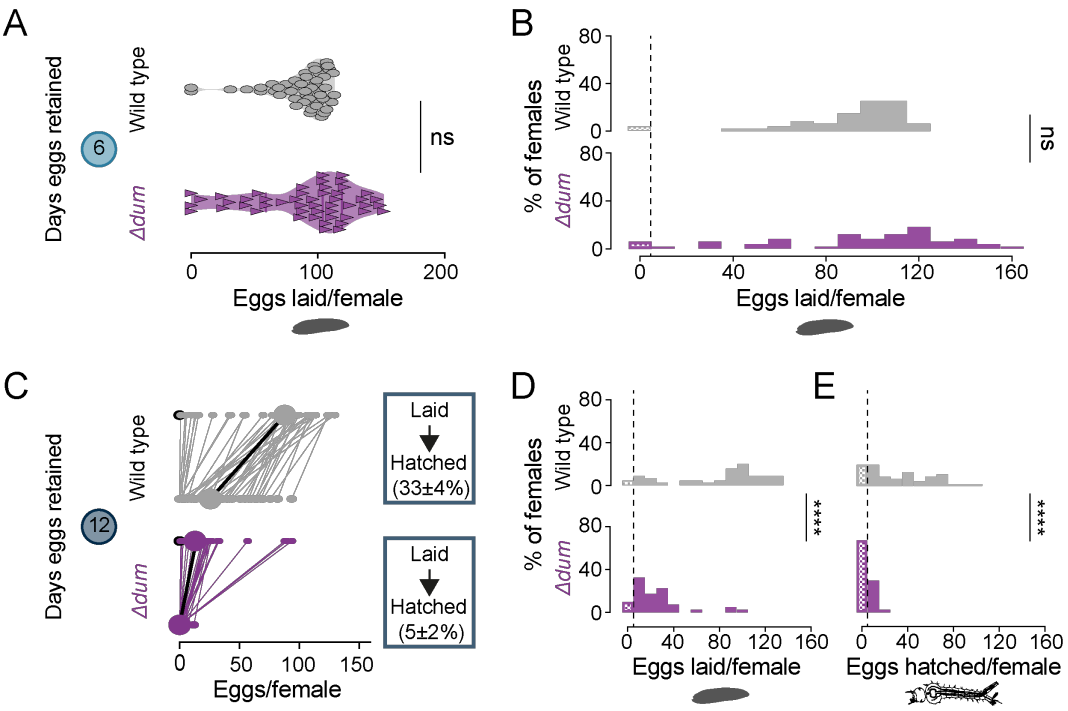

Figure 6.11 *tweedledum* mutants (*Δdum*) show defects in reproductive resilience during drought

(**A**) Eggs laid by females of the indicated genotype 6 days post-blood-meal. Data are plotted as violin plots with median and 1st/3rd quartiles and showing all data points. Each point represents the eggs laid by a single female (n=47-49/genotype). n.s., not significant (Mann-Whitney test).

(**B, D, E**) Distribution of eggs laid (B, D) or eggs hatched (E) in wild type and *Δdum* mutant females 6 days (B) and 12 days (D, E) post-blood-meal. Zero values are binned separately for each group. All other bins are groups of 10 starting with [1-10] and with closed/inclusive intervals. (B, D, E) The groups between each genotype for eggs laid and eggs hatched respectively were compared at each of the time points to determine significant difference (Mann-Whitney tests, **** $p<0.0001$). Distribution in (B) is analyzed from data in (A) and distributions in (D, E) are analyzed from data in (C).

(**C**) Number of eggs laid by (top) and hatched from (bottom) single wild type and *Δdum* mutant females 12 days post blood-meal, depicting extended egg retention. Females laying no eggs are depicted by open circles. Lines connect eggs laid by and hatched from the same individual. Larger circles and bold lines represent medians. Boxes show (mean ± S.E.M) of % eggs hatched from each egg retention group, n = 40-45 females/ group.

These results suggest that at minimum *tweedledum* is contributing to drought resilience, and future work will resolve if both *tweedledee* and *tweedledum* are required for this important phenomenon.

CHAPTER 7. Discussion

7.1 Flexibility enables a freshwater-centric lifestyle in variable environments

Aedes aegypti mosquitoes depend on freshwater availability for completing the aquatic larval and pupal stages of their life cycle (Bentley and Day, 1989; Day, 2016; Wallis, 1954). Adult *Aedes aegypti* females carrying mature eggs accordingly prefer to lay them at the edge of freshwater (Matthews et al., 2019). Fluctuating climates with unpredictable and intense droughts likely impose selective pressures on this species, which has evolved multiple reproductive strategies that contribute to its resilience and invasive potential. Decoupling of mating from host-seeking and subsequent blood feeding – such that either can take place first – and the appropriate coupling of both behaviors with egg-laying provides female *Aedes aegypti* mosquitoes with flexibility to maximize their reproductive output while still ensuring they have the required sperm and blood proteins for producing viable offspring. If faced with drought after being laid, embryos developmentally arrest in a state of diapause within the eggshell for several months as an added layer of protection, until freshwater that can support larval survival becomes available to stimulate hatching (Rezende et al., 2008).

We suggest that the ability of adult *Aedes aegypti* females to retain mature eggs in their ovaries without complete loss of viability for flexible lengths of time while searching for a freshwater egg-laying site is of significant adaptive value. While diapause provides a mechanism to “wait” for freshwater to become available so larval and pupal development can proceed under optimal conditions after hatching, this may be of

adaptive value on longer time-scales such as those correlating with seasonal changes. Instead, egg retention may be of adaptive value on shorter time-scales, such as those correlated with fluctuations that occur within a season on the order of days or weeks. Indeed, females strongly prefer laying eggs on moisture, and if moisture is removed after egg-laying during embryogenesis before the serosal cuticle is formed, subsequent hatch rates diminish significantly (Matthews et al., 2019; Rezende et al., 2008). Thus, egg retention occurring on shorter time-scales than diapause (days or weeks *vs.* months, respectively) may be a crucial and complementary strategy along with diapause to ensure offspring survival.

In this study, we demonstrated that *tweedledee* and *tweedledum,* a pair of linked, mosquito-specific genes, encode proteins that allow a female to retain her eggs for extended durations as needed without marked loss of viability, such as when access to freshwater is restricted due to drought. Females lacking both genes show a time-dependent phenotype. Their reproductive resilience dramatically worsens as length of egg retention increases from 6 to 12 days post-blood-meal, whereas wild type females continue to maintain a remarkable degree of reproductive resilience regardless of the duration of egg retention (Figure 6.7). Our findings highlight an example of plasticity in the innate reproductive behaviors of *Aedes aegypti* mosquitoes, which allows them to thrive in a remarkable range of ecosystems with distinct climates.

7.2 Providing protection to eggs: abundance in the right place, at the right time

Oocytes are stored within the ovaries of females in species separated by millions of years of evolution. Increased oocyte storage time carries the risk of increased damage, which females have evolved diverse strategies to mitigate (Greenblatt et al., 2019). Mammalian oocytes are maintained for decades and gradually released from their reserves. In humans, as a female and her oocyte reserve both age, oocytes become increasingly prone to meiotic segregation errors that result in higher rates of miscarriage and Down's syndrome (Webster and Schuh, 2017). Mammalian oocytes in reserve reside within primordial follicles where they are nurtured by maternally-derived nutrients that play a role in maintaining oocyte longevity (Webster and Schuh, 2017). Bidirectional exchange between germline (oocyte) and somatic (follicle) cells is critical for germline maintenance and occurs through both gap junction-mediated transfer of small molecules, as well as via paracrine secretion of nourishing factors from follicles (Kidder and Vanderhyden, 2010). In *Drosophila melanogaster* flies, oocytes are retained if access to protein or sperm is restricted, and extended oocyte storage results in lower capacity for embryonic development. In wild type fly oocytes, abundant expression of two heat shock protein chaperones, *Hsp26* and *Hsp27* contributes to maintenance of developmental capacity following extended oocyte retention (Greenblatt et al., 2019). These examples highlight a strong precedent for the existence of protective or nurturing mechanisms in *Aedes aegypti* ovaries that would enable the female to maintain viable eggs for extended durations post-maturation.

What is the mechanism by which a pair of abundantly expressed genes ensure long-term viability of eggs retained in the mosquito ovary? We have few clues to work with. The highly regulated spatiotemporal expression of these paired genes in the ovary suggests to us that they both contribute to egg viability during retention. After maturation, and in the hours post-egg-laying, expression of *tweedledum* is restricted within the ovaries to the follicular epithelial cells surrounding eggs. In contrast, *tweedledee* is basally expressed in all the reproductive states of the ovaries, although its upregulation by several orders of magnitude is concurrent with its expanded expression in the follicular epithelial cells surrounding mature eggs during egg retention, together with *tweedledum.* Since the follicular epithelial cells form a socket around mature eggs, the expression of both genes together in these cells may be most functionally relevant in protecting eggs during retention, such as by forming a secreted desiccation-resistant barrier or a coating required for long-term maintenance. The spatiotemporal similarities in *tweedledee* and *tweedledum* expression within follicular epithelial cells following egg maturation raise the plausibility that the secreted proteins physically interact. Future biochemical studies and empirical determination of the proteins' three-dimensional structures would reveal whether they could form a functional complex. The intrinsically disordered regions of the proteins may suggest a role for them in promoting phase separation, allowing for protective compartmentalization in the environment surrounding eggs (van Mierlo et al., 2021; Wright and Dyson, 2015).

On the way to being laid, mature eggs also interact with the calyx where *tweedledee* is additionally expressed. It is therefore possible that additional interaction between the

eggs and *tweedledee* while eggs are in transit facilitates egg competence for subsequent sperm entry and fertilization after extended retention, thereby ensuring viability. With future single-cell RNA sequencing of the ovaries to identify cell type markers, genetic tools could be developed in *Aedes aegypti* to visualize or disrupt the distinct *tweedledee* populations in a cell type-specific or temporally-controlled fashion. This would allow us to resolve whether the calyx and follicular epithelial cell expression programs of *tweedledee* serve distinct functions.

In this study, we generated and established both *Δdeedum* double mutants and a *Δdum* single mutant. Both strains have substantially similar phenotypes of reduced egg viability during extended retention. Our attempts to generate *Δdee* single mutants were unsuccessful. This leaves open the question of whether both *tweedledee* and *tweedledum* contribute to the *Δdeedum* phenotype or whether *tweedledum* is solely responsible.

7.3 Expression in the male reproductive system

The broader expression of *tweedledee* across cell types and tissues is also reflected in the male reproductive system; while both transcripts are expressed in the testes, only *tweedledee* is additionally expressed in the male accessory glands (MAGs). Our data from *Δdeedum* knockout females show that females lay significantly fewer eggs after extended retention even when they were mated with wild type males instead of *Δdeedum* mutant males, suggesting that the male expression of these genes likely does not contribute significantly to female reproductive resilience (Figure 6.6). A complementary experiment crossing *Δdeedum* mutant males with wild type females and assessing the number of eggs laid by and hatched from the females after extended retention would allow us to verify whether there is any contribution from the male to this egg viability phenotype. While out of the scope of this study, exploring whether male expression of *tweedledee* and *tweedledum* is otherwise functionally relevant to behavior or physiology would be an interesting avenue to explore whether these genes perform multiple, sexually dimorphic, or sexually antagonistic roles in *Aedes aegypti* mosquitoes.

7.4 Signal, waste, or both?

What is the function of the circulating forms of these proteins? Our proteomic analysis supports the hypothesis that these proteins are secreted, as we detect tryptic peptides from both proteins that represent N-terminal signal peptide-cleaved forms, both in the circulating hemolymph, as well as in the ovary. It is unclear if the circulating forms of these proteins are waste products destined for destruction after production in the ovaries, or if they serve a signaling function. One possibility is that tweedledee and

tweedledum sustain eggs in the ovary while also acting as a humoral signal to alert other organs – including the nervous system – of the female's reproductive status. There is a precedent for secreted egg-related proteins serving multiple roles. Vitellogenins are best known as egg yolk proteins, but also function as a hormone secreted into hemolymph, where they have multiple effects on behavior and longevity in social insects (Corona et al., 2007). In *Aedes albopictus,* vitellogenins have recently been implicated in regulating host-seeking behavior in response to the status of nutritional reserves, in addition to their role as yolk protein precursors (Dittmer et al., 2019). Bifunctionality and coordinated action of molecular pairs are common phenomena in insect reproduction. The hormones, 20-hydroxyecdysone and juvenile hormone III, act in concert to control metamorphosis across insects (Jia et al., 2017), while additionally modulating vitellogenesis after a blood meal in mosquitoes (Hansen et al., 2014; Raikhel and Lea, 1991; Roy et al., 2015) and defining caste-specific behavioral repertoires or traits in the Indian jumping ant, *Harpegnathos saltator* (Gospocic et al., 2021).

7.5 Evolutionary origins and catering to different natural histories

The evolutionary history of *tweedledee*, *tweedledum*, and the *conceptualogs* is intriguing. The lack of known domains poses a problem for understanding the function and evolutionary history of these proteins, and conventional homology searches fail to detect homologs that could provide clues. The two proteins have no homology to each other, to the conceptualogs, or to any other known protein. Structural homology-based approaches might be a path forward to identify genes with divergent sequence but

conserved three-dimensional protein structure and function. However, current protein structure prediction programs perform poorly on small proteins (Figure 5.4), especially when phylogenetic homology cannot be brought to bear to inform the analysis (Jumper et al., 2021).

Rapidly evolving genes typically show testis-biased expression across evolution (Witt et al., 2019; Witt et al., 2021), but in *Aedes aegypti,* ovary-specific genes evolve unusually fast with more frequently occurring signatures of positive selection as compared to genes with enriched expression in the testis (Whittle and Extavour, 2017). Our study reveals *tweedledee* and *tweedledum* as examples of such rapidly evolving, ovary-enriched genes present in mosquito genomes, but it remains an open question whether genes of this type exist outside of mosquitoes. Published transcriptomic data suggest the tissue-restricted and sexually dimorphic expression of these genes may be conserved across genera. In *Anopheles stephensi* (Jiang et al., 2014), the *conceptualog* is upregulated in ovaries 24 hours post-blood-meal, and in *Anopheles arabiensis,* the *conceptualog* is upregulated in the reproductive tissues of females compared to males (Papa et al., 2017). At the genomic level, what allows the syntenic locus, characterized in several blood-feeding mosquitoes by the conserved *scratch* and *peritrophin-like* genes, to 'trap' one rapidly divergent gene in the case of *Culex* and *Anopheles* mosquitoes, or two rapidly divergent genes in the case of *Aedes* mosquitoes? Together, these observations of shared synteny and gene expression indicate that the *Aedes tweedledee/tweedledum,* and the *Culex* and *Anopheles conceptualogs* are likely to have

evolved from a common ancestor, and that these genes may co-opt similar pathways across genera to function.

A look at the natural histories of different mosquito genera (see Chapter 1) suggests that they each employ distinct life history strategies. These involve differences in adult female behavioral parameters: flexibility in choosing a blood meal host, circadian control of host-seeking, mating frequency, and egg-laying site selection; differences in the potential for diapause or resistance to desiccation in embryos; and tolerance of larvae for different aquatic environments (Degner and Harrington, 2016; Wallis, 1954). The physiological and behavioral adaptations underpinning these strategies must co-evolve in each of the species, in turn determining the ecological niches that the species are able to exploit. Future comparative studies will resolve whether rapid divergence in the sequence of *tweedledee/tweedledum* and the *conceptualog* is accompanied by conservation, or by rapid divergence in their functions. This work thus highlights the importance of considering taxon-restricted genes as important points of study to understand the life-history strategies of a species, and to identify new inroads for breaking the cycle of mosquito-borne disease transmission.

7.6 Returning to the wild for lessons

Elegant genetic and genomic studies of wild animal populations have provided invaluable insights into how complex behaviors evolve in response to different environmental contexts. For example, in a study of two sister species of *Peromyscus* mice that build burrows with distinct architectures, genetic crosses combined with

quantitative trait locus analysis demonstrated how changes occurring in a single locus vs. in multiple loci with modularity can give rise to varied complex phenotypes (Weber et al., 2013). In mosquitoes, a study of wild-caught forest and domestic populations of *Aedes aegypti* allowed the identification of *Or4,* an olfactory receptor that underlies the human host preference of domestic *Aedes aegypti* mosquitoes. Mechanistically, tuning of *Or4* expression levels and the receptor's sensitivity to a ligand derived from human odor contributed to modulation of host preference (McBride et al., 2014). More recently, genomic sequencing of *Aedes aegypti* populations from different field sites across the ancestral home of the species in sub-Saharan Africa, coupled with evolutionary modeling revealed that human vs. non-human host preference is strongly correlated with and driven by the intensity of droughts/dry seasons, as well as urbanization-driven changes in population density (Rose et al., 2020).

Using the Liverpool laboratory strain of *Aedes aegypti,* our work identifies a genetic locus important for reproductive resilience during drought. Future comparative analysis of this *tweedledee* and *tweedledum* locus across wild populations derived from geographic regions with different climate parameters (e.g., precipitation seasonality, temperature, and intensity of dry seasons vs. monsoons) may allow us to home in on specific alleles and amino acid sites that might be of functional relevance in allowing populations to specifically adapt to their local climates. In examining the strain collection sites across Africa from Rose et al., 2020, it is evident that *Aedes aegypti* populations inhabit regions with vastly different precipitation seasonality. Do specific allelic variants of *tweedledee* or *tweedledum* in populations derived from distinct regions correlate with

different climate parameters of those regions? For example, are some specific alleles more frequently observed in individuals that have colonized regions with high precipitation seasonality or drought intensities, as compared to individuals in wetter regions with less fluctuating precipitation cycles? It would be especially interesting to consider climate parameters that are relevant on different time-scales, such as temperature or precipitation fluctuations within a day *vs.* within a month or a season. This might provide insight the time-scale on which egg retention provides a survival advantage. Additionally, is there an unexplored fitness cost associated with some alleles that is overridden by the high benefit of the reproductive resilience they confer? What fitness tradeoffs are relevant in driving the evolution of these genes? Together, such analyses would provide an inroad into further investigating the molecular evolution of *tweedledee* and *tweedledum* as enablers of drought resilience and provide an explanation for the rapid divergence rates of these genes.

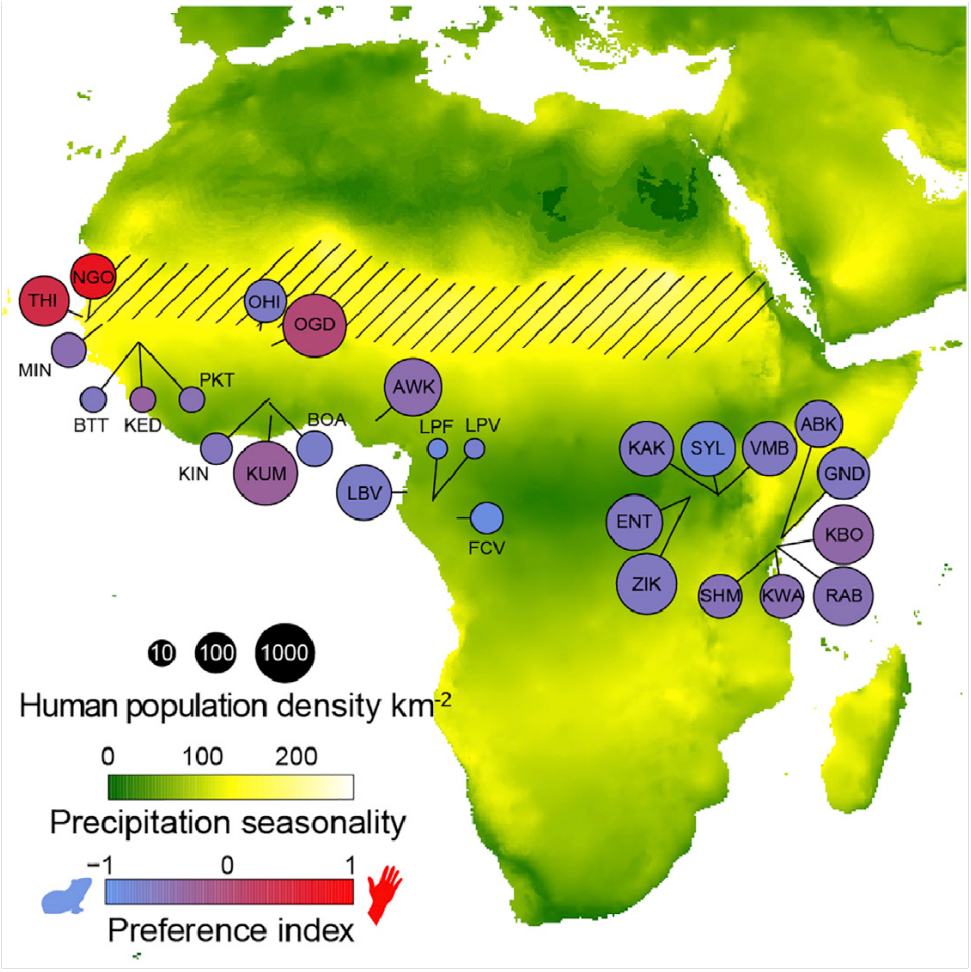

Figure 7.1 *Aedes aegypti* populations inhabit regions with diverse precipitation seasonality
Map of *Aedes aegypti* population collection sites (indicated by three-letter codes inside circles) shown with their respective human population density, precipitation seasonality, and resident *Aedes aegypti* population host preference index. Adapted from (Rose et al., 2020).

7.7 Invasiveness of *Aedes* mosquitoes

Aedes aegypti tweedledee and *tweedledum* both have orthologs in *Aedes albopictus,* another invasive mosquito species that is also a major vector for several viruses of concern to human health. Invasive species are those that have significantly increased in an area after their introduction, and that trigger changes to the native ecosystem as well as to human activities (Juliano and Lounibos, 2005). The distribution of *Aedes*

albopictus substantially overlaps across the world with that of *Aedes aegypti* (Figure 7.2), although ancestral *Aedes albopictus* populations originated in Asia whereas ancestral *Aedes aegypti* populations originated in sub-Saharan Africa (Juliano and Lounibos, 2005; Kraemer et al., 2015a; Kraemer et al., 2015b; Lounibos et al., 2016; Lounibos and Kramer, 2016). Where sympatric with *Aedes aegypti, Aedes albopictus* has been observed more frequently in rural habitats with vegetation, feeding on a range of mammalian hosts (Hawley, 1988). Particularly when invading regions without resident *Aedes aegypti,* however, *Aedes albopictus* has proven to be adept at colonizing urban areas wherein humans serve as the dominant blood meal hosts (Lounibos and Kramer, 2016). This versatility of *Aedes albopictus* is threatening. In many regions, *Aedes albopictus* populations have displaced *Aedes aegypti.* While both species lay eggs capable of desiccation resistance that hatch upon subsequent flooding, *Aedes albopictus* larvae have fared better than *Aedes aegypti* under limited resource and high competition contexts (Lounibos et al., 2016; Lounibos and Kramer, 2016). *Aedes albopictus* also likely succeeds in displacing *Aedes aegypti* because of satyrization, a form of reproductive interference that occurs asymmetrically (Lounibos and Kramer, 2016). In regions with species overlap, interspecific mating results in inviable offspring, but virgin *Aedes aegypti* females are worse affected than virgin *Aedes albopictus* females. The transfer of an accessory gland substance from *Aedes albopictus* males to *Aedes aegypti* females upon heterospecific mating blocks the *Aedes aegypti* females, which mate only once in a lifetime, from remating with a conspecific *Aedes aegypti* male. This is a unidirectional phenomenon, with *Aedes albopictus* females spared from

mating blocks (Bargielowski et al., 2015; Carrasquilla and Lounibos, 2015; Tripet et al., 2011).

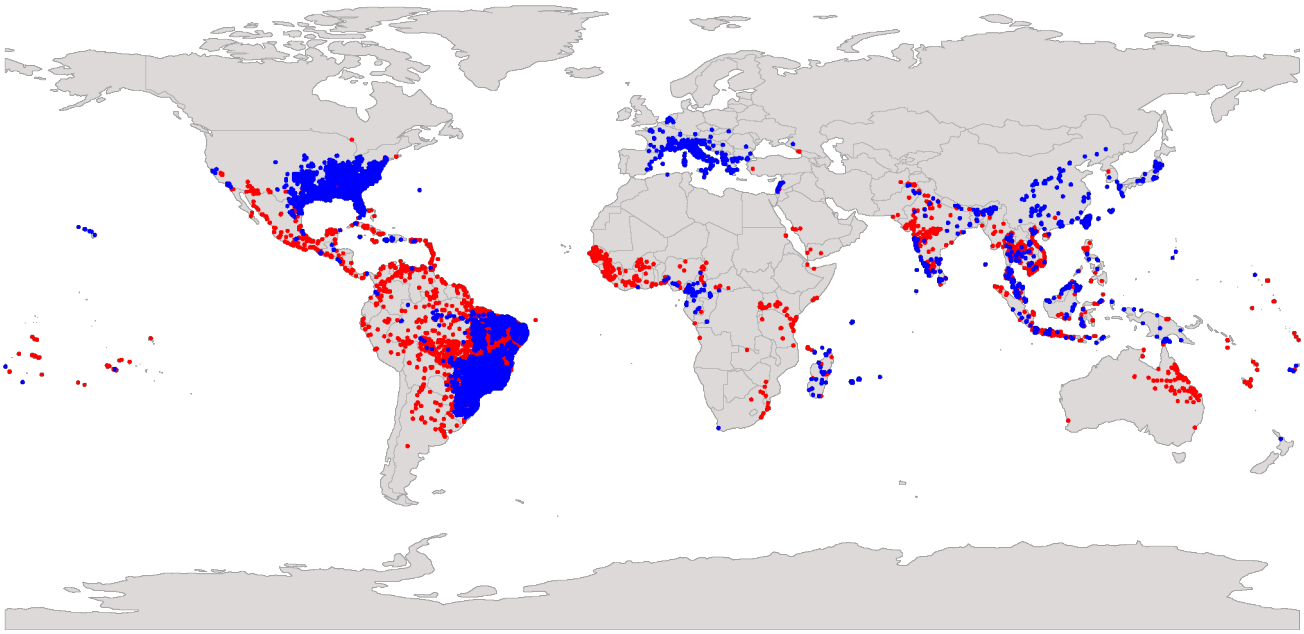

Figure 7.2 Occurrences of *Aedes aegypti* and *Aedes albopictus* mosquitoes globally from 1960-2013
Red points indicate occurrences of *Aedes aegypti* (as in Figure 1.2) and blue points indicate occurrences of *Aedes albopictus* from 1960-2013. Global geographical distribution re-plotted using occurrence data from (Kraemer et al., 2015a), which provides further information on the definition of what constitutes an occurrence.

Given the similarities and differences in the invasive capacities of these species that are sometimes sympatric, it would be interesting to investigate whether the versatility of *Aedes albopictus* in occupying regions with diverse climates is further facilitated by the *tweedledee* and *tweedledum* locus. Do *Aedes albopictus* females require an egg retention mechanism driven by *tweedledee* and *tweedledum* to be reproductively resilient during droughts? Do within-species vs. between-species differences at this locus contribute to differences in the invasive potential and reproductive resilience of

each species? A gene swap experiment would provide a fascinating approach to answer these questions (Prieto-Godino et al., 2017) – for example, could the *Aedes albopictus* form of *tweedledee* and *tweedledum* engineered using CRISPR-Cas9 into the *Aedes aegypti* genome confer reproductive resilience? What about vice versa? These experiments, also extended to include comparisons with *Culex* and *Anopheles conceptualogs,* would provide valuable insight into the trajectory of molecular evolution at this locus and into the functional consequences of the rapid evolution.

7.8 Final remarks

Overall, our data suggest a reproductive framework in *Aedes aegypti* females wherein they have evolved checkpoints to maximally utilize each blood meal that they obtain at great risk from a defensive human host. Be it preventing egg-laying when females are not mated, suppressing host-seeking while already developing or holding eggs, or retaining eggs for extended periods without dramatic loss of viability when freshwater is unavailable, *Aedes aegypti* females are experts at optimally using their blood meals for reproduction. Our work identifies *tweedledee* and *tweedledum* as late-stage reproductive checkpoint regulators in the *Aedes aegypti* adult female before she parts with her offspring. The time-dependent crash in reproductive resilience seen in *Δdeedum* mutants strongly supports the model that the pair of genes confer an important “insurance” for females bearing eggs to flexibly extend their retention, until freshwater suitable for offspring survival becomes available. This work thus illustrates the importance of considering taxon-restricted genes as important points of study to understand the life-history strategies of a species, and to identify new inroads for breaking the cycle of mosquito-borne disease transmission.

CHAPTER 8. Methods

8.1 Human and animal ethics statement

Behavioral experiments and blood-feeding methods using live hosts were approved and monitored by The Rockefeller University Institutional Review Board (IRB protocol LV-0652) and the Institutional Animal Care and Use Committee (IACUC protocol 17018), respectively. All human subjects gave their written informed consent to participate in this study.

8.2 Mosquito rearing and maintenance

Aedes aegypti wild type (Liverpool) and CRISPR-Cas9 knockout strains were reared using standard insectary conditions in an environmental chamber maintained at 70-80% relative humidity and 25-28°C with a photoperiod of 14 hours light: 10 hours dark as previously described (DeGennaro et al., 2013). Adults of all genotypes were provided *ad libitum* access to 10% sucrose and were housed in 30 cm^3 BugDorm-1 Insect Rearing Cages (MegaView Science) unless otherwise specified. Newly generated mutant strains were blood-fed on human volunteers until they were established. For stock maintenance, females were blood-fed on live mice or on defibrinated sheep blood (Hemostat Laboratories, DSB100) using an artificial membrane feeder (the “blood puck”) described below. All animals used for behavior experiments, regardless of genotype, were blood-fed using the blood puck.

8.3 Blood-feeding for behavior assays using the blood puck

For all behavior experiments requiring blood-fed mosquitoes, 5-16-day old females were fed sheep blood supplemented with 2 mM adenosine 5'-triphosphate (ATP) (Sigma Aldrich, A6419) in aqueous sodium bicarbonate buffer using a new artificial membrane feeder called the blood puck. Metal blood pucks were custom-made at The Rockefeller University Precision Instrumentation Technologies Resource Center and the Rockefeller High-Energy Physics Machine Shop. Three-dimensional designs for fabrication, and a bench manual for suggested use are provided (https://doi.org/10.5281/zenodo.5945525). The blood puck is a disc with one indented, rimmed face on which blood rests with Parafilm stretched over it. This allows the female mosquitoes to pierce the Parafilm membrane and feed on the blood beneath. The other face of the disc is fully flat and does not have Parafilm stretched across its surface.

Before assembling the blood puck, 8.1 mL of defibrinated sheep blood stored at 4°C was warmed to 42°C for 15-30 minutes in a water bath, and 1 mL aliquots of 20 mM ATP in 25 mM aqueous sodium bicarbonate stock stored at -20°C were slowly thawed on wet ice to room temperature. To assemble the feeding disc of the blood puck membrane-feeder, a 10x10 cm square of Parafilm M (Fisher Scientific, S37440) was first rubbed on both sides against a human skin surface free of cosmetics, such as the forearm or neck, then stretched evenly until translucent before setting aside. The blood puck disc was placed in a metal bead or water bath at 42°C for at least 10 minutes. It was then removed from the warming bath and thoroughly dried with a paper towel. Next, the Parafilm rubbed on human skin was stretched across the entire indented face

of the disc with the utmost care taken to ensure there were no holes in the Parafilm on the feeding side of the disc. Additional strips of Parafilm were used to seal the edges of the disc, and the stretched Parafilm was checked to ensure that it was taut enough to be pierced by a female mosquito's stylet. Working quickly to prevent heat dissipation from the pre-heated feeding disc and blood, 900 µL of ATP stock was added to the 8.1 mL of heated blood for a final concentration of 2 mM ATP, and vortexed thoroughly to mix. Care was taken to ensure the ATP was never heated and did not undergo multiple freeze-thaw cycles. The blood puck disc was held by its edges with the indented, rimmed side face-down and the flat side face-up. The blood + ATP mixture was pipetted through one of the two holes from the flat face. The disc was swirled laterally to evenly distribute the blood before gently placing the blood puck on top of a mesh face of the mosquito cage. In this configuration, the indented, rimmed side sat atop mesh of the cage with female mosquitoes beneath, while the flat side was face-up. Any excess blood dribbling out of the puck after placing on the mosquito cage was blotted with paper towels, and 1-2 additional metal discs (either additional blood pucks, or simple metal discs with both faces flat) pre-warmed to 42°C were placed on top of the feeding disc to maintain warmth. These discs were reheated and replaced as needed to maintain the feeding disc at an optimal temperature for mosquito blood-feeding. As needed, mosquitoes were activated by an experimenter exhaling their breath into the cage. Blood-feeding was conducted both at ambient room temperature conditions and in the environmental chamber with similarly high and reliable engorgement rates. Females were typically allowed to feed for 15 minutes, or until fully engorged, and a single blood puck could be used for 2-3 cages of ~400-450 females each with

replacement of rewarmed flat discs between transfer of the apparatus between cages. After feeding to repletion, typically 15-30 minutes per cage, the discs were taken off the cage, the Parafilm discarded into biohazard waste, and the metal discs rinsed under hot water to thoroughly remove all traces of blood. The blood puck was dried with paper towels for subsequent use.

After feeding, animals were cold anesthetized in a 4°C cold room to separate and discard males, as well as non-blood-fed and partially engorged females. Fully engorged females were selected by eye and returned to their original rearing conditions in a fresh cage with continuous access to 10% sucrose.

8.4 Preparation of mosquitoes for weighing

When blood meal size was measured by weighing (Figure 6.2B, 6.9), non-blood-fed females of all genotypes were each split into two cages of 80-100 females and sugar-starved for 20-24 hours prior to delivering the blood meal. During the sugar-starvation period in experiments involving subsequent weighing, females were offered deionized water-soaked cotton balls to prevent dehydration. Non-blood-fed controls and experimental group females engorged on blood were both immediately cold anesthetized at 4°C after offering the blood meal and weighed in respective groups of 5 each, as previously described (Jové et al., 2020b).

8.5 Preparation of mosquitoes at different reproductive time-points

To prepare groups of mosquito females at different reproductive time-points, all groups were age-matched within each experiment to the extent possible and maintained in mixed-sex cages for at least 5-7 days post-eclosion to ensure that most females were mated. The only exception was with the “virgin” group (Figure 2.4-2.5), for which females were separated at the pupal stage and maintained in single-sex cages. For all blood-feeding groups, females were provided sheep blood supplemented with 2 mM ATP, and only fully engorged females were selected by eye for subsequent experimental use. For egg retention groups, cages were carefully checked for any prematurely dumped eggs prior to collection of females for dissections. For all experiments in which females were required as soon after egg-laying as possible, i.e., groups where eggs were laid <5 hours prior (Figure 2.3D, 3.1-3.2, 3.5-3.6, 4.1, 4.3), we standardized 3 hours as the allotted time for individual females after they were aspirated into egg-laying vials at room temperature. The allotted time of 3 hours was determined based on our finding that ~80% of females complete egg-laying within 3 hours of transfer to egg-laying vials (Figure 2.3A-B). Eggs laid by *Aedes aegypti* females are initially white, and melanize within the first 1-2 hours of egg-laying (Isoe et al., 2019). Based on this, we postulated that any egg-laying vials with at least 10 melanized eggs are likely to have come from females that had completed laying their full clutch of ~100 eggs.

Females of the <5 hours post-egg-laying group used for ovary RNA-sequencing, ovary proteomics, and hemolymph proteomics experiments in Chapter 2 were tested

behaviorally to verify that they had restored attraction to humans using a long-range, live human stimulus olfactometer as described (Basrur et al., 2020). Briefly, females that had laid ≥10 melanized eggs were pooled into groups of 20, gently aspirated at room temperature into "start" canisters of the olfactometer, acclimated for 10 minutes, and the trial run for 5 minutes and 30 seconds as per standard assay protocol. Attracted females were defined as those that entered the trap proximal to the human arm. These attracted females were collected directly from the trap, and only these attracted females were dissected for ovary or hemolymph sample collection. Females that did not enter the attraction trap were discarded and not used for ovary or hemolymph sample collection.

For whole-mount ovary fluorescence RNA *in situ* hybridization experiments (Figure 4.1, 4.3), females were collected and used immediately from egg-laying vials that contained at least 10 melanized eggs, without further assessment of their attraction to humans. For groups that had laid eggs greater than 1 week prior to sample collection (Figure 3.1-3.2, 4.4), plastic cups (VWR HDPE Multipurpose Containers, H9009-664) half-filled with deionized water and lined with filter paper (GE Healthcare, WHA1001055) were introduced to the cage as continuously available egg-laying substrates between 3 and 6 days after blood-feeding. When dissected, 13 days had elapsed since the last blood-meal of this group. When groups in their second reproductive cycle were collected, either for behavior (Figure 2.2C) or for hemolymph proteomics (Figure 3.6), they were treated equivalently to the corresponding first reproductive cycle groups.

8.6 Live human olfactometer assay

Live human olfactometer assays for testing female mosquito attraction to a human forearm were performed as previously described (Basrur et al., 2020). The same subject was used as a stimulus in all experiments. Fabrication and assembly details, as well as a user guide are available at https://github.com/VosshallLab/Basrur_Vosshall2020. Experiments were conducted at 70-90% humidity and 25-28°C. Each trial consisted of approximately 20 female mosquitoes, grouped by reproductive condition. The groups of 20 were aspirated into "start" canisters at least 30 minutes before their trial. Females were given continuous access to 10% sucrose prior to sorting into canisters but were not provided any sucrose or water after being re-housed in the canister. Trials with non-blood-fed females were treated as positive controls and were interspersed throughout each experimental day. Experimental days were counted for final analysis only after ensuring average attraction to the live human arm stimulus of the non-blood-fed group was ≥50% across trials. All groups were run on each experimental day. Two trials were run simultaneously, one using each arm of the live experimenter as the stimulus. Groups were shuffled between ports to minimize bias.

8.7 Egg retention, laying, and hatching assay

For all egg retention experiments, to prevent accumulated condensation that could trigger premature egg ‘dumping’, special care was taken to ensure that all cages and sucrose-soaked cotton wicks for blood-fed female mosquitoes were not subjected to frequent fluctuating temperature and humidity, and closely monitored to remove any

accumulated droplets of water. Following the duration of egg retention, cages were thoroughly checked for any dumped eggs. If a small proportion of eggs was found prematurely dumped on the sugar-soaked cotton wicks, this was noted prior to set up of egg-laying. Although observed extremely rarely, if the cage floor was found to be covered with a large proportion of prematurely dumped eggs, suggesting that little to no egg retention was achieved, all females in such a cage were discarded and not used for further experimentation.

Only for the data shown in Figure 6.6, a single-female modular egg-laying assay setup was used as described (Matthews et al., 2019). The assay setup was modified to accommodate 28 females instead of 14, and each female was provided access to a single egg-laying substrate of deionized water instead of two substrate choices. Details of design and fabrication are available at https://github.com/VosshallLab/MatthewsYoungerVosshall2018.

For all other egg-laying behavior experiments, at the time of egg-laying, females with retained eggs were 14-21 days old, and aspirated out of their cages at room temperature into individual egg-laying vials. Egg-laying vials were made using plastic *Drosophila* vials (VWR, 25 mm diameter, 95 mm length, 75813-164) with 2-3 mL of deionized water, and a 55 mm diameter Whatman filter paper (GE Healthcare, WHA1001055) folded into a cone at the bottom of the vial to serve as a moist egg-laying substrate as previously described (Duvall et al., 2019; Matthews et al., 2019). Vials were kept plugged (Genesee Scientific, Flugs® Narrow Plastic Vials, 49-102) under

standard insectary conditions following transfer of females ready for egg-laying. All females were removed 20-24 hours after transfer under brief cold anesthesia and either discarded or stored at –20°C if required for further genotyping. Filter paper lined with laid eggs, and any eggs remaining on the sides of the vial or in the water, were removed from the vial at room temperature and placed briefly on a paper towel to remove excess moisture. The eggs were then manually counted by eye or under a dissection scope as needed and the number of eggs laid per female recorded. If most eggs from a female were unmelanized or submerged in the pool of water instead of lined on the filter paper, the sample was excluded. The egg-lined filter paper was returned to the emptied and dried vial within 24 hours of removing the female and terminating the egg-laying assay. All vials were kept under standard insectary conditions for 6-14 days prior to hatching.

Egg hatching was staggered to ensure that all egg papers were dried for the same length of time prior to hatching (6-14 days), and egg papers from distinct individuals were hatched and maintained separately. Eggs were hatched either by transferring egg papers into a small plastic cup (VWR, HDPE Multipurpose Containers, H9009-662) with 50-60 mL ‘hatch broth’ comprised of deoxygenated water with finely ground fish food (Pet Mountain, Tetramin Tropical Tablets Fish Food for Bottom Feeders, YT16110M), or by adding 20 mL of hatch broth directly to the egg-laying vial with the dry egg paper (Figure 2.7, and Figure 6.4 or Figure 6.11, respectively). Larvae hatched were provided with a fresh pinch of fish food as needed.

At least 5 days after hatching, the egg viability experiment was terminated. Egg papers were removed and larvae, sometimes mixed with pupae or eclosed adults, were either cold anesthetized at 4°C or killed by freezing at –20°C overnight before thawing and counting. Offspring from each individual female were separately poured onto Petri plates (Fisher Scientific, S33580A) or small plastic cups with fresh deionized water and photographed on a light board using a webcam (Logitech, C922x Pro Stream Webcam) mounted from above, ensuring that all offspring were captured in the field-of-view. Captured images were imported into FIJI/ImageJ (NIH), and the number of offspring from each individual female was counted using the Cell Counter plugin.

8.8 Bulk RNA-sequencing of mosquito ovaries

For ovary bulk RNA-sequencing (RNA-seq), 3 pairs of ovaries were used for each replicate, and 4 replicates were prepared per experimental group from 19-to-20-day old females. Mosquitoes were cold-anesthetized and kept on ice for up to 1 hour, or until dissections were complete. Ovaries were dissected on ice, in ice-cold RNase-free 1X phosphate-buffered saline (PBS) (Invitrogen, AM9625). They were moved using forceps into 0.5 mL Eppendorf LoBind microcentrifuge tubes (Sigma Aldrich, Z666521), and immediately snap-frozen on a cold block (Simport, S700-14) pre-chilled to –78°C on dry ice. Extreme caution was taken during the tissue dissection to ensure that there was no contamination from other mosquito tissues. Each dish and forcep was carefully cleaned with 70% ethanol and RNase-away (Thermo Fisher, 7003) after every dissection. All replicates for each experimental group were dissected in parallel to avoid artifacts and batch effects. Dissected tissue was stored at –80°C until RNA extraction.

RNA extraction was performed using the PicoPure Kit (Thermo Fisher, KIT0204) with the following modification for homogenizing tissue: instead of lysis buffer, 100 µL of TRIzol (Thermo Fisher, 15596026) was added to the collection tube on ice. Tissues were homogenized manually using a Pellet Pestle Motor (Kimble, 749540) and an RNase-Free pellet pestle (VWR, KT749510-0590) for 30 seconds following the addition of 140 µL of TRIzol to a total of 240 µL. Tubes stood at room temperature for 5 minutes before 48 µL of chloroform:isoamyl alcohol 24:1 was added (Sigma, C0549). Tubes were hand-shaken for 30 seconds and left to stand for 2 minutes before centrifuging at 12,000 RPM for 15 minutes at 4°C. The aqueous TRIzol layer was then removed and added into the PicoPure column, up to 130 µL at one time. Subsequent steps were performed according to PicoPure manufacturer's instructions, including DNase treatment.

Samples were run on a Bioanalyzer RNA Pico Chip (Agilent, 5067-1513) to determine RNA quantity and quality. RNA quantity was re-verified with a Qubit 2.0 Fluorometer using the RNA HS Assay Kit (Invitrogen, Q32855). The three biological replicates with the most consistent RNA yield across conditions were then used for library preparation and sequencing.

100 ng of total RNA was used to generate RNA-seq libraries using Illumina TruSeq stranded mRNA LT kit (Illumina, 20020594), following the manufacturer's protocol. Libraries prepared with unique dual indexes were pooled at equal molar ratios.

Sequencing was performed at The Rockefeller University Genomics Resource Center on the Illumina NovaSeq 6000 sequencer using V1.5 reagents, the SP flow cell, and NovaSeq Control Software V1.7.0 to generate 150 bp paired end reads, following manufacturer protocol. Data were demultiplexed and delivered as fastq files for each library. Sequencing reads have been deposited at the National Center for Biotechnology Information (NCBI) Sequence Read Archive (SRA) under BioProject PRJNA796320. The data discussed in this publication have been deposited in NCBI's Gene Expression Omnibus (Edgar et al., 2002) and are accessible through GEO series accession number GSE193470 (https://www.ncbi.nlm.nih.gov/geo/query/acc.cgi?acc=GSE193470).

8.9 Alignment and quantification of ovary RNA-seq data

Sequence and transcript coordinates for the *Aedes aegypti* mosquito genome and gene models were obtained by merging the Aaeg_L5 RefSeq annotation from NCBI with a manual chemoreceptor annotation. Information related to generating this annotation is available at https://github.com/VosshallLab/Jove_Vosshall_2020/tree/master/RNAseq_merged_annotation (Jové et al., 2020a). Transcript expression was calculated using the Salmon quantification software (version 0.8.2) (Patro et al., 2017), and gene expression levels as transcripts per million (TPMs) and counts were retrieved using Tximport (version 1.8.0) (Love et al., 2016; Love et al., 2018). A table of TPM counts for all reproductive conditions and replicates can be found on Zenodo (https://doi.org/10.5281/zenodo.5945525). Normalization and rlog transformation of raw read counts in genes were performed using DESeq2 (version 1.20.0) (Love et al.,

2014). The normalized and transformed counts were used to perform principal component analysis (PCA) using DESeq2, and to assess between-sample variability with hierarchical clustering and with calculation of sample distance correlations (Love et al., 2014).

8.10 Ovary collection and sample preparation for proteomics

To extract whole proteins from ovaries, 8 pairs of ovaries were used for each replicate, and 4 replicates were prepared per experimental group. Ovaries were dissected in a droplet of 1X PBS, as needed, and boiled for 5 minutes at 100°C in 150 µL MilliQ water. Samples were centrifuged at 12,000 RPM for 30 seconds. The water fraction was then decanted into a separate tube and set aside. Extraction solution (150 µL of 0.25% acetic acid) was added to the precipitate, and the tissue was homogenized with a 5 mm tungsten carbide bead in a bead mill homogenizer (Qiagen, Tissue Lyser II) at 30 Hz for 1.5 minutes. The water and acid fractions were centrifuged separately at 4°C, 8000 RPM for 30 minutes. The two supernatants were then combined and spun to dryness in an Eppendorf Speedvac at 60°C for 1-1.5 hours. The mass spectrometry proteomics data have been deposited to the ProteomeXchange Consortium via the PRIDE (Perez-Riverol et al., 2019) partner repository with the dataset identifier PXD030925. Ovary sample raw files begin with the code “MS205850LUM”.

8.11 Hemolymph collection and sample preparation for proteomics

To collect hemolymph, 5 females were used per replicate. Cold anesthetized females were kept on ice and decapitated using 2.5-mm cutting edge Vannas spring scissors

(Fine Science Tools, 15000-08) under a dissection microscope at 10X. Cold 30 µL1X PBS with 0.05% Tween (PBS-T) was pipetted as a bubble onto a 35 mm Petri plate (Falcon, 351008) on ice. The decapitated thorax was positioned close to the droplet without touching, and the thorax was gently squeezed using blunt forceps to release hemolymph from the decapitation site into the droplet of PBS-T. This was repeated such that each droplet of PBS-T consisted of pooled hemolymph from a total of 5 females for a single replicate. The PBS-T with hemolymph was pipetted into a 1.5 mL Eppendorf Protein LoBind tube (Thermo Fisher), and the Petri dish was washed with 10 µL PBS-T, and the 10 µL wash was combined with the ~30 µL from the initial extract. The samples were then heat-inactivated at 90°C for 10 minutes, snap-frozen on dry ice and stored in Eppendorf Protein LoBind tubes at -80°C until the subsequent steps could be carried out. For acetone precipitation of the extracted proteins, we ensured all samples, reagents, tubes, and tube racks were maintained at -20°C. Hemolymph samples from -80°C were quickly removed onto racks cooled to -20°C after which 6 volumes of acetone (~210 µL) cooled to -20°C were added. The sample tubes were vortexed for a few seconds until the frozen hemolymph samples fragmented and mixed well with the acetone. The tubes were then incubated upright at -20°C overnight. Following incubation, samples were spun down at 13,000 x g at 4°C for 10 minutes in a tabletop microcentrifuge. Most of the supernatant was removed with a pipette and discarded, leaving the protein pellet wet before storing at -80°C until subsequent steps. The mass spectrometry proteomics data have been deposited to the ProteomeXchange Consortium via the PRIDE (Perez-Riverol et al., 2019) partner repository with the

dataset identifier PXD030925. Hemolymph sample raw files begin with the code "MS195106LUM".

8.12 Liquid chromatography-mass spectrometry (LC-MS)

Dry protein pellets of both ovary and hemolymph samples were dissolved and reduced in 8 M urea (Fisher Scientific, 45000234)/70 mM ammonium bicarbonate (Fisher Scientific, 501656826)/20 mM dithiothreitol (Sigma Aldrich, 233153), followed by alkylation in the dark with 50 mM iodoacetamide (Sigma Aldrich, I1149). Samples were then diluted 2-fold and digested overnight with endoproteinase LysC (Fujifilm Wako Chemicals, WAKA Lysyl Endopeptidase, 129-02541). Samples were additionally diluted 2-fold and digested with trypsin (Promega, Sequencing Grade Modified Trypsin, Lyophil, PRV5111) for 6 hours. Digestions were halted by acidification and peptides were solid phase-extracted prior to analysis by LC-MS/MS. Peptide samples were analyzed by nano-flow LC-MS/MS (EasyLC 1200) coupled to a Fusion Lumos (Thermo Fisher) operated in High/High Data Dependent Acquisition (DDA) mode using Lock mass m/z 445.12003. Peptides were separated by reversed phase chromatography using 12 cm/75 µm, 3 µm C 18 beads (Nikkyo Technologies, NTCC-360/75-3-123 Column) with buffer A: 0.1% formic acid (Fisher Scientific, A11750), and buffer B: 80% acetonitrile (Fisher Scientific, A955) in 0.1% formic acid. For the hemolymph samples, a gradient from 2% buffer B/98% buffer A to 35% buffer B/65% buffer A in 70 minutes was used. For the ovary samples, a gradient from 2% buffer B/98% buffer A to 38% buffer B/62% buffer A in 90 minutes was used.

Data were queried against 'GCF_002204515.2_AaegL5.0_protein.fasta' database using MaxQuant software with the Andromeda search engine v.1.6. 6.0 (Cox et al., 2014). Oxidation of methionine and N-terminal protein acetylation were allowed as variables, and cysteine carbamidomethylation was defined as a fixed modification. Mass tolerance was set at 4.5 parts per million (ppm) for precursor ions and 20 ppm for fragment ions. Two missed cleavages were allowed for specific tryptic database searches. The 'match between runs' setting was enabled. False discovery rate (FDR) for proteins was set at 1% combined with a peptide FDR of 2%. Intensity based absolute quantitation (iBAQ) (Schwanhausser et al., 2011) values were used as a proxy for protein abundances. Data were processed using Perseus v.1.6.10.50 (Tyanova et al., 2016). Reverse database hits and contaminating proteins were removed, and it was required that a protein was to be measured (using iBAQ) in at least 3 of 4 replicates for least one of the experimental groups. Each $\log_2$-transformed iBAQ signal was normalized by subtracting the respective sample's median iBAQ signal. Missing values were assumed 'Missing Not At Random' (MNAR) (Lazar et al., 2016) and a random distribution of signals with a width of 0.3 and a downshift of 1.8 were used to impute missing values. The sample sets were assessed for quality and correlation using scatter plots and PCA. Tables of iBAQ values and other analyzed metrics are available on Zenodo (https://doi.org/10.5281/zenodo.5945525) for all reproductive conditions and replicates for both ovary and hemolymph proteomics datasets.

8.13 Whole-mount ovary fluorescence RNA *in situ* hybridization

The previously described hybridization chain reaction (HCR) technique (Choi et al., 2018; Younger et al., 2022) was modified to detect RNA in whole-mount ovaries. All reagents, including custom probes, amplifiers, Probe Hybridization Buffer, Amplification Buffer, and Probe Wash Buffer, were purchased from Molecular Instruments. Adult female mosquitoes were dissected ~20 days post-eclosion. They were grouped by reproductive condition, cold anesthetized at 4°C, and maintained on ice for 30 minutes while ovaries were dissected from each female in 0.1X PBS. Dissected ovaries were incubated in a solution of 4% paraformaldehyde, 1X PBS, and 0.03% Triton X-100**,** and rotated overnight at 4°C. Ovaries were then washed 4 times in 1X PBS containing 0.1% Tween-20 (0.1% PBS-T) for 10 minutes each. Subsequently, ovary samples were dehydrated on ice using a series of graded methanol/0.1% PBS-T washes for 10 minutes, as follows: 25% methanol in 0.1% PBS-T, 50% methanol in 0.1% PBS-T, 75% methanol in 0.1% PBS-T, and two washes in 100% methanol. Ovaries remained in 100% methanol at -20°C overnight. To rehydrate the ovaries, samples were washed for 10 minutes each on wet ice with a series of graded methanol/0.1% PBS-T solutions, as follows: 75% methanol in 0.1% PBS-T, 50% methanol in 0.1% PBS-T, 25% methanol in 0.1% PBS-T, and two washes of 0.1% PBS-T. Ovary tissue was then digested in 20 µg/mL Proteinase-K (Thermo Fisher, AM2548) with 0.1% PBS-T for 30 minutes at room temperature and subsequently washed twice in 0.1% PBS-T at room temperature for 10 minutes each. Tissues were then fixed in 4% paraformaldehyde in 0.1% PBS-T for 20 minutes at room temperature and washed 3 times in 0.1% PBS-T for 15 minutes each at room temperature.

Ovaries were incubated in Probe Hybridization Buffer for 5 minutes at room temperature, and subsequently in a 37°C hybridization oven for 30 minutes in pre-warmed Probe Hybridization Buffer. A solution of pre-warmed Probe Hybridization Buffer and probe sets, each at 8 µmol, was mixed, and used to incubate samples at 37°C in a hybridization oven for three nights. Ovaries were next washed 5 times for 10 minutes each in a 37°C hybridization oven using Probe Wash Buffer pre-warmed to 37°C. The samples were then washed twice with 5X saline-sodium citrate (SSC) buffer (Invitrogen, 15557044) containing 0.1% Tween-20 solution for 5 minutes each at room temperature. To pre-amplify, ovaries were incubated in room temperature Amplification Buffer for 10 minutes. 24 µmol hairpins were prepared by heating 8 µL of 3 µM stock of H1 and H2 hairpins, separately, each at 95°C for 90 seconds on an Eppendorf Mastercycler. The hairpins were cooled to room temperature for 30 minutes in the dark, as hairpins are photosensitive and subject to photobleaching. Hairpins were then added to 100 µL of Amplification Buffer in which ovaries were incubated on a rotator at room temperature in the dark overnight. Ovaries were next incubated in the dark in a solution of 1:1000 DAPI in 5X SSC with 0.1% Tween-20 at room temperature for one hour. Ovaries were finally washed four times for 10 minutes each in 5X SSC with 0.1% Tween-20 and mounted in SlowFade Diamond (Thermo Fisher, S36972) onto glass slides with confocal microscopy-compatible coverslips.

8.14 Ovary confocal imaging

Ovary images were acquired using an Inverted LSM 880 Airyscan NLO laser scanning confocal and multiphoton microscope (Zeiss). Either a 10x/0.45 NA objective, or an immersion-corrected 25x/0.8 NA or 63x/1.4 NA objective was used at a resolution of 1024 x 1024 pixels. If tiling was used, images were stitched with 10% or 12% overlap. Laser power, gain, and other parameters were individually optimized to acquire highest quality images for ovary samples acquired from non-blood-fed and post-egg-laying animals. Confocal images were viewed and processed using FIJI/ImageJ, and single slices were selected as representative images.

8.15 Identification or orthologs and conceptualogs

Orthologs for *tweedledee* and *tweedledum* in *Aedes albopictus* were identified using orthology relationships in VectorBase. We noted that the current release of the *Aedes albopictus* genome assembly (GCF_006496715.1 as of December 2021) contained multiples copies of the locus with *tweedledee*, *tweedledum*, *scratch* and *peritrophin-like*. With the currently available data, we were unable to ascertain whether the multiple copies of the locus reflect true duplication events, or incompletely collapsed haplotypes. We arbitrarily chose one locus for subsequent analyses with *Aedes albopictus* genes, but repeating analyses with genes in a second locus yielded no significant differences. *Conceptualogs* in *Culex quinquefasciatus* and all specified *Anopheles* species were found by searching syntenic genomic regions between annotated orthologs of *peritrophin-like* and *scratch* on VectorBase. *Anopheles* genome annotations were used for further analyses if *peritrophin-like, scratch* exon 1 and the *conceptualogs* were all

unambiguously annotated, and if all 3 genes were found on the same contig. *Aedes* and *Culex* protein sequences were obtained from NCBI. *Anopheles* protein sequences were also downloaded from NCBI if a RefSeq annotation was available, but if unavailable as with *Anopheles quadriannulatus* and *Anopheles culicifacies*, protein sequences were taken from VectorBase. Multiple sequence alignments and protein sequence identity matrices were generated using MUSCLE (Madeira et al., 2019). The annotation of *scratch* was fragmented, with both exons annotated as separate genes in *Aedes aegypti*, *Anopheles arabiensis*, *Anopheles culicifacies* and *Anopheles quadriannulatus*, likely due to the presence of a large >50 kb intron. To minimize the ambiguity of the *scratch* protein sequences in these species, we generated the multiple sequence alignment between only the first exon of *scratch* in each species. Gene accession numbers are available at https://doi.org/10.5281/zenodo.5945525.

8.16 Guanine+cytosine (GC) content analysis

GC content for all protein-coding genes from *Aedes aegypti* (AaegL5) was retrieved from Ensembl Metazoa BioMart (version 0.7) (Kinsella et al., 2011) using VectorBase as the gene source. The search was then limited to genes with a predicted cleavage site (SignalP 4.1) to filter for protein-coding genes with a predicted signal peptide.

8.17 Amino acid content analysis

All protein sequences with a predicted signal peptide encoded by the *Aedes aegypti* (AaegL5) genome were retrieved from Ensembl Metazoa BioMart (version 0.7) (Kinsella et al., 2011). The signal peptide predicted was cleaved for each protein using SignalP

4.1 (Nielsen, 2017), and the percent of each amino acid was then calculated for the cleaved sequence. Mean percent residue was calculated for 3,040 *Aedes aegypti* proteins (minimum protein length = 60 amino acids) with predicted signal peptides.

8.18 dN/dS ratio

We aligned coding sequences of 8,030 protein-coding *Aedes aegypti* genes to unique orthologs in *Aedes albopictus*, and coding sequences of 9958 protein-coding *Anopheles gambiae* genes to unique orthologs in *Anopheles stephensi*, as annotated in Ensembl Metazoa, via PRANK (Löytynoja, 2014) using the codon option. dN/dS values per gene were calculated with KaKs_calculator (Wang et al., 2010) using the YN model (Yang and Nielsen, 2000). Sliding window values of dN/dS for *Aedes tweedledee* and *tweedledum* were calculated using a custom script for KaKs_calculator available at https://github.com/LiZhaoLab/Kaks_Calculator.

8.19 Generation of *Δdeedum* double mutants

The *Δdeedum* double mutant was generated using CRISPR-Cas9 (Kistler et al., 2015). Wild type embryos of the *Aedes aegypti* Liverpool strain were injected at the Insect Transformation Facility at the University of Maryland Institute for Bioscience and Biotechnology Research with a gene-targeting mixture composed of 300 ng/μL Cas9 protein with NLS (PNA Bio, CP01-200) and 4 sgRNAs, each 40 ng/μL. Two of the sgRNAs targeted exon 2 of *tweedledee* and the other two targeted exon 2 of *tweedledum* (see https://doi.org/10.5281/zenodo.5945525). Coordinates on *Aedes aegypti* chromosome 2 for *tweedledee*: 113,795,266 - 113,794,685 and *tweedledum:*

113,807,172 - 113,806,119, as annotated in the AaegL5 genome (*40*). As described (*103*), DNA templates were generated for each sgRNA by annealing oligonucleotides using the NEBNext Ultra II Q5 master mix (NEB, M0544L). The HiScribe Quick T7 kit (NEB, E2050S) was then used for in vitro transcription, per manufacturer's instructions, with an overnight incubation of 17 hours at 37°C. Prior to mixing with Cas9 protein, sgRNAs were purified using SPRI beads (Beckman-Coulter, Ampure RNAclean, A63987) with elution in Ultrapure DNase/RNase-free distilled water (Invitrogen, 10977-015). The mutant allele was identified using polymerase chain reaction (PCR) and confirmed to be a double mutant, *Δdeedum,* in which both *tweedledee* and *tweedledum* were disrupted. The strain was backcrossed to wild type Liverpool animals for a minimum of four generations before inbreeding to homozygose. The homozygous *Δdeedum* strain was successfully established and behaviorally phenotyped. To verify wild type, +/*Δdeedum*, and *Δdeedum/Δdeedum* animals, 3 independent PCRs were run on each of the DNA template genotypes as described in Figure 6.1B. The corresponding genotyping primers are listed at https://doi.org/10.5281/zenodo.5945525.

8.20 Generation of *Δdum* mutant and attempted generation of *Δdee* mutant

Δdum, a *tweedledum* single mutant that was wild type at the *tweedledee* locus was recovered using the same mutagenesis procedure as the *Δdeedum* double mutant described above. The same genotyping strategy as that used for the *Δdeedum* double mutant was used with the *Δdum* single mutant to confirm that only *tweedledum* was mutated. With a distinct cocktail of sgRNAs, an allele with a deletion in *tweedledee*

(*Δdee*) that spared *tweedledum* was also isolated but attempts to homozygose and establish a *Δdee* mutant have been unsuccessful to date.

8.21 Photographs of ovaries and spermathecae

Mosquitoes were cold-anesthetized and kept on ice for up to 1 hour, or until dissections were complete. Ovaries and spermathecae were dissected on ice in 1X PBS. Ovaries were photographed using an AxioCam ERc 5s camera (Zeiss) attached to a stereo microscope (Zeiss, SteREO Discovery KMAT). Spermathecae were photographed using an iPhone X through the iDu Optics® LabCam® adapter attached to the eyepiece of a wide-field compound microscope (Swift, SW350B).

8.22 Statistical analysis

R (version 4.1.1) and GraphPad Prism 9 software were used for data visualization and statistical analysis except when specified otherwise in the sections above or in the figure legends.

8.23 Data and resource availability

All raw data reported here, along with a TPM count table from ovary RNA-seq, two protein abundance (iBAQ) tables from hemolymph and ovary proteomics respectively, and instructions for fabricating and using the blood puck are available on Zenodo (https://doi.org/10.5281/zenodo.5945525).

CHAPTER 9. References

Afify, A., and Galizia, C.G. (2015). Chemosensory cues for mosquito oviposition site selection. J Med Entomol *52*, 120-130.

Akbari, O.S., Antoshechkin, I., Amrhein, H., Williams, B., Diloreto, R., Sandler, J., and Hay, B.A. (2013). The developmental transcriptome of the mosquito *Aedes aegypti*, an invasive species and major arbovirus vector. G3 (Bethesda) *3*, 1493-1509.

Alfonso-Parra, C., Ahmed-Braimah, Y.H., Degner, E.C., Avila, F.W., Villarreal, S.M., Pleiss, J.A., Wolfner, M.F., and Harrington, L.C. (2016). Mating-induced transcriptome changes in the reproductive tract of female *Aedes aegypti*. PLoS neglected tropical diseases *10*, e0004451.

Anderson, W.A., and Spielman, A. (1971). Permeability of the ovarian follicle of *Aedes aegypti* mosquitoes. The Journal of cell biology *50*, 201-221.

Armbruster, P., Bradshaw, W.E., and Holzapfel, C.M. (1997). Evolution of the genetic architecture underlying fitness in the pitcher-plant mosquito, *Wyeomia smithii*. Evolution; international journal of organic evolution *51*, 451-458.

Armbruster, P., Bradshaw, W.E., Ruegg, K., and Holzapfel, C.M. (2001). Geographic variation and the evolution of reproductive allocation in the pitcher-plant mosquito, *Wyeomyia smithii*. Evolution; international journal of organic evolution *55*, 439-444.

Bargielowski, I.E., Lounibos, L.P., Shin, D., Smartt, C.T., Carrasquilla, M.C., Henry, A., Navarro, J.C., Paupy, C., and Dennett, J.A. (2015). Widespread evidence for interspecific mating between Aedes aegypti and Aedes albopictus (Diptera: Culicidae) in nature. Infection, genetics and evolution : journal of molecular epidemiology and evolutionary genetics in infectious diseases *36*, 456-461.

Basrur, N.S., De Obaldia, M.E., Morita, T., Herre, M., von Heynitz, R.K., Tsitohay, Y.N., and Vosshall, L.B. (2020). *Fruitless* mutant male mosquitoes gain attraction to human odor. eLife *9*, e63982.

Bentley, M.D., and Day, J.F. (1989). Chemical ecology and behavioral aspects of mosquito oviposition. Annual review of entomology *34*, 401-421.

Berthold, P., Helbig, A.J., Mohr, G., and Querner, U. (1992). Rapid microevolution of migratory behaviour in a wild bird species. Nature *360*, 668–670.

Berthold, P., and Querner, U. (1981). Genetic basis of migratory behavior in European warblers. Science *212*, 77-79.

Bertram, D.S. (1959). The ovary and ovarioles of mosquitos (an illustrated note, with glossary). World Health Organization, Geneva, Document WHO/Mal/236 https:// appswhoint/iris/handle/10665/64653

Bradshaw, W.E., Burkhart, J., Colbourne, J.K., Borowczak, R., Lopez, J., Denlinger, D.L., Reynolds, J.A., Pfrender, M.E., and Holzapfel, C.M. (2018). Evolutionary transition from blood feeding to obligate nonbiting in a mosquito. Proceedings of the National Academy of Sciences of the United States of America *115*, 1009-1014.

Brown, J.E., Evans, B.R., Zheng, W., Obas, V., Barrera-Martinez, L., Egizi, A., Zhao, H., Caccone, A., and Powell, J.R. (2014). Human impacts have shaped historical and recent evolution in *Aedes aegypti*, the dengue and yellow fever mosquito. Evolution; international journal of organic evolution *68*, 514-525.

Brown, M.R., Klowden, M.J., Crim, J.W., Young, L., Shrouder, L., and Lea, A. (1994). Endogenous regulation of mosquito host-seeking behavior by a neuropeptide. Journal of insect physiology *40*, 399-406.

Bungard, D., Copple, J.S., Yan, J., Chhun, J.J., Kumirov, V.K., Foy, S.G., Masel, J., Wysocki, V.H., and Cordes, M.H.J. (2017). Foldability of a Natural De Novo Evolved Protein. Structure *25*, 1687-1696.e1684.

Caldwell, J.M., LaBeaud, A.D., Lambin, E.F., Stewart-Ibarra, A.M., Ndenga, B.A., Mutuku, F.M., Krystosik, A.R., Ayala, E.B., Anyamba, A., Borbor-Cordova, M.J*., et al.* (2021). Climate predicts geographic and temporal variation in mosquito-borne disease dynamics on two continents. Nat Commun *12*, 1233.

Carrasquilla, M.C., and Lounibos, L.P. (2015). Satyrization without evidence of successful insemination from interspecific mating between invasive mosquitoes. Biology letters *11*, 20150527.

Chen, X.G., Jiang, X., Gu, J., Xu, M., Wu, Y., Deng, Y., Zhang, C., Bonizzoni, M., Dermauw, W., Vontas, J*., et al.* (2015). Genome sequence of the Asian Tiger mosquito, *Aedes albopictus*, reveals insights into its biology, genetics, and evolution. Proceedings of the National Academy of Sciences of the United States of America *112*, E5907-5915.

Chng, Y.R., Ong, J.L., Ching, B., Chen, X.L., Hiong, K.C., Wong, W.P., Chew, S.F., Lam, S.H., and Ip, Y.K. (2017). Aestivation induces changes in the mRNA expression levels and protein abundance of two isoforms of urea transporters in the gills of the African lungfish, *Protopterus annectens*. Front Physiol *8*, 71.

Choi, H.M.T., Schwarzkopf, M., Fornace, M.E., Acharya, A., Artavanis, G., Stegmaier, J., Cunha, A., and Pierce, N.A. (2018). Third-generation *in situ* hybridization chain reaction: multiplexed, quantitative, sensitive, versatile, robust. Development (Cambridge, England) *145*, 10.1242/dev.165753.

Clements, A.N. (1963a). The Physiology of Mosquitoes, Chapter 4: 72-108 (Oxford: Pergamon Press).

Clements, A.N. (1963b). The Physiology of Mosquitoes, Chapter 16: 295-310 (Oxford: Pergamon Press).

Clements, A.N. (2000). The biology of mosquitoes Vol. 1, Vol. 1 (New York, NY [etc.]: CABI).

Colton, Y.M., Chadee, D.D., and Severson, D.W. (2003). Natural skip oviposition of the mosquito Aedes aegypti indicated by codominant genetic markers. Med Vet Entomol *17*, 195-204.

Cook, B.I., Mankin, J.S., Marvel, K., Williams, A.P., Smerdon, J.E., and Anchukaitis, K.J. (2020). Twenty‐first century drought projections in the CMIP6 forcing scenarios. Earths Future *8*.

Cornel, A.J., Lee, Y., Almeida, A.P.G., Johnson, T., Mouatcho, J., Venter, M., de Jager, C., and Braack, L. (2018). Mosquito community composition in South Africa and some neighboring countries. Parasites & vectors *11*, 331.

Corona, M., Velarde, R.A., Remolina, S., Moran-Lauter, A., Wang, Y., Hughes, K.A., and Robinson, G.E. (2007). Vitellogenin, juvenile hormone, insulin signaling, and queen honey bee longevity. Proceedings of the National Academy of Sciences of the United States of America *104*, 7128-7133.

Cox, J., Hein, M.Y., Luber, C.A., Paron, I., Nagaraj, N., and Mann, M. (2014). Accurate proteome-wide label-free quantification by delayed normalization and maximal peptide ratio extraction, termed MaxLFQ. Mol Cell Proteomics *13*, 2513-2526.

Curtin, T.J., and Jones, J.C. (1961). The mechanism of ovulation and oviposition in *Aedes aegypti*. Annals of the Entomological Society of America *54*, 298-313.

Day, J.F. (2016). Mosquito oviposition behavior and vector control. Insects *7*.

DeGennaro, M., McBride, C.S., Seeholzer, L., Nakagawa, T., Dennis, E.J., Goldman, C., Jasinskiene, N., James, A.A., and Vosshall, L.B. (2013). *orco* mutant mosquitoes lose strong preference for humans and are not repelled by volatile DEET. Nature *498*, 487-491.

Degner, E.C., and Harrington, L.C. (2016). A mosquito sperm's journey from male ejaculate to egg: Mechanisms, molecules, and methods for exploration. Mol Reprod Dev *83*, 897-911.

Delmore, K., Illera, J.C., Pérez-Tris, J., Segelbacher, G., Lugo Ramos, J.S., Durieux, G., Ishigohoka, J., and Liedvogel, M. (2020). The evolutionary history and genomics of European blackcap migration. eLife *9*.

DeSiervo, M.H., Ayres, M.P., Virginia, R.A., and Culler, L.E. (2020). Consumer-resource dynamics in Arctic ponds. Ecology *101*, e03135.

Dittmer, J., Alafndi, A., and Gabrieli, P. (2019). Fat body-specific vitellogenin expression regulates host-seeking behaviour in the mosquito *Aedes albopictus*. PLoS biology *17*, e3000238.

Du, Y., and Millar, J.G. (1999). Oviposition responses of gravid Culex quinquefasciatus and Culex tarsalis to bulrush (Schoenoplectus acutus) infusions. Journal of the American Mosquito Control Association *15*, 500-509.

Duvall, L.B., Basrur, N.S., Molina, H., McMeniman, C.J., and Vosshall, L.B. (2017). A peptide signaling system that rapidly enforces paternity in the *Aedes aegypti* mosquito. Current biology : CB *27*, 3734-3742.

Duvall, L.B., Ramos-Espiritu, L., Barsoum, K.E., Glickman, J.F., and Vosshall, L.B. (2019). Small-molecule agonists of *Ae. aegypti* neuropeptide Y receptor block mosquito biting. Cell *176*, 687-701.

Edgar, R., Domrachev, M., and Lash, A.E. (2002). Gene Expression Omnibus: NCBI gene expression and hybridization array data repository. Nucleic acids research *30*, 207-210.

Fallon, A.M., Hagedorn, H.H., Wyatt, G.R., and Laufer, H. (1974). Activation of vitellogenin synthesis in the mosquito *Aedes aegypti* by ecdysone. Journal of insect physiology *20*, 1815-1823.

Gloria-Soria, A., Ayala, D., Bheecarry, A., Calderon-Arguedas, O., Chadee, D.D., Chiappero, M., Coetzee, M., Elahee, K.B., Fernandez-Salas, I., Kamal, H.A.*, et al.* (2016). Global genetic diversity of *Aedes aegypti*. Molecular ecology *25*, 5377-5395.

Gospocic, J., Glastad, K.M., Sheng, L., Shields, E.J., Berger, S.L., and Bonasio, R. (2021). Kr-h1 maintains distinct caste-specific neurotranscriptomes in response to socially regulated hormones. Cell *184*, 5807-5823 e5814.

Greenblatt, E.J., Obniski, R., Mical, C., and Spradling, A.C. (2019). Prolonged ovarian storage of mature *Drosophila* oocytes dramatically increases meiotic spindle instability. eLife *8*.

Gu, L., Chen, J., Yin, J., Sullivan, S.C., Wang, H.-M., Guo, S., Zhang, L., and Kim, J.-S. (2020). Projected increases in magnitude and socioeconomic exposure of global droughts in 1.5 and 2 °C warmer climates. Hydrol Earth Syst Sci *24*, 451-472.

Guan, Y., Liu, L., Wang, Q., Zhao, J., Li, P., Hu, J., Yang, Z., Running, M.P., Sun, H., and Huang, J. (2018). Gene refashioning through innovative shifting of reading frames in mosses. Nat Commun *9*, 1555.

Guillén, Y., Rius, N., Delprat, A., Williford, A., Muyas, F., Puig, M., Casillas, S., Ramia, M., Egea, R., Negre, B.*, et al.* (2014). Genomics of ecological adaptation in cactophilic *Drosophila*. Genome Biol Evol *7*, 349-366.

Gwadz, R.W., and Craig Jr., G.B. (1968). Sexual receptivity in female *Aedes aegypti*. Mosquito News *28*, 586-593.

Hagedorn, H.H. (1974). The control of vitellogenesis in the mosquito, *Aedes aegypti*. Amer Zool *14*, 1207-1217.

Hagedorn, H.H., and Fallon, A.M. (1973). Ovarian control of vitellogenin synthesis by the fat body in Aedes aegypti. Nature *244*, 103-105.

Hansen, I.A., Attardo, G.M., Rodriguez, S.D., and Drake, L.L. (2014). Four-way regulation of mosquito yolk protein precursor genes by juvenile hormone-, ecdysone-, nutrient-, and insulin-like peptide signaling pathways. Front Physiol *5*, 103.

Harbach, R. (2013). Mosquito Taxonomic Inventory.

Harrington, L.C., Edman, J.D., and Scott, T.W. (2001). Why do female *Aedes aegypti* (Diptera: Culicidae) feed preferentially and frequently on human blood? J Med Entomol *38*, 411-422.

Harrington, L.C., Fleisher, A., Ruiz-Moreno, D., Vermeylen, F., Wa, C.V., Poulson, R.L., Edman, J.D., Clark, J.M., Jones, J.W., Kitthawee, S*., et al.* (2014). Heterogeneous feeding patterns of the dengue vector, *Aedes aegypti*, on individual human hosts in rural Thailand. PLoS neglected tropical diseases *8*, e3048.

Hawley, W.A. (1988). The biology of Aedes albopictus. J Am Mosq Control Assoc Suppl *1*, 1-39.

Heames, B., Schmitz, J., and Bornberg-Bauer, E. (2020). A Continuum of Evolving De Novo Genes Drives Protein-Coding Novelty in Drosophila. J Mol Evol *88*, 382-398.

Heimroth, R.D., Casadei, E., and Salinas, I. (2018). Effects of experimental terrestrialization on the skin mucus proteome of African lungfish (*Protopterus dolloi*). Front Immunol *9*, 1259.

Hopp, M.J., and Foley, J.A. (2003). Worldwide fluctuations in dengue fever cases related to climate variability. Clim Res *25*, 85–94.

Hudson, B.N.A. (1956). The behaviour of the female mosquito in selecting water for oviposition. The Journal of experimental biology *33*, 478-492.

IPCC (2021). IPCC, 2021: Climate Change 2021: The Physical Science Basis. Contribution of Working Group I to the Sixth Assessment Report of the Intergovernmental Panel on Climate Change, V. Masson-Delmotte, P. Zhai, A. Pirani, S.L. Connors, C. Péan, S. Berger, N. Caud, Y. Chen, L. Goldfarb, M.I. Gomis*, et al.*, eds.

Isoe, J., Koch, L.E., Isoe, Y.E., Rascon, A.A., Jr., Brown, H.E., Massani, B.B., and Miesfeld, R.L. (2019). Identification and characterization of a mosquito-specific eggshell organizing factor in *Aedes aegypti* mosquitoes. PLoS biology *17*, e3000068.

Jia, Q., Liu, S., Wen, D., Cheng, Y., Bendena, W.G., Wang, J., and Li, S. (2017). Juvenile hormone and 20-hydroxyecdysone coordinately control the developmental timing of matrix metalloproteinase-induced fat body cell dissociation. The Journal of biological chemistry *292*, 21504-21516.

Jiang, X., Peery, A., Hall, A.B., Sharma, A., Chen, X.G., Waterhouse, R.M., Komissarov, A., Riehle, M.M., Shouche, Y., Sharakhova, M.V.*, et al.* (2014). Genome analysis of a major urban malaria vector mosquito, *Anopheles stephensi*. Genome Biol *15*, 459.

Johnson, B.R. (2018). Taxonomically Restricted Genes Are Fundamental to Biology and Evolution. Front Genet *9*, 407.

Jones, J.C., and Wheeler, R.E. (1965). Studies on spermathecal filling in *Aedes aegypti* (Linnaeus). II. Experimental. The Biological bulletin *129*, 532-545.

Jové, V., Gong, Z., Hol, F.J.H., Zhao, Z., Sorrells, T.R., Carroll, T.S., Prakash, M., McBride, C.S., and Vosshall, L.B. (2020a). Sensory discrimination of blood and floral nectar by *Aedes aegypti* mosquitoes. Neuron *108*, 1163–1180.

Jové, V., Venkataraman, K., Gabel, T.M., and Duvall, L.B. (2020b). Feeding and quantifying animal-derived blood and artificial meals in *Aedes aegypti* mosquitoes. Journal of visualized experiments : JoVE.

Judson, C.L. (1968). Physiology of feeding and oviposition behavior in *Aedes aegypti* (L.) Experimental dissociation of feeding and oogenesis. J Med Entomol *5*, 21-23.

Juliano, S.A., and Lounibos, L.P. (2005). Ecology of invasive mosquitoes: effects on resident species and on human health. Ecology Letters *8*, 558-574.

Jumper, J., Evans, R., Pritzel, A., Green, T., Figurnov, M., Ronneberger, O., Tunyasuvunakool, K., Bates, R., Žídek, A., Potapenko, A.*, et al.* (2021). Highly accurate protein structure prediction with AlphaFold. Nature *596*, 583-589.

Khalturin, K., Hemmrich, G., Fraune, S., Augustin, R., and Bosch, T.C. (2009). More than just orphans: are taxonomically-restricted genes important in evolution? Trends in genetics : TIG *25*, 404-413.

Kidder, G.M., and Vanderhyden, B.C. (2010). Bidirectional communication between oocytes and follicle cells: ensuring oocyte developmental competence. Can J Physiol Pharmacol *88*, 399-413.

Kinsella, R.J., Kahari, A., Haider, S., Zamora, J., Proctor, G., Spudich, G., Almeida-King, J., Staines, D., Derwent, P., Kerhornou, A.*, et al.* (2011). Ensembl BioMarts: a hub for data retrieval across taxonomic space. Database (Oxford) *2011*, bar030.

Kistler, K.E., Vosshall, L.B., and Matthews, B.J. (2015). Genome engineering with CRISPR-Cas9 in the mosquito *Aedes aegypti*. Cell reports *11*, 51-60.

Klowden, M.J. (1994). Endogenous regulation of the attraction of *Aedes aegypti* mosquitoes. Journal of the American Mosquito Control Association *10*, 326-332.

Klowden, M.J. (1995). Blood, sex, and the mosquito. Bioscience *45*, 326 – 331.

Klowden, M.J. (1996). Endogenous factors regulating mosquito host-seeking behaviour. Ciba Foundation symposium *200*, 212-223; discussion 223-232.

Klowden, M.J. (1999a). The check is in the male: male mosquitoes affect female physiology and behavior. Journal of the American Mosquito Control Association *15*, 213-220.

Klowden, M.J. (1999b). Physiological control of host-seeking behavior by mosquitoes. Wiadomosci parazytologiczne *45*, 561.

Klowden, M.J., and Lea, A.O. (1978). Blood meal size as a factor affecting continued host-seeking by *Aedes aegypti* (L.). The American journal of tropical medicine and hygiene *27*, 827-831.

Klowden, M.J., and Lea, A.O. (1979a). Abdominal distention terminates subsequent host-seeking behaviour of *Aedes aegypti* following a blood meal. Journal of insect physiology *25*, 583-585.

Klowden, M.J., and Lea, A.O. (1979b). Humoral inhibition of host-seeking in *Aedes aegypti* during oocyte maturation. Journal of insect physiology *25*, 231-235.

Korgaonkar, A., Han, C., Lemire, A.L., Siwanowicz, I., Bennouna, D., Kopec, R.E., Andolfatto, P., Shigenobu, S., and Stern, D.L. (2021). A novel family of secreted insect proteins linked to plant gall development. Current biology : CB *31*, 1836-1849 e1812.

Kraemer, M.U., Sinka, M.E., Duda, K.A., Mylne, A., Shearer, F.M., Brady, O.J., Messina, J.P., Barker, C.M., Moore, C.G., Carvalho, R.G.*, et al.* (2015a). The global compendium of *Aedes aegypti* and *Ae. albopictus* occurrence. Sci Data *2*, 150035.

Kraemer, M.U., Sinka, M.E., Duda, K.A., Mylne, A.Q., Shearer, F.M., Barker, C.M., Moore, C.G., Carvalho, R.G., Coelho, G.E., Van Bortel, W.*, et al.* (2015b). The global distribution of the arbovirus vectors *Aedes aegypti* and *Ae. albopictus*. eLife *4*, e08347.

Kraemer, M.U.G., Reiner, R.C., Jr., Brady, O.J., Messina, J.P., Gilbert, M., Pigott, D.M., Yi, D., Johnson, K., Earl, L., Marczak, L.B.*, et al.* (2019). Past and future spread of the arbovirus vectors *Aedes aegypti* and *Aedes albopictus*. Nat Microbiol *4*, 854-863.

Lazar, C., Gatto, L., Ferro, M., Bruley, C., and Burger, T. (2016). Accounting for the multiple natures of missing values in label-free quantitative proteomics data sets to compare imputation strategies. Journal of proteome research *15*, 1116-1125.

League, G.P., Degner, E.C., Pitcher, S.A., Hafezi, Y., Tennant, E., Cruz, P.C., Krishnan, R.S., Garcia Castillo, S.S., Alfonso-Parra, C., Avila, F.W.*, et al.* (2021). The impact of

mating and sugar feeding on blood-feeding physiology and behavior in the arbovirus vector mosquito *Aedes aegypti*. PLoS neglected tropical diseases *15*, e0009815.

Lehane, M.J. (2005). The biology of blood-sucking in insects (chapter 2) (Cambridge: Cambridge University Press).

Li, J. (1994). Egg chorion tanning in *Aedes aegypti* mosquito. Comp Biochem Physiol A Physiol *109*, 835-843.

Liang, S., Hapuarachchi, H.C., Rajarethinam, J., Koo, C., Tang, C.S., Chong, C.S., Ng, L.C., and Yap, G. (2018). Construction sites as an important driver of dengue transmission: implications for disease control. BMC Infect Dis *18*, 382.

Liesch, J., Bellani, L.L., and Vosshall, L.B. (2013). Functional and genetic characterization of neuropeptide Y-like receptors in *Aedes aegypti*. PLoS neglected tropical diseases *7*, e2486.

Lounibos, L.P., Bargielowski, I., Carrasquilla, M.C., and Nishimura, N. (2016). Coexistence of Aedes aegypti and Aedes albopictus (Diptera: Culicidae) in Peninsular Florida Two Decades After Competitive Displacements. J Med Entomol *53*, 1385-1390.

Lounibos, L.P., and Kramer, L.D. (2016). Invasiveness of *Aedes aegypti* and *Aedes albopictus* and vectorial capacity for chikungunya virus. The Journal of infectious diseases *214*, S453-s458.

Love, M.I., Hogenesch, J.B., and Irizarry, R.A. (2016). Modeling of RNA-seq fragment sequence bias reduces systematic errors in transcript abundance estimation. Nature biotechnology *34*, 1287-1291.

Love, M.I., Huber, W., and Anders, S. (2014). Moderated estimation of fold change and dispersion for RNA-seq data with DESeq2. Genome Biol *15*, 550.

Love, M.I., Soneson, C., and Patro, R. (2018). Swimming downstream: statistical analysis of differential transcript usage following Salmon quantification. F1000Res *7*, 952.

Löytynoja, A. (2014). Phylogeny-aware alignment with PRANK. Methods in molecular biology (Clifton, NJ) *1079*, 155-170.

Madeira, F., Park, Y.M., Lee, J., Buso, N., Gur, T., Madhusoodanan, N., Basutkar, P., Tivey, A.R.N., Potter, S.C., Finn, R.D.*, et al.* (2019). The EMBL-EBI search and sequence analysis tools APIs in 2019. Nucleic acids research *47*, W636-W641.

Matthews, B.J., Dudchenko, O., Kingan, S.B., Koren, S., Antoshechkin, I., Crawford, J.E., Glassford, W.J., Herre, M., Redmond, S.N., Rose, N.H.*, et al.* (2018). Improved reference genome of *Aedes aegypti* informs arbovirus vector control. Nature *563*, 501-507.

Matthews, B.J., McBride, C.S., DeGennaro, M., Despo, O., and Vosshall, L.B. (2016). The neurotranscriptome of the *Aedes aegypti* mosquito. BMC Genomics *17*, 32.

Matthews, B.J., Younger, M.A., and Vosshall, L.B. (2019). The ion channel ppk301 controls freshwater egg-laying in the mosquito Aedes aegypti. eLife *8*.

McBride, C.S. (2016). Genes and odors underlying the recent evolution of mosquito preference for humans. Current biology : CB *26*, R41-46.

McBride, C.S., Baier, F., Omondi, A.B., Spitzer, S.A., Lutomiah, J., Sang, R., Ignell, R., and Vosshall, L.B. (2014). Evolution of mosquito preference for humans linked to an odorant receptor. Nature *515*, 222-227.

Nielsen, H. (2017). Predicting Secretory Proteins with SignalP. Methods in molecular biology (Clifton, NJ) *1611*, 59-73.

Papa, F., Windbichler, N., Waterhouse, R.M., Cagnetti, A., D'Amato, R., Persampieri, T., Lawniczak, M.K.N., Nolan, T., and Papathanos, P.A. (2017). Rapid evolution of female-biased genes among four species of *Anopheles* malaria mosquitoes. Genome research *27*, 1536-1548.

Parks, J.J., and Larsen, J.R. (1965). A morphological study of the female reproductive system and follicular developmpent in the mosquito *Aedes aegypti* (L). Trans Am Microsc Soc *84*, 88-98.

Patro, R., Duggal, G., Love, M.I., Irizarry, R.A., and Kingsford, C. (2017). Salmon provides fast and bias-aware quantification of transcript expression. Nat Methods *14*, 417-419.

Perez-Riverol, Y., Csordas, A., Bai, J., Bernal-Llinares, M., Hewapathirana, S., Kundu, D.J., Inuganti, A., Griss, J., Mayer, G., Eisenacher, M.*, et al.* (2019). The PRIDE database and related tools and resources in 2019: improving support for quantification data. Nucleic acids research *47*, D442-D450.

Powell, J.R., Gloria-Soria, A., and Kotsakiozi, P. (2018). Recent History of Aedes aegypti: Vector Genomics and Epidemiology Records. Bioscience *68*, 854-860.

Powell, J.R., and Tabachnick, W.J. (2013). History of domestication and spread of Aedes aegypti--a review. Mem Inst Oswaldo Cruz *108 Suppl 1*, 11-17.

Prieto-Godino, L.L., Rytz, R., Cruchet, S., Bargeton, B., Abuin, L., Silbering, A.F., Ruta, V., Dal Peraro, M., and Benton, R. (2017). Evolution of acid-sensing olfactory circuits in Drosophilids. Neuron *93*, 661-676.e666.

Raikhel, A.S., and Lea, A.O. (1991). Control of follicular epithelium development and vitelline envelope formation in the mosquito; role of juvenile hormone and 20-hydroxyecdysone. Tissue Cell *23*, 577-591.

Renfree, M.B. (1979). Initiation of development of diapausing embryo by mammary denervation during lactation in a marsupial. Nature *278*, 549-551.

Rezende, G.L., Martins, A.J., Gentile, C., Farnesi, L.C., Pelajo-Machado, M., Peixoto, A.A., and Valle, D. (2008). Embryonic desiccation resistance in *Aedes aegypti*: presumptive role of the chitinized serosal cuticle. BMC Dev Biol *8*, 82.

Riehle, M.A., and Brown, M.R. (2002). Insulin receptor expression during development and a reproductive cycle in the ovary of the mosquito *Aedes aegypti*. Cell and tissue research *308*, 409-420.

Rose, N.H., Sylla, M., Badolo, A., Lutomiah, J., Ayala, D., Aribodor, O.B., Ibe, N., Akorli, J., Otoo, S., Mutebi, J.P*., et al.* (2020). Climate and urbanization drive mosquito preference for humans. Current biology : CB *30*, 3570-3579 e3576.

Roy, S., Saha, T.T., Johnson, L., Zhao, B., Ha, J., White, K.P., Girke, T., Zou, Z., and Raikhel, A.S. (2015). Regulation of gene expression patterns in mosquito reproduction. PLoS Genet *11*, e1005450.

Ryan, S.J., Carlson, C.J., Mordecai, E.A., and Johnson, L.R. (2019). Global expansion and redistribution of Aedes-borne virus transmission risk with climate change. PLoS neglected tropical diseases *13*, e0007213.

Santos, M.E., Le Bouquin, A., Crumière, A.J.J., and Khila, A. (2017). Taxon-restricted genes at the origin of a novel trait allowing access to a new environment. Science *358*, 386-390.

Sappington, T.W., Kokoza, V.A., Cho, W.L., and Raikhel, A.S. (1996). Molecular characterization of the mosquito vitellogenin receptor reveals unexpected high homology to the *Drosophila* yolk protein receptor. Proceedings of the National Academy of Sciences of the United States of America *93*, 8934-8939.

Schmidt, H., Greshake, B., Feldmeyer, B., Hankeln, T., and Pfenninger, M. (2013). Genomic basis of ecological niche divergence among cryptic sister species of non-biting midges. BMC Genomics *14*, 384.

Schwanhausser, B., Busse, D., Li, N., Dittmar, G., Schuchhardt, J., Wolf, J., Chen, W., and Selbach, M. (2011). Global quantification of mammalian gene expression control. Nature *473*, 337-342.

Šmarda, P., Bures, P., Horova, L., Leitch, I.J., Mucina, L., Pacini, E., Tichy, L., Grulich, V., and Rotreklova, O. (2014). Ecological and evolutionary significance of genomic GC content diversity in monocots. Proceedings of the National Academy of Sciences of the United States of America *111*, E4096-4102.

Spielman, A., and D'Antonio, M. (2001). Mosquito: The Story of Man's Deadliest Foe (Hyperion).

Steffan, W.S., RD; Evenhuis, NL (1980). Biological observations of Toxorhynchites amboinensis (Diptera: Culicidae) in the laboratory. Journal of Medical Entomology *17*, 515-518.

Stewart, N.B., and Rogers, R.L. (2019). Chromosomal rearrangements as a source of new gene formation in Drosophila yakuba. PLoS Genet *15*, e1008314.

Sun, J., Hiraoka, T., Dittmer, N.T., Cho, K.H., and Raikhel, A.S. (2000). Lipophorin as a yolk protein precursor in the mosquito, *Aedes aegypti*. Insect biochemistry and molecular biology *30*, 1161-1171.

Tripet, F., Lounibos, L.P., Robbins, D., Moran, J., Nishimura, N., and Blosser, E.M. (2011). Competitive reduction by satyrization? Evidence for interspecific mating in nature and asymmetric reproductive competition between invasive mosquito vectors. The American journal of tropical medicine and hygiene *85*, 265-270.

Tunyasuvunakool, K., Adler, J., Wu, Z., Green, T., Zielinski, M., Žídek, A., Bridgland, A., Cowie, A., Meyer, C., Laydon, A.*, et al.* (2021). Highly accurate protein structure prediction for the human proteome. Nature *596*, 590-596.

Tyanova, S., Temu, T., Sinitcyn, P., Carlson, A., Hein, M.Y., Geiger, T., Mann, M., and Cox, J. (2016). The Perseus computational platform for comprehensive analysis of (prote)omics data. Nat Methods *13*, 731-740.

Tyndale-Biscoe, C.H., Hearn, J.P., and Renfree, M.B. (1974). Control of reproduction in macropodid marsupials. The Journal of endocrinology *63*, 589-614.

Valzania, L., Mattee, M.T., Strand, M.R., and Brown, M.R. (2019). Blood feeding activates the vitellogenic stage of oogenesis in the mosquito *Aedes aegypti* through inhibition of glycogen synthase kinase 3 by the insulin and TOR pathways. Developmental biology *454*, 85-95.

van Mierlo, G., Jansen, J.R.G., Wang, J., Poser, I., van Heeringen, S.J., and Vermeulen, M. (2021). Predicting protein condensate formation using machine learning. Cell reports *34*, 108705.

Villarreal, S.M., Pitcher, S., Helinski, M.E.H., Johnson, L., Wolfner, M.F., and Harrington, L.C. (2018). Male contributions during mating increase female survival in the disease vector mosquito *Aedes aegypti*. Journal of insect physiology *108*, 1-9.

Wallis, R.C. (1954). A study of oviposition activity of mosquitoes. Am J Hyg *60*, 135-168.

Wang, D., Zhang, Y., Zhang, Z., Zhu, J., and Yu, J. (2010). KaKs_Calculator 2.0: A toolkit incorporating gamma-series methods and sliding window strategies. Genomics, Proteomics Bioinformatics *8*, 77-80.

Weber, J.N., Peterson, B.K., and Hoekstra, H.E. (2013). Discrete genetic modules are responsible for complex burrow evolution in Peromyscus mice. Nature *493*, 402-405.

Webster, A., and Schuh, M. (2017). Mechanisms of aneuploidy in human eggs. Trends Cell Biol *27*, 55-68.

Whittle, C.A., and Extavour, C.G. (2017). Rapid evolution of ovarian-biased genes in the yellow fever mosquito (*Aedes aegypti*). Genetics *206*, 2119-2137.

WHO (2017). Global vector control response 2017–2030 (Geneva: World Health Organization, ISBN 978-92-4-151297-8).

Witt, E., Benjamin, S., Svetec, N., and Zhao, L. (2019). Testis single-cell RNA-seq reveals the dynamics of de novo gene transcription and germline mutational bias in Drosophila. eLife *8*.

Witt, E., Svetec, N., Benjamin, S., and Zhao, L. (2021). Transcription factors drive opposite relationships between gene age and tissue specificity in male and female *Drosophila* gonads. Molecular biology and evolution *38*, 2104-2115.

Wright, P.E., and Dyson, H.J. (2015). Intrinsically disordered proteins in cellular signalling and regulation. Nature reviews Molecular cell biology *16*, 18-29.

Xie, C., Bekpen, C., Kunzel, S., Keshavarz, M., Krebs-Wheaton, R., Skrabar, N., Ullrich, K.K., and Tautz, D. (2019). A *de novo* evolved gene in the house mouse regulates female pregnancy cycles. eLife *8*.

Yang, Z., and Bielawski, J.P. (2000). Statistical methods for detecting molecular adaptation. Trends Ecol Evol *15*, 496-503.

Yang, Z., and Nielsen, R. (2000). Estimating synonymous and nonsynonymous substitution rates under realistic evolutionary models. Molecular biology and evolution *17*, 32-43.

Younger, M.A., Herre, M., Goldman, O.V., Lu, T.-C., Caballero-Vidal, G., Qi, Y., Gilbert, Z.N., Gong, Z., Morita, T., Rahiel, S.*, et al.* (2022). Non-canonical odor coding in the mosquito. BioRxiv DOI_101101/20201107368720v2.

Zhao, L., Saelao, P., Jones, C.D., and Begun, D.J. (2014). Origin and spread of de novo genes in *Drosophila melanogaster* populations. Science *343*, 769-772.